NASA TR R-102

NATIONAL AERONAUTICS AND SPACE ADMINISTRATION

TECHNICAL REPORT
R-102

AN ANALYSIS OF ERRORS AND REQUIREMENTS OF AN OPTICAL GUIDANCE TECHNIQUE FOR APPROACHES TO ATMOSPHERIC ENTRY WITH INTERPLANETARY VEHICLES

By DAVID P. HARRY, III, and ALAN L. FRIEDLANDER

1961

For sale by the Superintendent of Documents, U.S. Government Printing Office, Washington 25, D.C. Yearly subscription, $15; foreign $19; single copy price varies according to size - - - - - - - - - Price 65 cents

TECHNICAL REPORT R-102

AN ANALYSIS OF ERRORS AND REQUIREMENTS OF AN OPTICAL GUIDANCE TECHNIQUE FOR APPROACHES TO ATMOSPHERIC ENTRY WITH INTERPLANETARY VEHICLES

By DAVID P. HARRY, III, and ALAN L. FRIEDLANDER

Lewis Research Center
Cleveland, Ohio

CONTENTS

TECHNICAL REPORT R-102

AN ANALYSIS OF ERRORS AND REQUIREMENTS OF AN OPTICAL GUIDANCE TECHNIQUE FOR APPROACHES TO ATMOSPHERIC ENTRY WITH INTERPLANETARY VEHICLES

By David P. Harry, III, and Alan L. Friedlander

SUMMARY

An analysis of guidance-system performance and requirements for the control of interplanetary vehicles approaching an entry corridor or grazing pass of any planet is presented. A measurement scheme based on a clock and optical instruments (to obtain trajectory knowledge) and inertial instruments (to measure corrective maneuvers) is hypothesized and could be a self-contained system. Errors in all measurements and control action are considered, and the effects of uncertainties in planet terrain or size are studied. The feasibility study is characterized by two-body hyperbolic trajectories and entry corridors specified only in terms of altitude and direction of rotation. A range of entry velocities from about parabolic to twice parabolic is considered.

A multiple-correction, but not continuous, control technique based on the variance in trajectory elements and including the effects of past history is found capable of performing the entry approach. For example, with instrument errors of 40-second-arc standard deviation, the vehicle can be guided to entry corridors slightly larger than the minimum limit due to the uncertainty in planet terrain at a velocity-increment cost chargeable to the system of 1 percent of entry velocity.

Definition of the uncertainties in planet terrain is beyond the scope of this analysis, but the effects on the system are predictable. Since the velocity-increment cost of correcting the residual errors in midcourse guidance causes large uncertainties in the total velocity-increment requirements, the tradeoff criteria between midcourse residual errors and velocity-increment costs are investigated.

Evaluations of guidance-system performance are obtained by simulating the system on a digital computer using Monte Carlo techniques of statistical analysis. System requirements consistent with the demands of manned interplanetary missions are interpreted as the worst probable requirements, and the probability of success is predicted using extreme-value statistics.

INTRODUCTION

It has become generally accepted that launch guidance is insufficient to perform interplanetary missions without some later corrections. The problems of navigation and control associated with determining and executing these corrections can be considered in several groups, after launch:

(1) Post-injection corrections place the vehicle on a desired departure trajectory.

(2) Midcourse maneuvers correct the trajectory to intercept the target planet.

(3) Homing, approach, or terminal corrections establish the desired arrival trajectory at the destination planet.

This study is concerned with guidance of the approach phases of interplanetary missions; that is, guidance in the region from about the sphere of influence of a target planet down to the sensible atmosphere. The time elapsed during the approach phase may vary from 12 hours to several days, depending on mission velocity. This period of coasting flight is interrupted only at discrete intervals where thrust is used to modify the trajectory toward the desired target. The requirements for an integrated navigation-control system to be used in executing an approach to atmospheric entry or a grazing pass of the planet are analyzed.

It has been shown in reference 1 that entry from high-energy trajectories is aerodynamically feasible and that weight savings relative to the use of retrothrust can be substantial. The ac-

curacy requirements for entry, however, are exacting. For example, to enter the Earth's atmosphere from a parabolic approach trajectory allowing 10-g maximum deceleration rate, the target tolerance with a lifting vehicle modulated (scheduled variation) to a maximum lift-drag ratio of 1 is ±33 miles, and with a ballistic vehicle the tolerance is ±3.5 miles.

Accuracy in guiding to an entry corridor must be accomplished using real instrumentation; that is, measurements subject to finite errors. In general, errors in initial trajectory and uncertainties in planet size or terrain must be considered. Also, the vehicle must execute corrective maneuvers using imperfect controls and sensors.

All vehicles must be guided to within specified entry corridors, and high success probability will be demanded for manned missions. Representative design criteria, such as propellant requirements, result when the worst probable circumstances are considered.

Missions to planets such as Venus or Mars, as well as a return to Earth, are of primary interest. As a result, a fully vehicle-contained navigation system is hypothesized that uses only a clock and optical instruments to obtain trajectory information. Control and measurement of corrective maneuvers by inertial instruments, possibly accelerometers and gyroscopes, are assumed.

The primary trajectory knowledge, then, is obtained from two range observations, an increment of rotation about the target planet, and an increment of time. The scheme is characterized as an $R_1,R_2,\Delta\varphi,\Delta\tau$ scheme. Previous, but less comprehensive, analyses of other schemes have been reported. The use of range, range rate, and the rate of angular rotation about the target planet (ref. 2) might represent instrumentation such as radar or radio and a gyroscopically stabilized reference direction. This might be characterized as an $R,\dot{R},\dot{\theta}$ scheme. Since the accuracy of this scheme depends largely on the rate $\dot{\theta}$, errors increase at long range as the angular rate becomes very small. Also briefly considered in reference 2 is a scheme based on the radar determination of range and range rate at two successive points, an $R_1,\dot{R}_1,R_2,\dot{R}_2$ scheme, which is not directly capable of determining the orientation of the orbit and may, in addition, require large power supplies. Another scheme using successive range and angular-position measurements (ref. 3) might represent an optical system with a planet scanner and star tracker, and is characterized as an $R_1,\varphi_1,R_2,\varphi_2,R_3,\varphi_3$, or $3(R,\varphi)$ scheme. Though no rates are used, accuracy is dependent on second differences in measured quantities. The scheme herein $(R_1,R_2,\Delta\varphi,\Delta\tau)$ is based on finite first differences and has advantages in the accuracy of trajectory determination. Consequently, more efficient guidance is possible.

Of particular concern herein is evaluation of interactions between various component systems related to the overall guidance system. Where feasible, these component requirements are minimized, so that the complexity, cost, and weight can be reduced and/or the reliability increased. The design of components is considered only to the extent that a model for the functional form of errors and their effect on guidance can be evaluated. Since it is desired to determine minimal component requirements, considerable importance is placed on the logic of interpreting and acting on relatively poor knowledge. A fairly sophisticated guidance logic is developed to utilize the available data derived from instruments of reduced performance capability.

The assumed guidance system is synthesized on a digital computer using two-body conic trajectories and a two-dimensional analysis. The performance of the system is evaluated with Monte Carlo techniques; that is, by statistical interpretation of results of many random approach "runs." The analysis was conducted at the NASA Lewis Research Center, and some results have been presented in reference 4.

Many factors beyond the scope of this analysis would enter into a specific mission study. Results are presented herein to illustrate the feasibility of the guidance system to perform the approach to entry, and to determine approximate guidance-system and propellant requirements. Where stringent component requirements are determined, the needs for additional research or development are pointed out.

Tradeoff criteria between guidance accuracy and entry-corridor tolerance are shown with respect to guidance-system requirements. The costs of initial errors in trajectory are shown to illustrate the costs of inaccuracies in the midcourse guidance system, and the effects of mission energy level are presented. All results are shown in nondimensional units valid for any planet. A

sample of the optimization of guidance logic is shown, and the calculation methods are shown in detail in appendixes.

ANALYSIS

Results to be presented represent evaluation of an integrated navigation and control system hypothesized to guide an interplanetary vehicle to a corridor that will permit safe entry. In the following analysis the two-body trajectory relations in nondimensional form are considered first, and the target of guidance is defined. The techniques of correcting trajectory errors are described briefly.

The second section of analysis considers the measurement scheme used in trajectory determination and the techniques of data reduction, including discussion of advantages and disadvantages. The error sensitivity of the system to errors in measurement instruments is then considered, and the effects of mission energy and initial errors in trajectory and the use of redundant data are illustrated.

The logic of acting on measured data, including significant errors, is considered with the objective of reducing total propellant requirements, increasing the tolerance to errors in component systems, decreasing the number of corrective maneuvers, and assuring simultaneously a safe entry. Finally, the techniques of simulating vehicles on a digital computer and evaluating performance by Monte Carlo methods of statistical inference are described.

TRAJECTORY RELATIONS

The range of interest is restricted to within the sphere of influence of the target planet but above its sensible atmosphere, and two-body conic trajectories (specifically, hyperbolas) are assumed. Governing equations can be expressed as laws of conservation of energy and angular momentum (refs. 5 and 6). The total energy (per unit mass) is the kinetic energy plus the potential energy, and the angular momentum is the product of circumferential velocity and the distance from the origin at the center of the planet:

$$\mathscr{E}=\frac{v^2}{2}-\frac{GM}{r} \tag{1}$$

$$h=r(v\cos\gamma) \tag{2}$$

Symbols are defined in appendix A.

Nondimensional units.—The nondimensional units used herein are based on the radius of the planet and the parabolic escape velocity at the surface. These constants are noted in table I for planets of current or probable future interest, and the same nondimensional scheme is used in references 2 and 3. Then,

TABLE I. APPROXIMATE CONSTANTS FOR CONVERTING NONDIMENSIONAL TO REAL UNITS

Parameter	Earth	Venus	Mars
Distance (radius), miles (Int. naut. miles)	3,960 ~4,000 (~3,500)	3,750 (~3,250)	2,108 ~2,100 (1,800)
Escape velocity, ft/sec	36,700	34,400	17,100
Time, min	9.45	9.6	10.9
Acceleration, ft/sec^2	63.8	59.7	26.1

$$\mathscr{E}_e\equiv 0=\frac{v_e^2}{2}-\frac{GM}{r_o} \tag{3}$$

Defining now,

$$\left.\begin{aligned} R&\equiv\frac{r}{r_o}\\ V&\equiv\frac{v}{v_e}\end{aligned}\right\} \tag{4}$$

so that range R is measured in radii from the center of the planet, and velocity V in escape velocities. Working equations become, with the notation of figure 1,

$$E\equiv\frac{\mathscr{E}}{v_e^2/2}=V^2-\frac{1}{R} \tag{5}$$

$$H\equiv\frac{h}{v_e r_o}=RV_\theta=R(V\cos\gamma) \tag{6}$$

In general, upper-case (capital) letters refer to nondimensional units, and lower-case symbols refer to the same variable in real units such as miles, seconds, and so forth. All conversion factors can be derived as functions of the planet radius and escape velocity. This nondimensional system of units permits analysis valid for any planet. Results of this analysis are not valid for Moon approaches, since the range used in numerical evaluation is less than the range of valid two-body assumptions.

Target of guidance.—The target of the approach guidance problem considered is a safe atmospheric entry or grazing pass of the planet. Reference 1 shows the relation between an entry corridor and

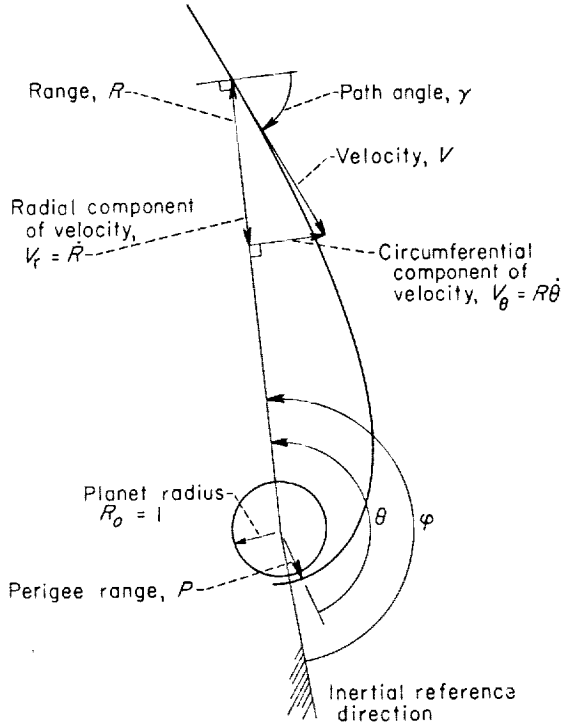

FIGURE 1.—Trajectory notation.

the perigee ($R_p \equiv P$) or the approach trajectory that would result if there were no atmosphere. As indicated schematically in figure 2, the mean range of the two boundary perigees that define a corridor is used as the target perigee. The orientation of the plane of motion is undefined, but it is of interest to guide the vehicle to the desired direction of rotation around the planet.

Equations (5) and (6) evaluated at the perigee where $R=P$ and $\gamma=0$ become

$$E = V_p^2 - \frac{1}{P} \tag{5a}$$

$$H = V_p P \tag{6a}$$

so that

$$E = \frac{H^2}{P^2} - \frac{1}{P} \tag{7}$$

and the perigee range can be obtained with the quadratic equation as

$$\left.\begin{aligned} P &= \frac{1}{2E}\left(\pm\sqrt{1+4EH^2}-1\right) && E \neq 0 \\ P &= H^2 && E = 0 \end{aligned}\right\} \tag{8}$$

The target perigee P_{tar} is assumed to be 1 radius, or tangent to the surface of the planet. The effect of variation in target perigee is shown in reference 2 and also will be considered briefly herein.

Corrective maneuvers.—Velocity increments ΔV required for trajectory modification will be considered representative of propellant expenditure. In nondimensional units, ΔV is measured in escape velocities.

Discussion of corrective maneuvers and the derivation of error relations are treated in appendix B, where (1) the method of determining the desired ΔV is shown and the basic cost of idealized maneuvers is illustrated, (2) a measurement scheme is hypothesized and the effect of measurement errors on the vehicle's knowledge of orbital elements is presented, and (3) the effects of inexact control devices are considered.

The major assumptions introduced in appendix B are summarized as follows:

(1) Corrective maneuvers are applied circumferentially (perpendicular to range) in the plane of motion and are impulsive in effects on trajectory modification.

(2) The effect of finite propulsion devices is approximated by introducing periods of coasting flight equivalent to the firing time of fixed acceleration-rate devices.

(3) Errors in ΔV measurements are assumed uncorrelated with control errors. This assumption permits investigation of the effects of reduced control requirements.

(4) Instrument calibrations, in terms of standard deviations, are assumed available to the vehicle.

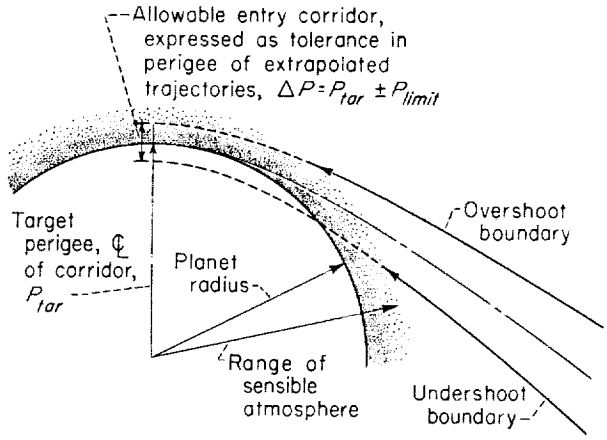

FIGURE 2.—Entry corridor and target perigee.

It will be shown with numerical evaluations that the performance of the guidance system is insensitive to errors in corrective maneuvers when multiple corrections are permitted. The following conclusions are drawn in appendix B:

(1) The ΔV for a given trajectory modification varies as $1/R$, and it is concluded that correction should be made at the maximum feasible range.

(2) The added ΔV cost of specifying a given direction of rotation around the planet is about 0.022 escape velocity (800 ft/sec) for an entry velocity of 1.1 escape velocities (40,400 ft/sec). (Parenthetical values represent approximate values for an approach to Earth throughout this analysis.)

TRAJECTORY DETERMINATION

It is not the purpose of this analysis to consider details of the instrumentation system hypothesized to supply guidance information to the vehicle. It is essential, however, to specify a system in sufficient detail to permit realistic evaluation of the problems, costs, and requirements of approach guidance. Importance is placed on the interaction of various vehicle system components for the purpose of avoiding implied demands on components not considered. As an example, requirements for a dynamic attitude control system during corrective maneuvers might be implied by specifying accurate ΔV control.

The following discussion will illustrate first the measurement scheme to be analyzed. Then the data-reduction techniques and the method of introducing redundant data will be described. The logic used in acting on measured data and the basic error sensitivity of the system will not be considered in this section, but are treated in subsequent sections.

Measurement scheme.—The measurement scheme analyzed herein includes a clock and visual or infrared optical instruments. Range, the distance from the center of the planet to the vehicle, is found from the apparent size of the planet by

$$R=\frac{1}{\sin(\omega/2)} \tag{9}$$

as shown schematically in figure 3. Increments of vehicle rotation around the planet $\Delta\varphi$ are determined from motion of the planet against the star background as viewed from the vehicle, or by occultation methods (ref. 7). The stars, shown behind the planet in two dimensions, could also be 180° away behind the vehicle. In the plane of motion,

$$\Delta\varphi=\varphi_1-\varphi_2 \tag{10}$$

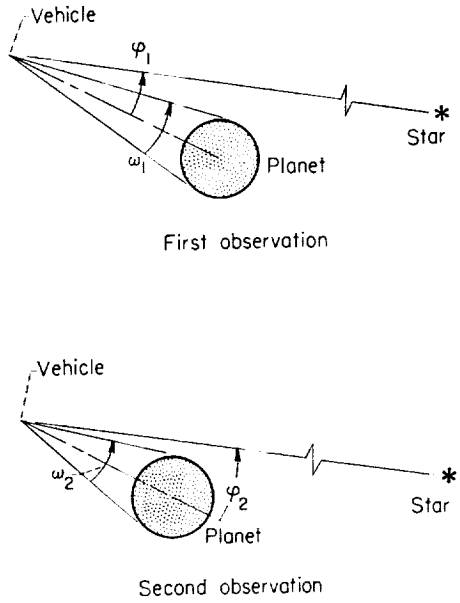

FIGURE 3.—Schematic sketch of use of apparent size and occultation methods in measurement scheme.

Two range determinations, the $\Delta\varphi$, and the time increment $\Delta\tau$ lead to trajectory calculations similar to "two positions and time of flight" methods (e.g., ref. 8).

The image created by the hypothetical telescope is shown schematically in figure 4 for two successive points along an approach trajectory. Two stars, the minimum number needed to

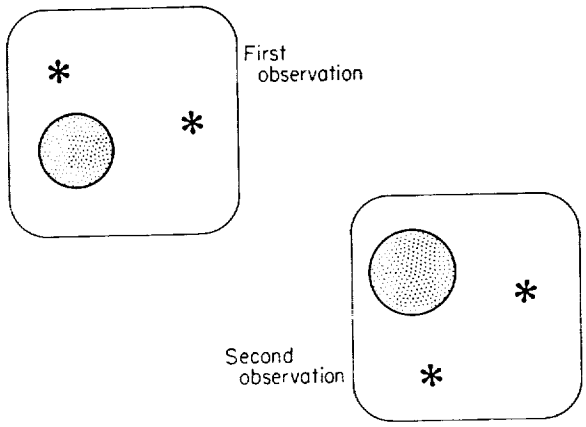

FIGURE 4.—Schematic illustration of image created by hypothetical telescope.

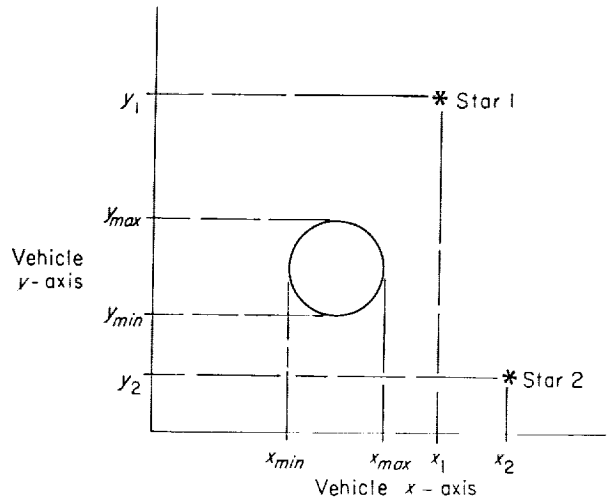

FIGURE 5.—Data to be read from telescope image showing minimum of two stars.

determine the trajectory in three dimensions, are shown; but more would be desirable to check identity in successive readings by triangulation. However, it is not necessary to identify or catalog specific stars.

Data scaled from the image are shown in figure 5 and may be read in some plane relative to the image, such as the vehicle x-y plane. The scale factor must be known, of course, to relate distances on the image to angular measurements. Star coordinates and the maximum and minimum intercepts of the planet in two directions would be read. Errors in measurement are assumed in the process of picking (detection) points from the image. Thus, both y_{max} and y_{min} are subject to measurement errors of standard deviation σ_{meas}, and so forth.

Errors reflect not only the optical system that creates the image but, more important, errors in obtaining data from the image. Reduced accuracy requirements therefore will permit lighter and more reliable optical systems and also less complex and more reliable electronic components associated with the reduction of data from the image.

For the analysis herein it would be unduly tedious to generate the image and random errors in reading data from it. The methods by which these data are calculated are presented in appendix C. The assumption is made that the vehicle has reasonable choice of star positions. It is then possible to relate the measured values of range R and angular displacement $\Delta\varphi$ to the actual values along the true trajectory, R_a and $\Delta\varphi_a$. From appendix C,

$$\left.\begin{aligned} R &= R_a\left(1-\frac{\sqrt{R_a^2-1}}{2}\,\delta_{meas}+\delta_{R,o}\right) \\ \Delta\varphi &= \Delta\varphi_a+\sqrt{2}\delta_{meas} \end{aligned}\right\} \tag{11}$$

The error in planet size or the planet surface radius $\delta_{R,o}$ is included to take into account planet terrain or surface definition uncertainties.

The variance of these values is shown in appendix C to be

$$\left.\begin{aligned} \sigma_R^2 &= R^2\left(\frac{R^2-1}{4}\,\sigma_{meas,ex}^2+\sigma_{R,o,ex}^2\right) \\ \sigma_{\Delta\varphi}^2 &= 2\sigma_{meas,ex} \end{aligned}\right\} \tag{12}$$

where calibration of the instruments is again assumed by the use of $\sigma_{meas,ex}$. Uncertainties in planet size and optical definition of the planet surface establish an accuracy limit for the guidance system, even with otherwise perfect systems. Predictable phenomena such as oblateness, for example, would not normally be considered an uncertainty. Herein, measured range is used in computing σ_R aboard the vehicle (eq. (12)), while the actual error in range (eq. (11)) is assumed to depend on the actual range.

The method of trajectory determination using R_1, R_2, $\Delta\varphi$, and $\Delta\tau$, along with the variances $\sigma_{R,1}^2$, $\sigma_{R,2}^2$, $\sigma_{\Delta\varphi}^2$, and $\sigma_{\Delta\tau}^2$ is presented in later sections. At this point, however, some advantages of using this measurement scheme may be summarized as follows:

(1) The accuracy of the attitude control system is not reflected in the accuracy of the measurement scheme. Thus, the requirements for attitude control result from corrective-maneuver accuracy requirements, which will be shown to be decades less exacting. This is contingent on the ability of the optical device to obtain the image sufficiently fast to allow slight motion of the vehicle, a problem analogous to that of photographing a moving object.

(2) Data are then obtained in essentially zero time relative to trajectory times, and the computational problems associated with range variation during a single reading are avoided.

(3) Attitude control during coasting periods is not required. An attitude knowledge, in contrast to active control, may be useful in avoiding search modes prior to data acquisition, and also in permitting consideration of oblateness corrections in data reduction.

Some potential disadvantages of the measurement scheme should be noted, but study to evaluate effects is beyond the scope of the present analysis:

(1) Failure to obtain the same pair of stars in successive readings may, after failure of a search, result in loss of data for periods of the approach.

(2) The apparent size of the planet varies from minutes of arc to 180° during approach, and the use of several lens systems may be required.

(3) Problems associated with obtaining data from the image are not analyzed.

Data-reduction techniques.—The simultaneous equations that must be solved to determine the orbital elements can be expressed in two dimensions as

$$\left.\begin{aligned}\Delta\tau+\tau_{go,2}-\tau_{go,1}=0\\ \Delta\varphi+\theta_2-\theta_1=0\end{aligned}\right\} \tag{13}$$

where τ_{go} is the time to perigee passage, a function of range and two orbital elements such as perigee P and energy E. Equations are shown in appendix D. True anomaly θ, or the angular displacement from the perigee, is also a function of P, E, and R. Equations (13) express the conditions that the measured increments of angular displacement and time agree with the increments calculated from range and orbital elements. In functional notation consistent with the least-squares adjustment to be used,

$$\left.\begin{aligned}F_1(P,E,R_1,R_2,\Delta\tau,0)=0\\ F_2(P,E,R_1,R_2,0,\Delta\varphi)=0\end{aligned}\right\} \tag{14}$$

Literature on least-squares methods is extensive (e.g., refs. 9 and 10). The development shown in appendix E is that of reference 11.

To solve for unknown values of the orbital elements, P and E, the elements are interpreted as unknown parameters in the least-squares solution. Thus, the pair (or "set") of equations is uniquely determined (two equations and two unknowns), and no adjustment of the observations (R_1, R_2, $\Delta\tau$, $\Delta\varphi$) is made. The least-squares reduction is, in a sense, a method used to expedite convergence of the iterative solution, a particularly efficient method in that convergence of about a decade in both unknown parameters is obtained in each iteration loop. Simultaneously, the expected variances of the adjusted parameters (σ_P^2, σ_E^2) are computed for use in guidance logic.

In general, however, the vehicle does have some knowledge of its orbital elements from previous data reduction, namely, P and E and estimates σ_P^2 and σ_E^2. To make use of this knowledge without the need to re-reduce previous data with new sets, the orbital elements are treated as observations, or measurements. Thus, a history of vehicle knowledge is propagated using the terms P, E, σ_P^2, and σ_E^2. The least-squares condition equations are overdetermined, and there are no unknown parameters.

The results of data reduction are again the adjusted values P, E, σ_P^2, and σ_E^2, but also the adjusted values of the other observations, from which R_2 and $\sigma_{R,2}^2$ are useful.

If guidance logic and the results of data reduction do not cause a corrective action, coasting flight is continued, the trajectory knowledge is used in successive data reductions, and so on. However, if corrective maneuvers are used, the orbital elements are modified as discussed in appendix B, and errors in measuring the ΔV will add additional uncertainty to the modified elements. Assuming that the expected errors in data reduction are uncorrelated with the errors in measuring corrective maneuvers, the modified variance is

$$\left.\begin{aligned}\sigma_P^2=\sigma_{P,(data\ reduction)}^2+\sigma_{P,(\Delta V\ measurement)}^2\\ \sigma_E^2=\sigma_{E,(data\ reduction)}^2+\sigma_{E,(\Delta V\ measurement)}^2\end{aligned}\right\} \tag{15}$$

Trajectory determination, and thus guidance performance, is influenced by inaccuracy in measuring ΔV, but only indirectly by control errors, since the accuracy of trajectory knowledge is not reduced, even though the desired trajectory may not be attained.

More comprehensive methods of using redundant data are available (e.g., refs. 5 and 8). The method just described is used herein to maintain simplicity. The need for computational ease in Monte Carlo evaluations is obvious. The use of

vehicle-contained computers, however, also makes simplicity desirable to reduce complexity and calculation-speed requirements. Where significant weight reduction may not be possible, the gains probably would be attained in reliability (ref. 12).

As indicated in discussion of the costs of corrective maneuvers (appendix B), it is desirable to improve the trajectory at as long a range as possible; and with this method of using redundant data, corrective action can be taken after each increment of coasting flight.

Additional considerations on the data-reduction methods are presented in the next section in relation to the error sensitivity of the measurement scheme.

ERROR SENSITIVITY IN TRAJECTORY DETERMINATION

The basic sensitivity of data reduction and trajectory determination to errors in measurement reflects directly on the ability of the system to perform the approach guidance mission. Consequently, error sensitivity will be considered in some detail.

The terms of the coefficient matrix of the linearized condition equations (appendix D, eqs. (D27)) can be solved algebraically for error coefficients, such as $\partial P/\partial R$. Considerable effort is required, however, and the resulting terms are sufficiently complex that numerical evaluation is necessary before trends are apparent. Also, since it is desired to investigate the effects of several errors simultaneously, the least-squares solution used in simulation of data reduction is also used to evaluate error sensitivity.

The sensitivity of the measurement scheme to errors will be expressed as the standard deviation of the orbital elements, σ_P and σ_E. The caution generally exercised in interpreting linearized error coefficients multiplied by errors is warranted here, since the mechanics are identical. The linearization and use of expected errors are the same as hypothesized in data reduction, however, so that the standard deviations represent the expected errors computed during data reduction aboard a vehicle. Note that the true or actual error in readings does not directly influence the expected error, since the expected standard deviations from calibration of instruments are used in computation. Indirectly, though, large variation may be anticipated because real errors cause changes in the nominal point about which linearization is made.

The expected errors in perigee and energy determination, due to assumed measurement errors and the planet terrain uncertainties, are considered first, followed by illustration of the effects of trajectory energy level and initial perigee. Finally, the effects on trajectory determination of using redundant data and the effects of errors in corrective maneuvers are considered briefly.

The effects of individual component accuracy on the overall accuracy in trajectory determination are presented in appendix F in terms of error coefficients. The major results can be summarized as follows:

(1) With errors of the relative size considered herein, errors in time measurement have insignificant effect relative to other errors.

(2) The measurement scheme considered herein utilizes a common image in observing range (vector) and star positions. If, in contrast, separate instruments are assumed, the error sensitivity due to planet observations is about equal to that due to star-position observations. In a qualitative sense, the results presented could be interpreted for a system using a gyroscopic reference direction, but quantitative results may differ significantly.

(3) The uncertainties in planet size or terrain contribute significant error at short range that for the measurement scheme herein is a physical limitation to guidance accuracy rather than an instrument accuracy problem. Consideration leading to the assumption of $\sigma_{R,o}=0.0002$ radius (0.8 mile, 0.7 Int. naut. mile) as a representative value for analysis purposes is discussed in appendix F.

Basic measurement sensitivity.—The standard deviations in perigee and energy determination, σ_P and σ_E, are shown in figure 6 as functions of the range increment between readings, $\Delta R=R_1-R_2$, for several values of R_2. Since the effects of errors in time, distance, and angles are considered, specific numerical values are assumed: 0.0002-radian (40-sec-arc) angular error, 0.01-percent timing error, and 0.0002-radius (0.8-mile) surface uncertainty. The sensitivities are illustrated for a trajectory of 0.2 energy ($v_h=16{,}400$ ft/sec) and 1 perigee (tangent to the surface), with shaded areas to point out the combinations of range and increment size ΔR that are of interest with the

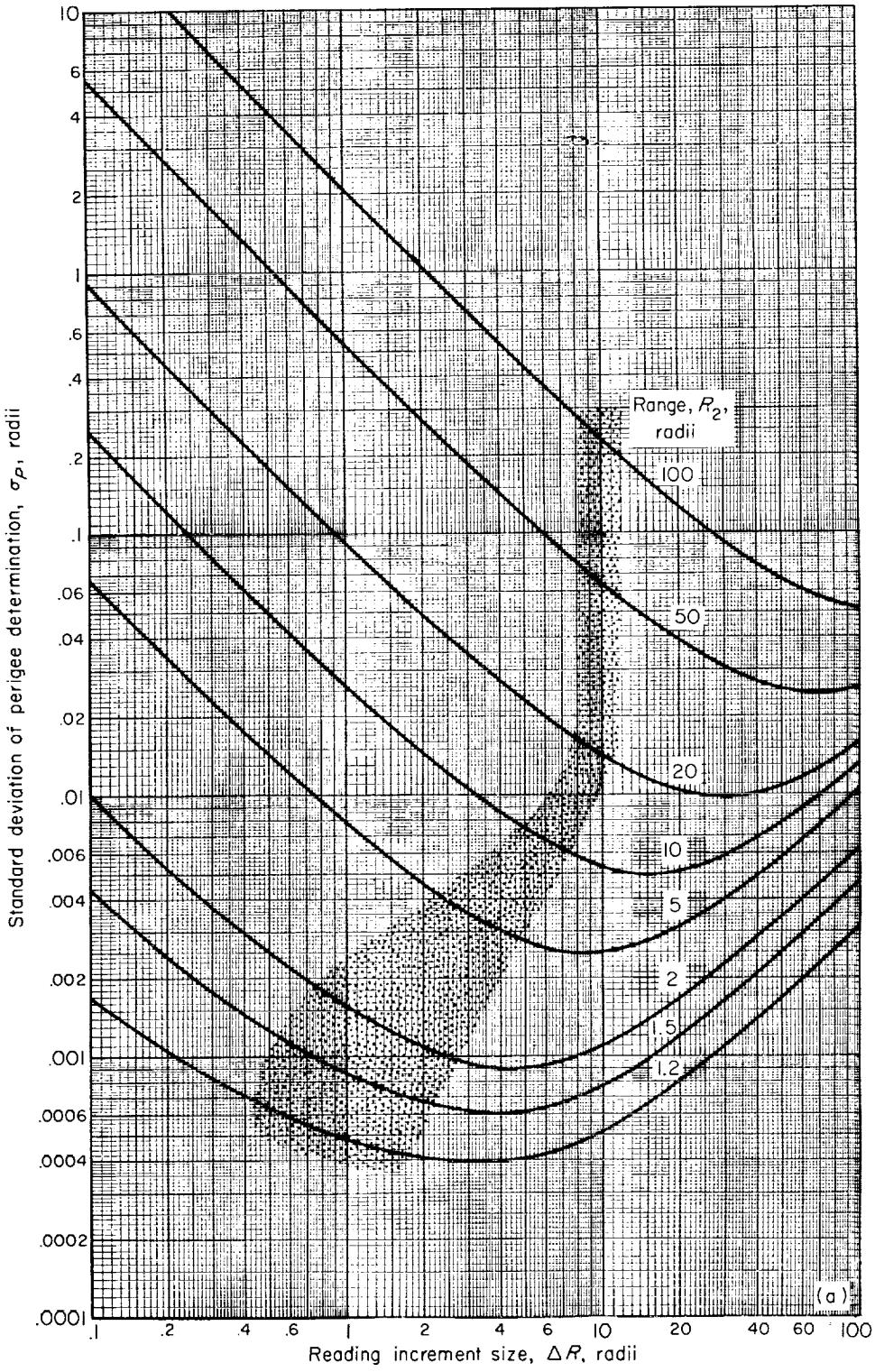

(a) Expected errors in perigee determination.

FIGURE 6. - Basic measurement sensitivity. Assumed values from table II.

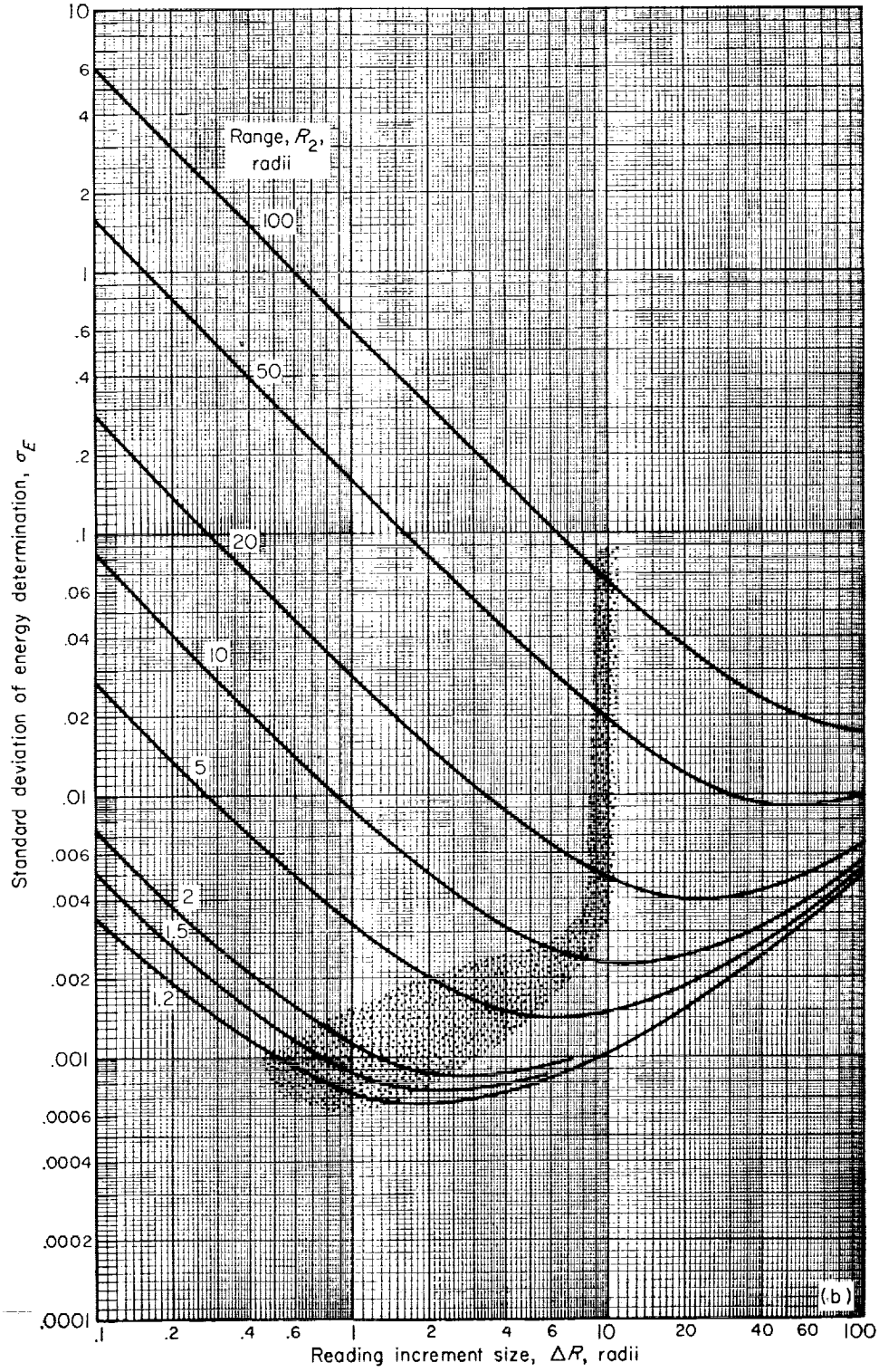

(b) Expected errors in energy determination.

FIGURE 6.—Concluded. Basic measurement sensitivity. Assumed values from table II.

multiple-correction guidance scheme to be analyzed. The curves are shown for range R_1 as large as 200 radii and errors as large as 10 radii for completeness, but two-body assumptions and linearization have doubtful validity at these extremes.

The expected error in perigee determination is shown in figure 6(a). In the range of interest, σ_P varies from 0.0005 radius (2 miles, 1.7 Int. naut. miles) for $R_2=1.2$ radii and $\Delta R=1$ radius, to 0.23 radius (920 miles, 800 Int. naut. miles) for $R_2=100$ and $\Delta R=10$ radii. The variation in accuracy along a probable trajectory is then about 460 to 1. At long range, the increment size for maximum accuracy is approximately the same as the range R_2. At short range, the optimum increment size for a single increment is 2 or 3 times R_2. Shorter than optimum increments are used in multiple-correction schemes, primarily because of the influence of redundant data and the increasing cost of correction as R_2 decreases.

The standard deviation of energy determination is illustrated in figure 6(b). In the range of interest, σ_E varies from 0.0007 (equivalent to an uncertainty in hyperbolic velocity of 97 ft/sec) with $R_2=1.2$ radii and $\Delta R=1$ radius, to 0.065 (9000 ft/sec) with $R_2=100$ and $\Delta R=10$ radii. The optimum step size is roughly the final range R_2, or $R_2\approx R_1/2$, so that steps about half the distance from the initial range to the center of the planet result in maximum accuracy.

The errors in energy using the measurement scheme of this analysis are significantly larger than those of other systems, such as the range, range-rate, and angular-rate scheme of reference 2. This, however, does not constitute a difficulty in guidance, since the energy is not intentionally varied or controlled during the approach, and the entry vehicle is not sensitive to small variation in energy and thus entry velocity (ref. 1). More important, though, σ_P for the subject scheme varies much less with range than σ_P for the $R,\dot{R},\theta$ scheme, where the variation from 100 to 1.2 radii is 20,000:1 relative to the 460:1 of figure 6(a). At short range, the two schemes are of the same order in accuracy capability, but a more precise comparison than decades requires assumption of details not of interest here. On the other hand, at long range, the $R_1,R_2,\Delta\tau,\Delta\varphi$ measurement scheme is clearly decades more precise than the $R,\dot{R},\theta$ scheme. This is reflected in the ability to guide close to the target perigee at long range and thus require less corrective ΔV. Note, however, that computational complexity is significantly increased by the use of time increments in data reduction.

The foregoing results were presented for a particular trajectory, $P=1$, $E=0.2$. The effects of variation in trajectory energy and perigee are considered next. The problems due to linearization around nominal points indicated by measurements that may vary from the true point because of errors are pointed out.

Variation in basic measurement sensitivity with perigee.—The indicated and true perigee will generally differ from the target perigee, herein assumed as 1 radius. The variation of σ_P for several range values and increment sizes is shown in figure 7 as a function of perigee. The energy of 0.2 and the same measurement errors are assumed as previously, and the logarithmic representation is shown only for the range of interest. (As $R\to P$ the errors decrease and curves cross, as shown in ref. 2, but this is considered beyond the range of interest here.)

The trend of principal interest here is that of increasing σ_P with perigee. For example, the error in perigee determination for a trajectory with $P=10$ radii is about 5 times that for $P=1$ radius. This approximation is almost unaffected by range R_2 or increment size ΔR in the region of interest. As a result of the decrease in accuracy with increasing perigee, larger errors in trajectory will cause larger errors in trajectory determination, so that control is poorer at long range. The ΔV cost of control may increase, then, even more than the obvious increase due to larger initial trajectory errors would indicate.

An order-of-magnitude evaluation of linearization can be made as follows, considering for example a reading interval of 10 radii ending at $R_2=100$ radii. If the true perigee were 1 radius, the standard deviation σ_P should be about 0.23 radius. If readings were such that an error of $+2\sigma$ resulted, the indicated reading would be about $P=1.5$ radii, and σ_P would be evaluated as 0.27, or about one-fifth too large. Estimating for $R_2=100$, $\Delta R=5$, and $P=10$ radii, the ratio of indicated to true σ_P is almost 2:1. At short range, where errors are decades less, the errors in computing σ_P should be small, if not negligible. The effect of varying the target of guidance should

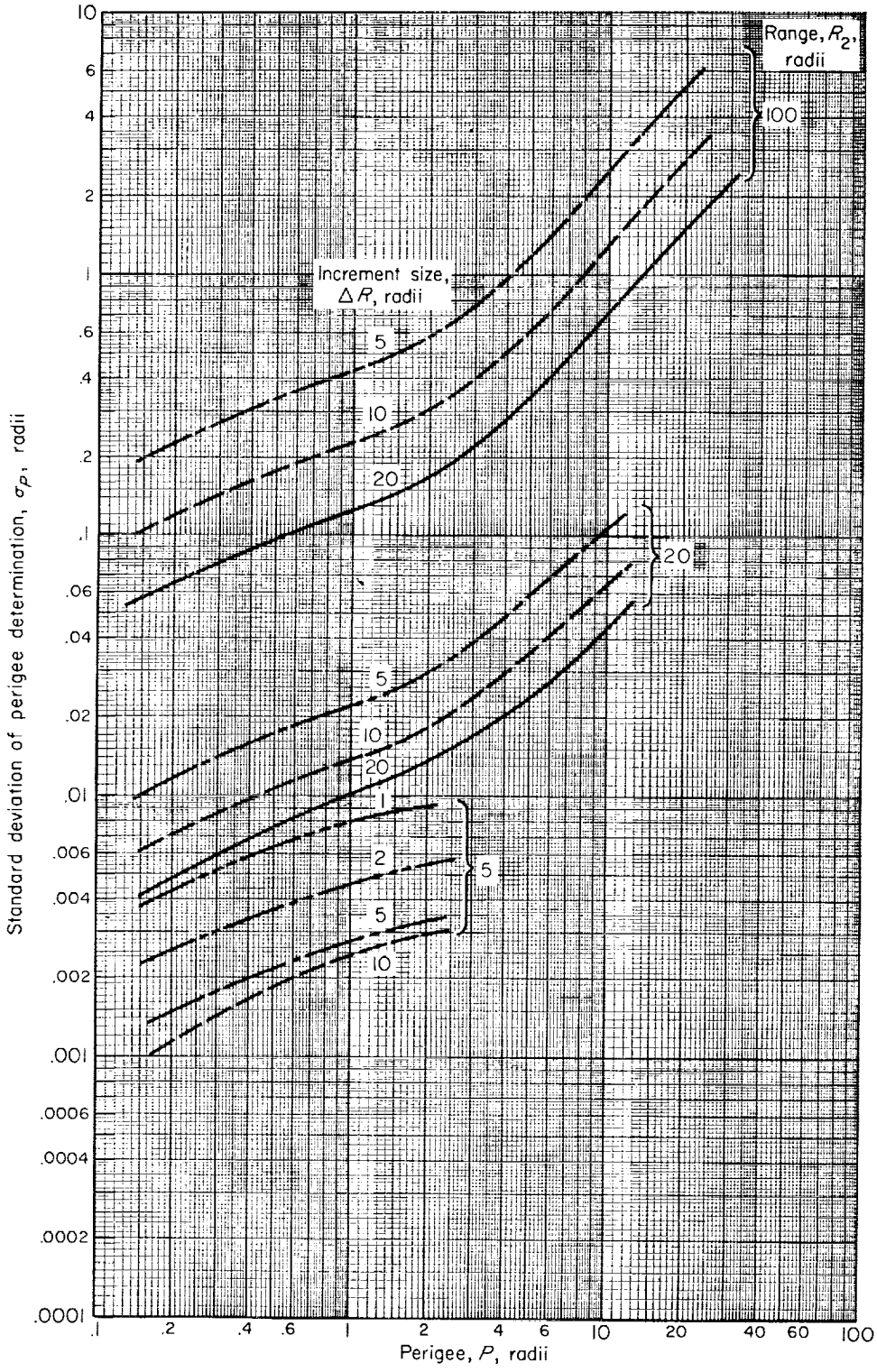

FIGURE 7.—Variation in basic measurement sensitivity with perigee. Assumed values from table II.

be relatively small for the range of entry altitudes that may be considered.

The variation in the sensitivity of energy determination with perigee is not illustrated, since effects on the guidance problem are relatively unimportant.

Variation in basic measurement sensitivity with trajectory energy.—The ability to determine trajectory elements over a range of energy level is significant to guidance in two ways: first, the effect of changes in energy on linearization, as discussed with perigee variation, and, second, the ability to guide the vehicle with high approach velocities.

The standard deviation of perigee determination σ_P for the same assumed errors and $P=1$ radius is shown in figure 8(a) as a function of energy level. The variation from parabolic to more than 3 units hyperbolic represents entry velocities from about 1 to 2 escape velocities (37,000 to 74,000 ft/sec). The hyperbolic velocity varies from zero to $\sqrt{3}$ escape velocities (0 to 64,000 ft/sec), and for this large variation σ_P increases only as much as 50 percent at long range, $R_2=100$ radii. At short range σ_P is almost constant, even decreasing slightly because of changes in the R_2:ΔR relation as energy increases.

Since the perigee is the primary control parameter, the guidance problem for approach to entry should not be significantly more difficult even with high approach velocities. Naturally, the ΔV cost of correction will be greater, and other factors affecting guidance will be considered later. Error coefficients for the $R,\dot{R},\dot{\theta}$ measurement scheme illustrating a decrease in expected perigee errors with increasing energy are noted in reference 2.

The standard deviation of energy determination σ_E, however, increases rapidly with energy level. For the purpose of illustration, σ_E is shown in figure 8(b) as σ_E/E, showing that probable errors are approximately proportional to energy at long range. At short range, the increase in σ_E is less than proportional to E for E up to about 1 unit (v_h=37,000 ft/sec), but σ_E does increase. For higher energy, the increase becomes proportional to energy.

The significance of increased energy errors at high energy is reflected best in numerical evaluations of guidance performance. It is concluded, however, that the ability to determine the perigee accurately is more important than the ability to determine the energy, and that the characteristics illustrated in figure 8 are desirable.

Effects of redundant data.—The previous illustrations of probable errors considered only a single increment of calculation. Consider now the effects of previous knowledge on the computation of perigee along an approach trajectory of $P=1$ radius and $E=0.2$ using the measurement errors as previously. These were 0.0002 radian in angular measurement, 0.0002 radius in surface uncertainty, and 0.01 percent in timing. It is also necessary to assume the sampling rate, or the sequence of increment sizes, along the approach. For the example illustrated in figure 9, increments of 15 radii are used initially at long range and 0.3 R_1 proportional steps at short range. The transition is at 45 radii, where $0.3R_1<15$, and the cutoff point is at 1.2 radii. Logarithmic scales are used to illustrate the variation in σ_P as a function of range R_2, where each point represents the knowledge of all previous data reductions. The past history is introduced as described in sections on data reduction.

The value of σ_P with redundant data is 0.00049 radius, while the expected standard deviation of just the last point alone is indicated as 0.00067 in figure 9. Thus, perigee determination is improved by one-third through the use of redundant data. Greater improvement would not be expected, since σ_P for earlier data is much greater (up to two decades) than σ_P for later data-reduction increments.

The one-third gain due to redundant data is useful in guidance, since it implies roughly one-third smaller entry-corridor sizes. On the other hand, more sophisticated methods of incorporating past history may not greatly improve accuracy but would complicate the computation problem. The reason for large tolerances to inaccuracy in measurement of corrective maneuvers, to be shown, is that loss of even all previous history results in only one-third reduction of knowledge at the time of loss, and less after additional increments of measurement.

GUIDANCE LOGIC

As stated previously, the broad objectives of guidance are (1) to ensure control to the specified entry corridor, (2) to minimize total propellant requirements, and (3) to establish and relax where

595488—61——3

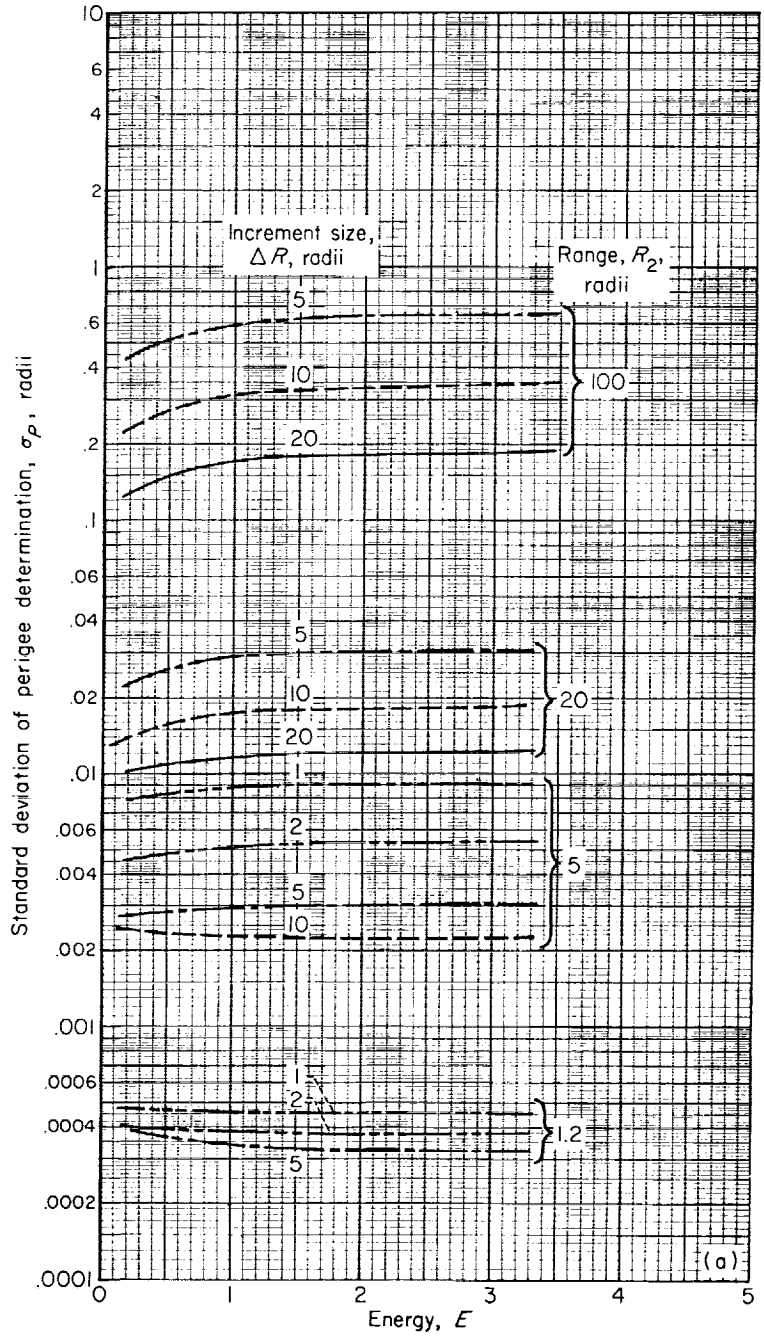

(a) Expected errors in perigee determination.

FIGURE 8.—Variation in basic measurement sensitivity with energy. Assumed values from table II.

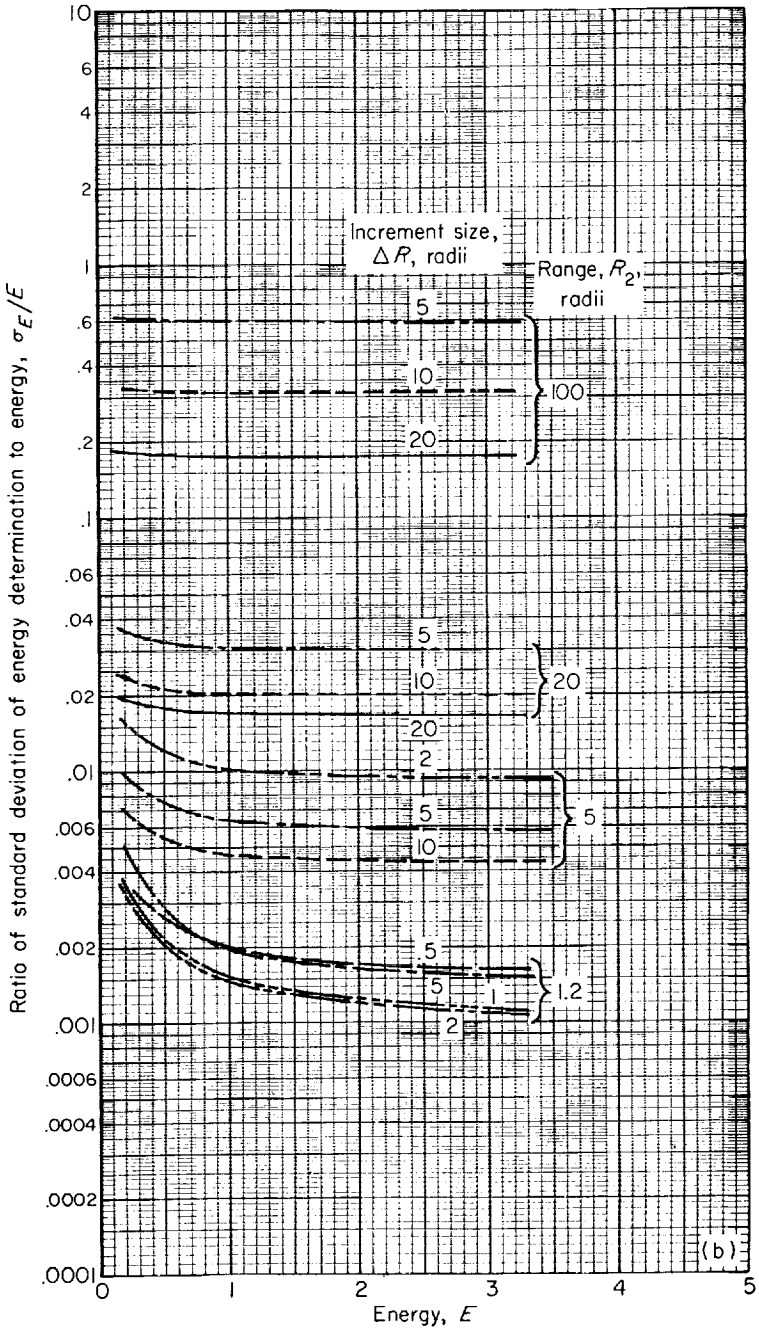

(b) Expected errors in energy determination.

FIGURE 8.—Concluded. Variation in basic measurement sensitivity with energy. Assumed values from table II.

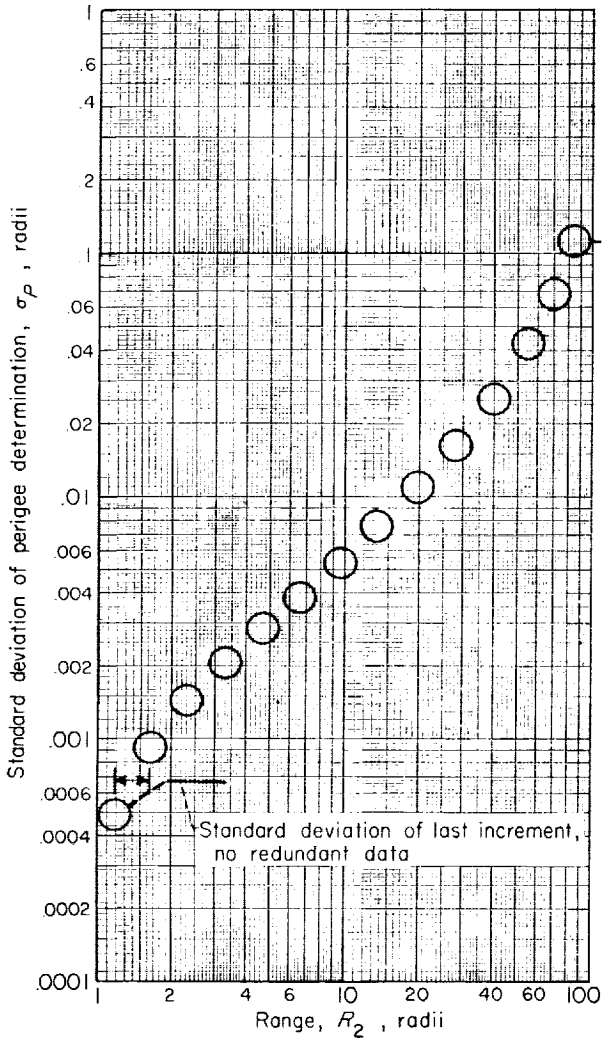

FIGURE 9.—Illustration of effects of redundant data on trajectory determination. Assumed values from table II, except $\Delta R_{max}=15$ radii.

possible the demands on guidance-system components. To achieve these objectives, a method of obtaining and reducing data has been presented, but without discussion of the number or spacing of data-acquisition points. The first function of guidance logic to be considered, then, is the functional logic of a data-sampling schedule. The mechanics of corrective maneuvers and the associated computation have also been described, and the second group of guidance logic forms the link from measured trajectory errors to the desired correction. The presentation of numerical values for particular functions of logic is avoided. An example of the optimization of numerical values, and also of the need for various functions, is shown in connection with statistical performance calculations.

It is of interest to note that the execution of the logic of guidance in a self-contained computer system is negligible compared to data reduction. Thus, computer size is little influenced by the use of the logic to be described.

Data-sampling rate.—Several schemes for determining the rate of data acquisition and corrective maneuvers are proposed in the literature (e.g., ref. 13). It has been found in this analysis and in the studies reported in reference 2, however, that the importance of the first and last points outweighs the importance of the scheme used in intermediate increments. As illustrated in discussing figure 9, the accuracy of guidance is almost completely determined by the accuracy in the last increment before cutoff. The first increment or the first few increments of trajectory determination and correction are important in reducing the ΔV cost of initial errors, as discussed in appendix B.

The sampling rate used in this analysis is shown in figure 10 as a function of the range of the first reading R_1 of a pair. At long range, for the first few readings, a constant increment size is used, or

$$\Delta R=\Delta R_{max} \tag{16}$$

so that the increment size for the correction of initial errors may be varied independently of the remainder of the sampling-rate schedule.

At close range, two factors have been found important. First, the last data should be obtained at the shortest range consistent with sufficient time to act on the data before entry; and second, the last increment must be long enough to obtain good accuracy. The range of the last data point R_{cut} is computed from the range of the sensible atmosphere, the time required to reduce data, the times used in orienting and reorienting the vehicle, and the estimated time needed actually to execute the largest ΔV used after the final data point. The computation is indicated in appendix D. A minimum increment is specified as $\Delta\tau_{min}$ to establish the minimum spacing of data points, where $\Delta\tau_{min}$ is arbitrary but should be at least the time required to reduce data. It is possible, then, to predict when the last reading increment should begin, and also when the second-last reading in-

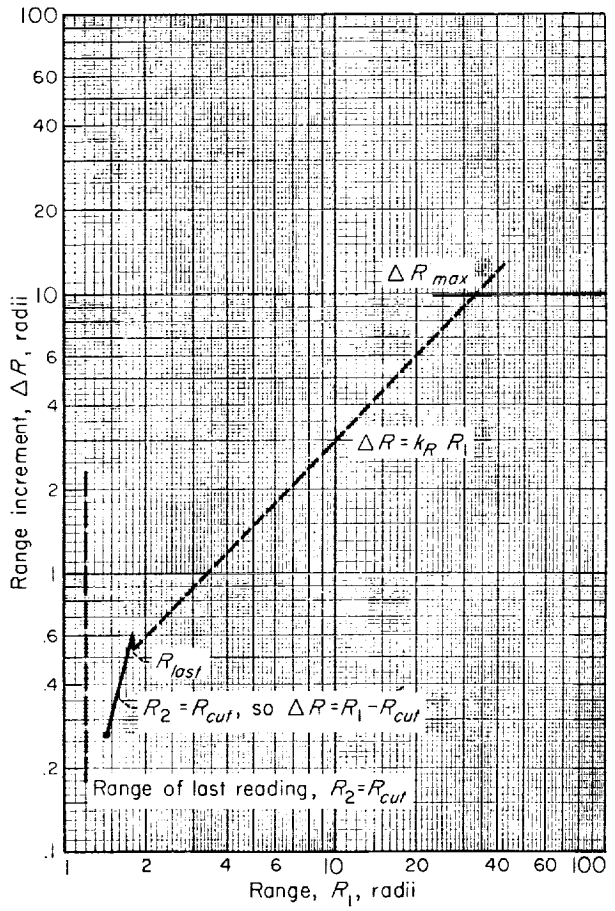

FIGURE 10. Sampling-rate schedule.

crement should begin. The range R_{last} distinguishes the minimum range from which two complete data increments are possible. Thus, for $R > R_{last}$, two (or more) readings are started; while for $R < R_{last}$, only one complete increment may be accomplished. Finally, then, for $R_1 < R_{last}$, the second point of the pair is $R_2 = R_{cut}$, and the increment size becomes

$$\Delta R = R_1 - R_{cut} \qquad R_1 < R_{last} \tag{17}$$

With the sampling rate for the initial and final increments defined, the increment size for intermediate readings is herein assumed to be proportional to R_1, or

$$\Delta R = k_R R_1 \begin{cases} R_{last} < R_1 \\ \Delta R < \Delta R_{max} \end{cases} \tag{18}$$

As will be illustrated in the presentation of numerical results, the proportional step-size coefficient k_R can be varied from 0.1 to 0.5 with only small effects on guidance-system performance. Also, unpublished results indicate that other functional forms of scheduling, such as increments proportional to time, are acceptable. It is concluded, therefore, that the particular functional form of the sampling-rate schedule is not important to guidance-system performance.

The sampling-rate schedule is simulated for computation as presented; but, to prevent requiring the vehicle to monitor its position, a time increment is computed (using vehicle knowledge) and passive coasting is assumed. In other words, the second reading is made after increments of passive coasting flight during which only the clock is monitored. Since, at long range, trajectory knowledge is less accurate, the specific range R_2 desired may differ from the range at which the reading occurs. At short range, where time and range increments should be accurately executed, trajectory determination is sufficiently precise, and the schedule can be closely approximated.

Correction logic.—The guidance computer must have a means to determine, for each of the data-reduction increments, (1) whether a correction is desirable, (2) the size of the correction, and (3) whether the ΔV is within the efficient limits of the propulsion devices. The logic developed to perform these functions is shown as a block diagram in figure 11, which includes terms analogous to dead band and damping as well as limitations on ΔV. On the right of the diagram is the logic used normally for the purpose of minimizing total ΔV and the number of corrective impulses; on the left are modifications for the final correction before entry, which are oriented principally to ensure guidance accuracy.

In a qualitative sense, if uncertainties in perigee determination are larger than the miss distance, expenditure of ΔV is not justified. In a quantitative sense, however, neither the "true" miss distance nor the "true" error in perigee determination is known to the vehicle, and control action must be based on statistical estimates available from data reduction; namely, P and σ_P. A dead band based on the indicated miss distance $P - P_{tar}$ and the expected error in perigee determination

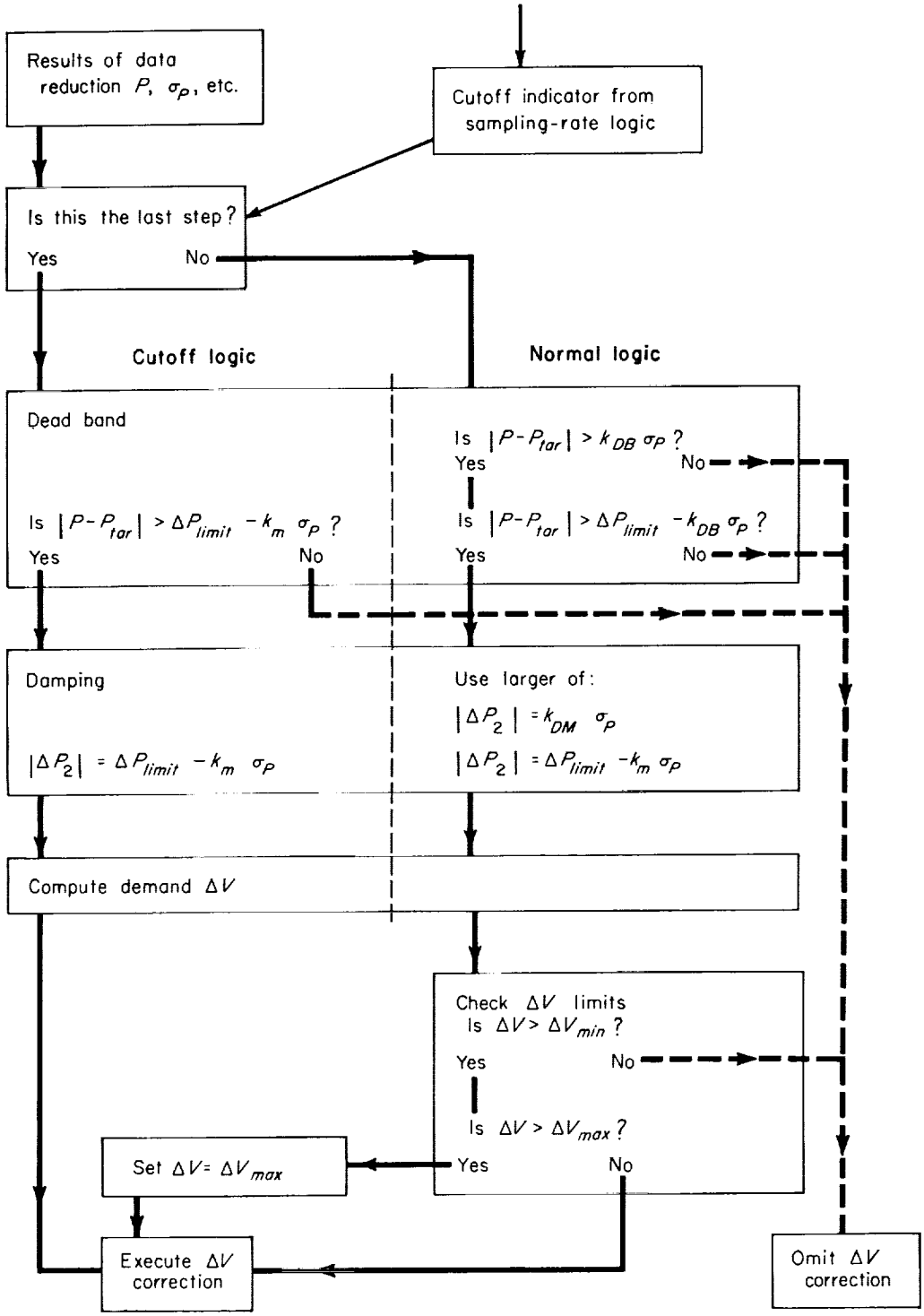

FIGURE 11. Block diagram of correction velocity-increment control logic.

σ_P is used herein to cause omission of ΔV expenditure when knowledge is insufficient (in a statistical sense). An arbitrary "dead-band" coefficient k_{DB} is introduced so that desirable dead-band sizes may be determined by optimization of results. A corrective maneuver is used only when

$$|P-P_{tar}|>k_{DB}\sigma_P \tag{19}$$

Where the indicated error is less than the dead band (e.g., 0.5 sigma), the coasting trajectory is continued.

Unnecessary ΔV is omitted, in a statistical sense, if the vehicle is within the desired corridor size limits, $P_{tar}\pm\Delta P_{limit}$, by specifying an additional dead-band criterion. Thus, unless the indicated error is larger than ΔP_{limit} less a safety factor $k_{DB}\sigma_P$, correction is omitted. Or, coasting flight is continued unless

$$|P-P_{tar}|>\Delta P_{limit}-k_{DB}\sigma_P \tag{20}$$

The dead band used with cutoff logic (the left side in fig. 11) is modified to shift emphasis from efficient control to high accuracy for the final correction. A "miss coefficient" k_m is introduced that is a larger "safety factor" than k_{DB} (e.g., 2.5 sigmas), so that coasting is continued unless

$$|P-P_{tar}|>\Delta P_{limit}-k_m\sigma_P \tag{21}$$

Equation (21) differs from equation (20) only by the arbitrary constant, but the larger coefficient allows correction of smaller errors.

Damping action is incorporated into the guidance logic by causing ΔV to be less than that required to correct to the centerline of the entry corridor P_{tar}, for the purpose of preventing overcorrection due to errors. In normal logic the damping is related to both the significance of the knowledge and the specified corridor size, as with dead bands. The intentional error in trajectory after correction ΔP_2 is the larger of

$$|\Delta P_2|=k_{DM}\sigma_P \tag{22a}$$

$$|\Delta P_2|=\Delta P_{limit}-k_m\sigma_P \tag{22b}$$

where the damping coefficient k_{DM} is introduced to permit optimization of results. The miss coefficient is used again for convenience and to allow somewhat earlier correction close to P_{tar}. The cutoff logic uses only the target-oriented damping (eq. (22b)). The sign convention used herein is shown in appendix D.

Limitations on velocity increments.—The use of engines or thrust devices having limited ΔV capability for individual corrective maneuvers is considered by supplying the guidance computer with the maximum and minimum ΔV that are to be allowed. For example, ΔV_{max} may be limited for an uncooled engine, or ΔV_{min} may be limited to reduce startup losses (if a large engine is used to make small corrections).

When ΔV corrections greater than ΔV_{max} are specified by the foregoing logic, the guidance computer arbitrarily substitutes the maximum allowable correction ΔV_{max}, as indicated in figure 11.

If, on the other hand, ΔV smaller than ΔV_{min} is demanded, control logic arbitrarily overrides the foregoing logic and omits corrective action altogether, except at the cutoff point. Since guidance accuracy is seriously affected by the omission of a final trimming correction, the (slight) inefficiency that results is unavoidable. It should be noted that the use of ΔV_{min} to cause omission of small corrections is somewhat analogous to a dead band and that, as ΔV_{min} is increased, the number of corrective maneuvers used during the approach to entry decreases.

COMPUTATIONAL METHODS

Numerical results used in evaluating guidance-system performance are computed through the use of Monte Carlo techniques. Thus, a random trajectory is generated, and the data that would be acquired under ideal conditions are calculated. Then, indicated readings are computed using random errors and are reduced by the methods described. Guidance logic is executed and any corrective action is calculated. Random errors are used to compute the true corrective action, which is then used to modify the true trajectory, and so forth. The result is the simulation of one sample approach to entry, and the performance of the guidance system is evaluated by the statistical interpretation of many sample cases.

The most important advantage of the Monte Carlo technique is that there is no limit to the complexity of the physical problems that can be solved. A formidable practical limitation, however, is the size and speed of the computer used for simulation.

It should also be noted that the simulation of the computations that would be made aboard the vehicle points out computational difficulties. Thus, where unusual combinations of errors and/or logic lead to breakdown of calculation techniques, such as divergence of iterative solutions, for example, the situations that cause trouble can be avoided by using modified logic or improved calculation techniques.

Random errors used herein are approximately normally distributed and are generated by the method described and evaluated in reference 14. The details of the use of these errors in computation are shown in appendix D.

The performance of the vehicle of interest, namely the one that may attempt to execute the mission, can then be predicted from the statistics generated by simulating many random vehicles. In contrast to predicting the expected or most probable performance, the maximum miss distance and ΔV requirements are of interest herein. Results are interpreted, therefore, for the worst probable requirements on the system, as an initial step in determining the success probability in the range demanded for manned missions.

The significance of the maximum requirements from a given sample of an approximately continuous distribution can be estimated using the statistics of extreme values (ref. 15). The mean number of exceedances $\bar{x}_m$ in N future trials over the m^{th} largest result in n previous trials, and the variance σ_m^2, are

$$x_m = m\frac{N}{n+1}, \qquad \sigma_m^2 = \frac{m(n-m+1)}{(n+1)^2} \times \frac{N(N+n+1)}{n+2} \tag{23}$$

For the special case of one future sample, the mean number of exceedances over the largest previous result and the variance become

$$\bar{x}_m = \frac{1}{n+1} \approx \frac{1}{n}, \qquad \sigma_m^2 = \frac{n}{(n+1)^2} \approx \frac{1}{n} \tag{24}$$

so both the number of exceedances and the variance in the number of exceedances are inversely proportional to the number of previous samples n. The majority of results presented herein illustrate the worst case in 100 samples, so that the mean number of exceedances in the next sample is about 1 percent and the variance of $\bar{x}_m$ is 1 percent. The success probability is thus about 99 percent.

The maximum value itself, however, is only roughly estimated by 100 samples. Before application of analyses to an actual mission, statistical evaluation much more exacting should be made. Further increase in sample size is not considered warranted for the subject analysis, primarily because of the preliminary nature of the investigation. Other factors, including the many assumptions of trajectory and measurement errors, computing-time considerations, and the ability to establish trends with 100 samples, influence the restriction. It should be noted that, where additional samples have been evaluated, the prediction of exceedances has been good.

The use of conventional statistical methods, such as references 9, 10, or 16, which generally require foreknowledge of distribution type, is avoided, principally because the changes in logic and so forth that may make prediction desirable are usually made to alter the distribution type intentionally, thus invalidating the prediction.

STATISTICAL PERFORMANCE EVALUATION

Numerical results are presented in nondimensional units but can readily be translated to real units for a particular planet if the escape velocity and surface radius of that planet are known. The input assumptions of the reference case are presented herein for Mars, Venus, and Earth to illustrate the differences and similarities in the guidance problem of approach to these three planets.

The guidance factors used in presenting the reference case are, for the most part, stated but not discussed. The effects of variations in guidance logic and the method of its optimization are then presented. Next, the requirements on system component performance are discussed, with emphasis on the propulsion and attitude control system associated with corrective maneuvers.

The remaining considerations of the statistical performance evaluation include (1) the effects of assumed initial errors in trajectory, which may contribute the majority of the ΔV cost of guidance and so are presented in terms of the ΔV attributable to midcourse errors and in terms of the influence reflected on the approach guidance system; (2) the effects of entry-corridor size limitations; and (3) the effects of mission energy on the ap-

proach guidance problem, illustrated for a range of basic measurement-error assumptions.

Discussion of numerical results based on many assumed values leads unavoidably to presentation of many values for later discussion because of the interaction of the many variables considered.

REFERENCE CASE

The reference case used herein represents the result of a restricted optimization of guidance logic within a framework of assumed trajectory parameters and measurement errors. A reiteration of the many considerations leading to selection of one particular sample for use as a reference is unduly repetitious. Since many factors influence the results, a tabulation of assumed values is presented before discussion of numerical results, but discussion of individual assumptions is deferred to more appropriate context.

Assumed input to reference case.—The numerical values assumed in computing the guidance performance of the reference case are tabulated in nondimensional units in the second column of table II. The real units in the third column refer

TABLE II.—ASSUMED INPUT TO REFERENCE CASE

Parameter	Assumed value	Approximate equivalent			
		Real units	Earth	Venus	Mars
Initial and target trajectory					
Initial energy, nominal, E_i	0.2	v_h, ft/sec	16, 400	15, 500	7, 700
Standard deviation of E_i, $\sigma_{E,i}$	0.01	v_h, ft/sec	180	172	85
Initial perigee, nominal, P_i	1 radius	Miles	4, 000	3, 750	2, 100
[1] Standard deviation of P_i, $\sigma_{P,i}$	2 radii	Miles	8, 000	7, 500	4, 200
Initial range, nominal, R_i	100 radii	Miles	400, 000	375, 000	210, 000
Standard deviation of R_i, $\sigma_{R,i}$	10 radii	Miles	40, 000	37, 500	21, 000
Target perigee, mean, P_{tar}	1 radius	Miles	4, 000	3, 750	2, 100
Allowable miss distance, ΔP_{limit}	0.0025 radius	Miles	10	9. 4	5. 2
Instrument errors					
Basic measurement error, σ_{meas}	0.0002 radian		0. 8	or 40-sec arc 0. 75	0. 42
Planet terrain uncertainty, $\sigma_{R,o}$	0.0002 radius	Miles	or 0.01 percent		
Clocking error, $\sigma_{\Delta t}$	0.0001		or 80-sec arc		
ΔV Control, direction, σ_β	0.0004 radian		or 0.1 percent		
ΔV Control, magnitude, $\sigma_{\Delta V}$	0.001		or 80-sec arc		
ΔV Measurement, direction, $\sigma_{\delta\beta}$	0.0004 radian		or 0.1 percent		
ΔV Measurement, magnitude, $\sigma_{\delta\Delta V}$	0.001				
Propulsion factors					
Acceleration capability, A_v	0.1	ft/sec^2	6. 4	6. 0	2. 6
Last impulse size estimate, ΔV_{last}	0. 01 escape velocity	ft/sec	367	344	171
Max. ΔV limit, ΔV_{max}	0.1 escape velocity	ft/sec	3, 670	3, 440	1, 710
Min. ΔV limit, ΔV_{min}	0.001 escape velocity	ft/sec	36. 7	34. 4	17. 1
Guidance factors					
Dead-band coefficient, k_{DB}	0.5				
Damping coefficient, k_{DM}	0.5				
Combined cutoff miss coefficient, k_m	2.5				
Max. range increment, ΔR_{max}	10 radii	Miles	40, 000	37, 500	21, 000
Proportional range increment coefficient, k_R.	0.3				
Min. time increment, $\Delta\tau_{min}$	0.5	Min	4. 7	4. 8	5. 4
Lost time, $\Delta\tau_{stop}$	0.5	Min	4. 7	4. 8	5. 4
Range of sensible atmosphere, R_{atm}	1.02 radii	Miles, altitude	80	75	42
New data coefficient, k_{new}	0.1				

[1] The standard deviation of the linear normal distribution used to generate a bivariate distribution.

to the approximate equivalents shown in the last three columns for approaches to Earth, Venus, and Mars. Ratios, coefficients, and angular measurements are unaffected by the nondimensional system.

The first group of assumptions is related to the initial trajectory and the target of guidance. The nominal energy E_i is assumed to be 0.2, representing a hyperbolic velocity of about 0.45 escape velocity or an entry velocity of about 1.1 escape velocities (40,400 ft/sec approaching Earth). The standard deviation in initial energy $\sigma_{E,i}$ is assumed to be 0.01 and is not considered further herein, but two reasons for using errors in initial energy are (1) to avoid coincidental unique solutions possible with fixed values and (2) to make some allowance for midcourse variations in velocity. The initial nominal value of perigee P_i is assumed to be the target perigee P_{tar}, 1 radius, or tangent to the planet surface. This implies that the midcourse guidance system has sufficient resolution to aim at the surface instead of the center of the planet. The linear components of the perigee error $\sigma_{P,i}$ used to generate a bivariate distribution, are assumed to be 2 radii, thus allowing initial errors up to, say, 6 radii for particularly bad samples. The initial range R_i of 100 radii and standard deviation $\sigma_{R,i}$ of 10 radii are assumed and will not be considered further. The large error in initial range is used, first, to maintain the previous assumption that coasting flight between readings is used to avoid the need for the vehicle to monitor its range, and, second, to prevent the development of unique sampling-rate schedules keyed to a particular initial range. The assumed entry corridor ΔP_{limit} of ± 0.0025 radius (± 10 miles or 8.7 Int. naut. miles approaching Earth) will be considered further.

The second group of assumed values includes the errors in measurement instruments and the planet terrain uncertainty, as were discussed previously in connection with the basic accuracy of trajectory determination. These assumptions will all be considered later except the clocking error $\sigma_{\Delta\tau}$, assumed to be 0.01 percent. This error, representing about 10 seconds per day, is not a stringent requirement but nevertheless has little influence on results.

The third group of assumed values specifies the control propulsion devices, though the last impulse size ΔV_{last} is possibly better considered a function of guidance logic. Values of A_v, ΔV_{max}, and ΔV_{min} are assumed to be 0.1, 0.1, and 0.001, respectively, and are considered later. Since ΔV_{max} as assumed is much larger than the maximum requirement, it is essentially unspecified for the reference case.

Assumed or optimized values of guidance logic are listed in the last group. The range of the sensible atmosphere R_{atm}, assumed 1.02 radii (80-mile or 70-Int.-naut.-mile altitude for Earth), and the "new data coefficient" k_{new} will not be considered further, the latter term representing the increase in range or time-increment steps used when the data reduction fails. Thus, if breakdown of data reduction occurs, the original step size is increased by 10 percent and a new second reading is generated, and so forth, until a valid result is obtained. Of particular note is the close correspondence of time increments for the three planets, namely, 4.7, 4.8, and 5.4 minutes. Thus, the times associated with computer speed and dynamic attitude control represent roughly the same equipment requirement for approaches to any of these three planets.

Results of reference case.—The accuracy of guidance for the reference case is illustrated in figure 12(a), where the number of vehicles completing the approach with a given true absolute miss distance $|\Delta P_a|$ is shown as a function of miss distance. The assumed allowable miss distance of 0.0025 radius (± 10 miles) is indicated, and all vehicles are guided within the entry corridor by at least 0.00025 radius (1 mile). No significance is placed on the distributions of miss distance herein, except where the specified corridor is missed. Though the sample size of 100 vehicles is insufficient to specify probabilities of success greater than 99 percent, any known miss of the target corridor indicates a success probability of 98 percent or less and is categorically rejected herein. *Thus, unless notation is made of vehicles missing the corridor, it should be assumed that the desired accuracy is attained.*

The frequency distribution of total ΔV requirements is shown in figure 12(b). The number of vehicles requiring a given ΔV_{tot} is shown as a function of the total velocity increment. Two important effects are immediately obvious. First, the average, mean, or mode does not reflect requirements on the guidance system. For example, the most frequent requirement is 0.007, the mean

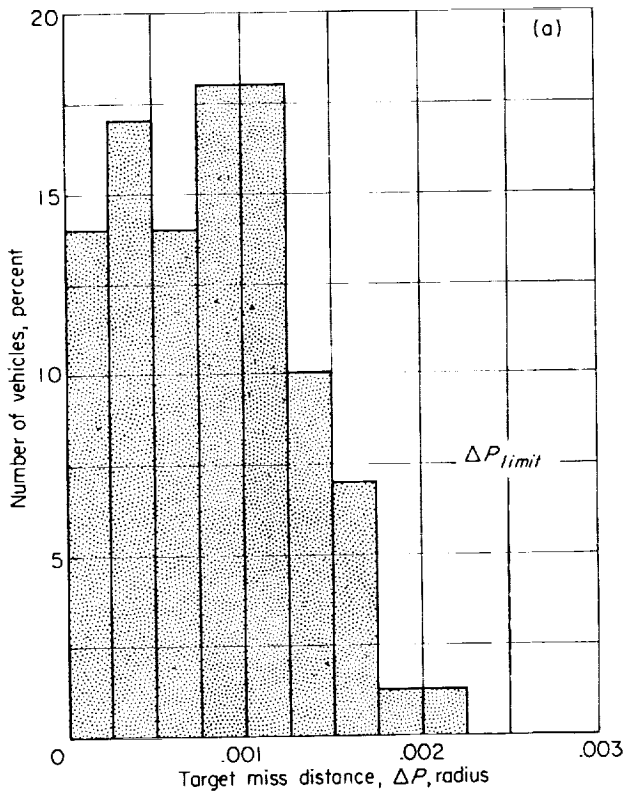

(a) Frequency distribution of target miss distance.

FIGURE 12.—Results of reference case. Assumed values from table II.

is 0.014, and the average is 0.016; while to obtain a predicted probability of success of 99 percent the system must be capable of 0.042 escape velocity. Second, the distribution is poorly defined, particularly in the high ΔV requirement region of interest.

Avoiding, momentarily, the problem of accurately defining ΔV_{tot}, the cumulative frequency distribution of ΔV expenditure is shown in figure 12(c). The ideal velocity increment ΔV_{id} is the velocity increment needed to correct the initial error in perigee to the nearest boundary of the entry corridor at the range of guidance initiation, and is interpreted herein as the ΔV chargeable to errors in midcourse guidance. This ΔV_{id} is not easily expressed analytically, but is a function of range, energy, and perigee; assumed errors σ_R, σ_E, and σ_P; and the entry-corridor size. The method of computation is shown in appendix D.

The dashed curve in figure 12(c) is the cumulative frequency distribution of ΔV_{id} from 10,000 samples, and so should closely approximate the parent distribution. The curve agrees satisfactorily with the points of the 100-sample reference case except at the extreme values, as anticipated. From equation (23), the predicted numbers of exceedances over ΔV_{id} of about 0.047, 0.041, and 0.0367 escape velocity are 0.01, 0.1, and 1 percent, respectively. Predicting from the reference case, a ΔV_{id} of 0.0336 escape velocity should be exceeded 1 percent of the time, with a standard deviation of 1 percent (from ref. 15), while the same ΔV_{id}

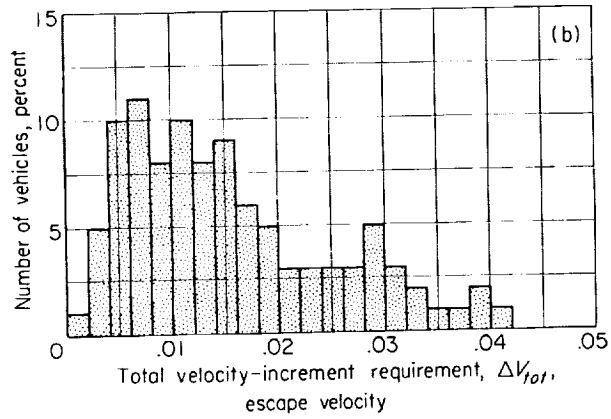

(b) Frequency distribution of total velocity-increment requirements.

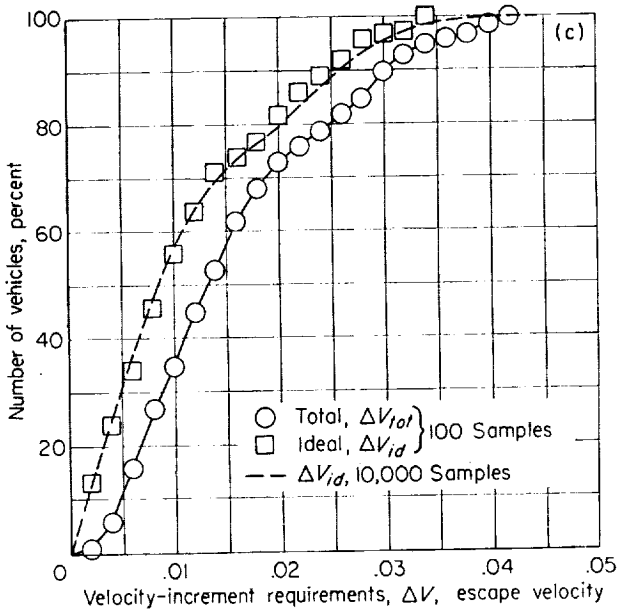

(c) Cumulative frequency distribution of velocity-increment requirements.

FIGURE 12.—Continued. Results of reference case. Assumed values from table II.

from the large sample is exceeded 2 percent of the time; thus, the reference case is in error by 1σ, a typical result.

The poor definition of $\Delta V_{tot,max}$ is largely a result of insufficient resolution in the ΔV required to correct the assumed errors in initial conditions rather than of poor resolution in evaluating the costs due to errors in the approach guidance system.

The ΔV capability that must be supplied to the vehicle, in addition to the $\Delta V_{id,max}$, to attain the desired success probability is defined as

$$\Delta V_{xs} \equiv \Delta V_{tot,max} - \Delta V_{id,max} \tag{25}$$

where ΔV_{xs} is interpreted as the velocity-increment capability requirement chargeable to inaccuracies in the approach guidance system and will be used extensively herein. In other words, ΔV_{xs} is the "excess" ΔV required, because of approach guidance errors and planet terrain uncertainties, over that which an "ideal" system with "ideal" knowledge would require.

It will be demonstrated that the excess velocity-increment requirements are not a strong function of initial perigee errors, and as a result, ΔV_{xs} can be used to evaluate $\Delta V_{tot,max}$ requirements using any given $\Delta V_{id,new}$ evaluated for conditions reasonably close to those used in determining ΔV_{xs}. This procedure, written as

$$\Delta V_{tot,max} = \Delta V_{id,new} + \Delta V_{xs}$$

is used herein to adjust total velocity-increment requirements with accurately determined $\Delta V_{id,new}$. (Computing speed is about 500 times greater than that of the complete approach guidance system.) Naturally, this technique does not aid in assuming initial errors; therefore, $\Delta V_{tot,max}$ remains a strong function of the midcourse guidance system and beyond the scope of this analysis.

The approach guidance system is optimized using ΔV_{xs} as the principal criterion for good performance. Thus, the ΔV requirements are minimized for those samples resulting in maximum total requirements. A distinction is made between the desired "difference of maximums,"

$$\Delta V_{xs} \equiv \Delta V_{tot,max} - \Delta V_{id,max} \tag{26}$$

and the "maximum difference,"

$$\Delta V_{xs} \neq (\Delta V_{tot} - \Delta V_{id})_{max} \tag{27}$$

since in many cases the "maximum difference" exceeds the "difference of maximums," but the "maximum difference" is ignored herein because the total ΔV requirements for the (midcourse+approach) system are not influenced.

From the ranked data used in plotting figure 12(c), the ΔV_{xs} is 0.0067 escape velocity (245 ft/sec) with a probability of exceedance of 1 percent with a standard deviation of 1 percent. From the 10,000-sample evaluation, a $\Delta V_{id,max}$ of 0.0403 escape velocity is exceeded in a predicted 0.1 percent of the time, and the maximum total velocity increment of 0.047 escape velocity (1725 ft/sec) should be exceeded about 1.0 ± 1.0 σ percent of the time in one additional sample.

Frequency distributions of the number and size of individual corrective maneuvers are shown in figures 12(d) and (e). The number of ΔV during the approach varies from 1 to 6, with a mean of between 3 and 4 corrections. The system requirement is considered the capability for 6 corrective maneuvers.

The size of individual ΔV (fig. 12(e)) varies up to 0.038 escape velocity, larger than the largest ΔV_{id} in the 100 samples of the reference case. No correction is made about 11½ times per vehicle, and a small trimming correction up to

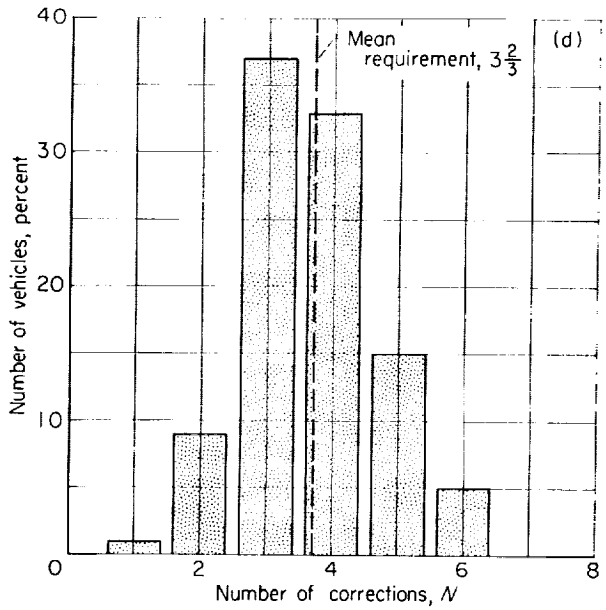

(d) Frequency distribution of number of corrective maneuvers.

FIGURE 12.—Continued. Results of reference case. Assumed values from table II.

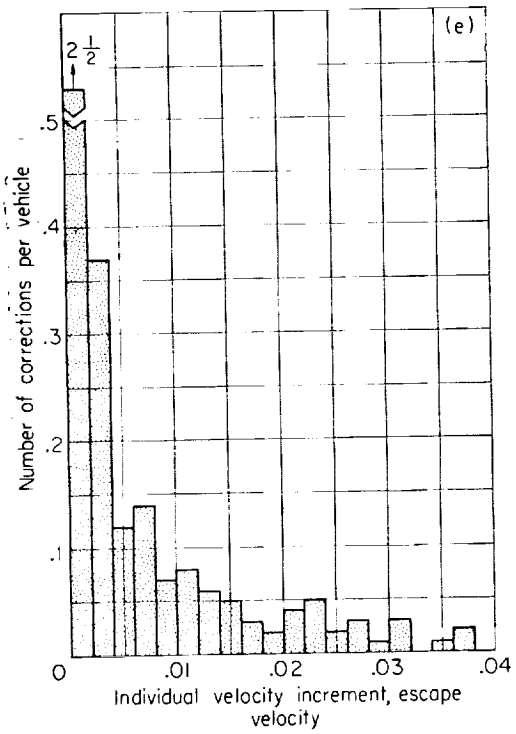

(e) Frequency distribution of individual corrective maneuvers.

FIGURE 12.—Concluded. Results of reference case. Assumed values from table II.

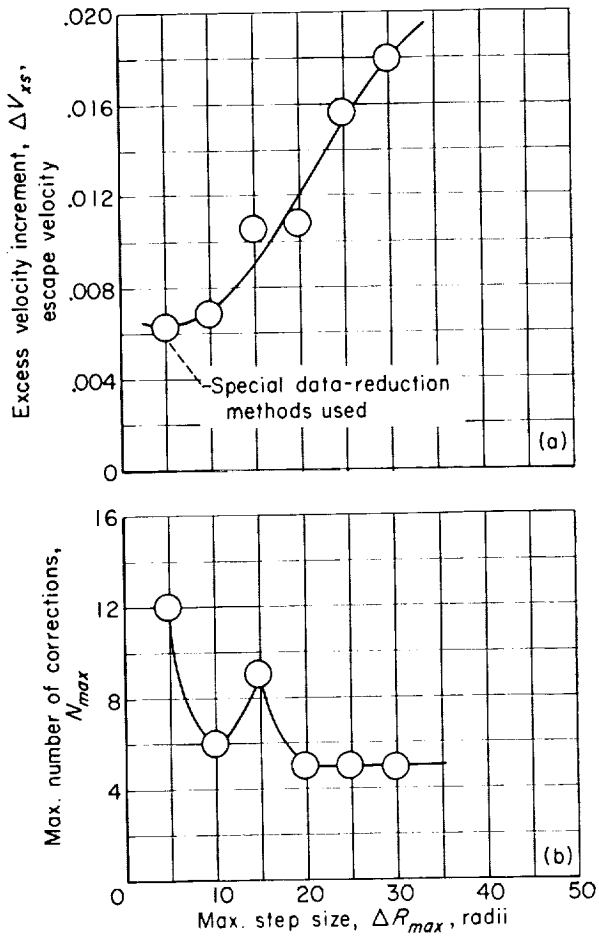

(a) Effect of maximum step size on velocity-increment requirements.

(b) Effect of maximum step size on number of corrective maneuvers.

FIGURE 13.—Effects of guidance logic. Assumed values from table II.

0.002 escape velocity (75 ft/sec) is used an average of 2½ times per vehicle. An average of 1 larger correction is used during each approach, usually at the first point, followed by up to 5 trimming corrections.

The assumed values of the reference case will be used throughout this analysis except where noted otherwise, such as in the next section where the effects of guidance logic on the optimization of performance criteria are discussed.

EFFECTS OF GUIDANCE LOGIC

Other factors affect the performance of the approach guidance system in a fashion similar to the factors considered specifically "guidance logic," particularly the minimum limit on individual velocity-increment size ΔV_{min}. This discussion, nevertheless, will be restricted to analysis of the effects of optimization of arbitrary coefficients that are uniquely the logic of guidance; namely, the factors defining the sampling-rate schedule and the dead-band and damping coefficients.

The primary criteria in optimization have been described as the excess velocity-increment requirement ΔV_{xs} and the maximum number of corrective maneuvers N_{max}. In many respects, however, additional criteria for selecting good performance must be introduced; for example, the sensitivity of the system to larger measurement errors. Even so, the selection of some factors remains arbitrary.

Data-sampling rate.—The logic of determining the size of reading increments is shown in figure 10. The effect of maximum step size ΔR_{max} on the excess velocity-increment requirements is illustrated in figure 13(a) for variation of ΔR_{max} around the reference point at 10 radii (40,000 miles, 35,000 Int. naut. miles). The excess velocity increment ΔV_{xs} decreases with ΔR_{max},

since smaller steps permit correction at longer range, where ΔV requirements to correct a given error in perigee are less (see appendix B). For small initial steps, such as 5 radii, the data-reduction methods are modified to permit rejection of bad data and the acquisition of more data until useful results are obtained. The maximum number of corrective maneuvers during the approach N_{max} is shown as a function of ΔR_{max} in figure 13(b). Decrease of ΔR_{max} from 10 to 5 radii increases N_{max} from 6 to 12 in addition to causing complications in data reduction, though the large N_{max} at 5 or 15 radii could be reduced (partially) by reoptimization. The reference value at $\Delta R_{max}=10$ radii is selected to cause near-optimum ΔV_{xs} without data-reduction complications.

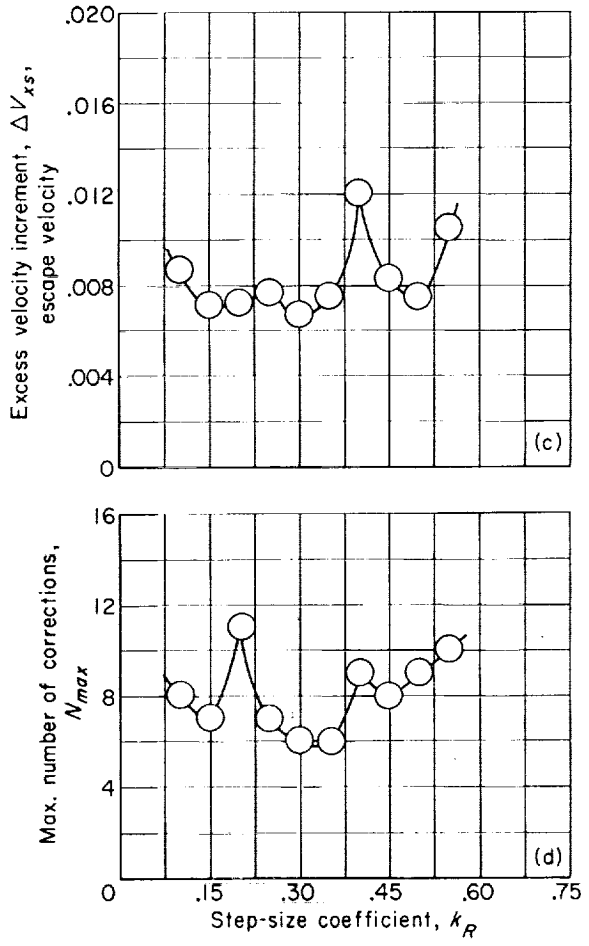

(c) Effect of step-size coefficient on velocity-increment requirements.

(d) Effects of step-size coefficient on number of corrective maneuvers.

FIGURE 13.—Continued. Effects of guidance logic. Assumed values from table II.

The effect of the proportional step-size coefficient k_R on ΔV_{xs} and N_{max} is shown in figures 13(c) and (d). The sampling-rate schedule between the first and last few corrections is assumed proportional to the range of the initial reading of a pair and defined numerically by k_R. Combinations of relatively low ΔV_{xs} and N_{max} are possible over a wide range of k_R, representing increments of from 15 to 50 percent of the range of the first reading. The large scatter is due principally to the mismatch of logic. It is concluded, however, that the sampling rate between the first and last corrections has relatively little effect on system performance and can be used as a variable in optimization of other logic. The reference value of $k_R=0.3$ is selected to allow greater tolerance to component system errors, and, in general, choice of optimum values is not obvious.

The logic of increment size at the cutoff of active guidance prior to entry is defined numerically by the time increments associated with data reduction and corrective maneuvers and is discussed under "Requirements on System Components."

Dead band and damping.—The logic of the final correction prior to entry is considered first. The dead band and damping for the last increment are both alined to the specified corridor size and defined numerically by the coefficient k_m, or "miss coefficient." The purpose of using modified logic (fig. 11) just prior to cutoff is to ensure a high probability of guiding to within the limits $\pm\Delta P_{limit}$. The effect of k_m in controlling the maximum target miss distance ΔP_{max} is shown in figure 13(e). As anticipated, increasing k_m results in increased accuracy at cutoff, with a minimum of $1.5(\sigma)$ required to cause all vehicles to hit the specified entry corridor of ± 0.0025 radius (± 10 miles).

Partly because of the use of k_m in normal logic as well as at cutoff, k_m has some unexpected effects on ΔV_{xs} (fig. 13(f)). For k_m larger than 2.0, the correction at cutoff is increased as k_m is increased, and the total velocity increment due to approach guidance increases from 0.0052 to 0.0108 as k_m varies from 2 to 3. Unexpected, however, is the increase in ΔV_{xs} as k_m is decreased from 2.0. The increase is due to the reduction of required corrections in the increments prior to cutoff and

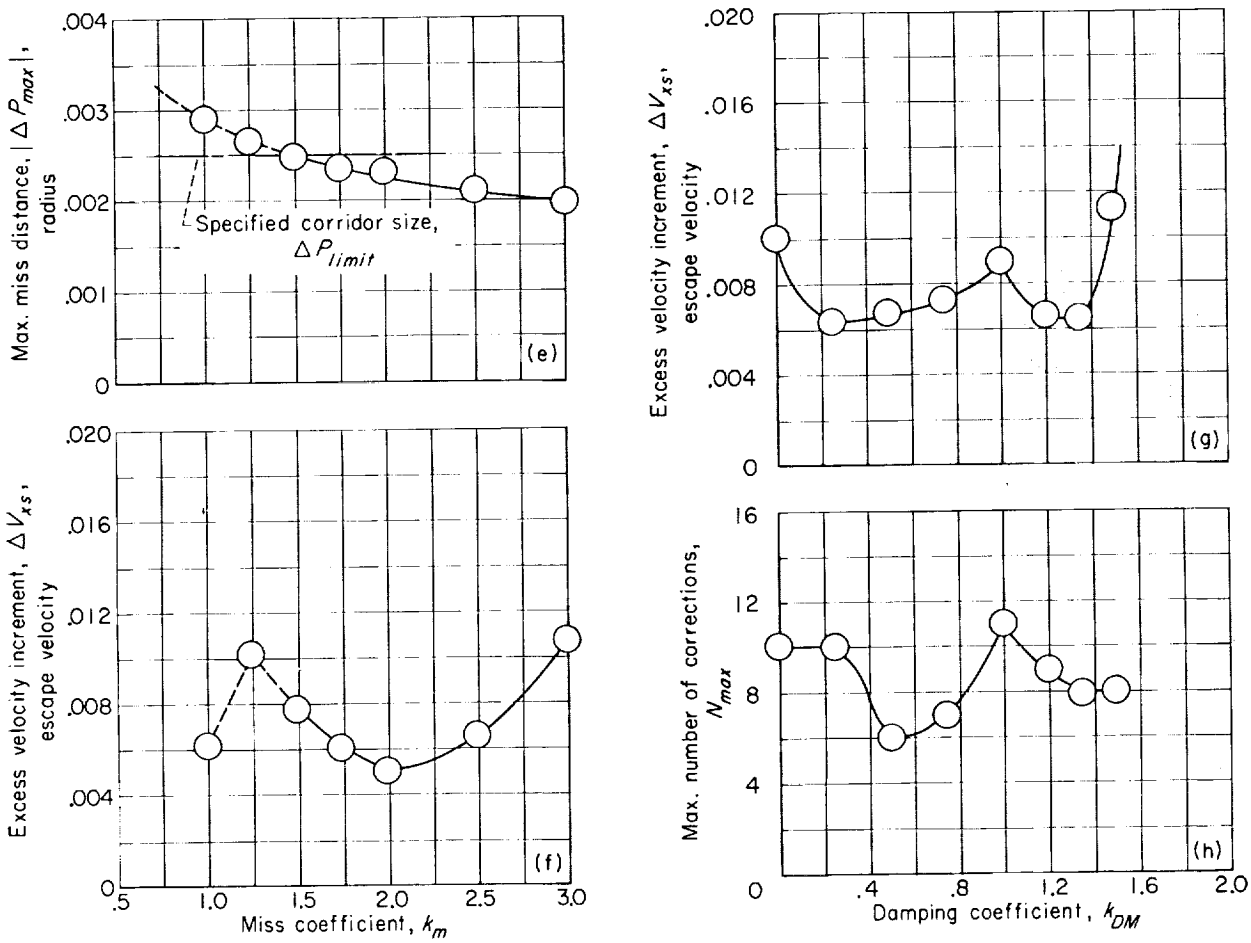

(e) Effect of miss coefficient on maximum target miss distance.

(f) Effect of miss coefficient on velocity-increment requirements.

(g) Effect of damping coefficient on velocity-increment requirements.

(h) Effect of damping coefficient on number of corrective maneuvers.

FIGURE 13.—Continued. Effects of guidance logic. Assumed values from table II.

results in increased ΔV at the final correction, which is larger since range is reduced. No importance is placed on the low ΔV_{xs} at k_m of 1, since the desired accuracy is not obtained with k_m below 1.5; but the trend is typical of the interactions in logic that can occur and results from reduced corrections in both the last few increments and the last increment.

The reference value of k_m is selected as 2.5 to give greater margin in parametric studies, which results in an increase in ΔV_{xs} from 0.0052 for k_m of 2 to 0.0067 escape velocity, a difference of 0.0015 escape velocity (55 ft/sec).

The effects of the dead band in normal logic are insignificant because of the large ΔV_{min} used in the reference case. As a result, but not a general conclusion, the dead band could be omitted from the logic of the reference case, and the effects are not shown.

The effect of varying the damping coefficient k_{DM} on ΔV_{xs} is shown in figure 13(g). The ΔV_{xs} is relatively large at k_{DM} equal to 0, 1, and 1.5 or greater, but two regions of good performance occur, one with "light" damping and the second with "heavy" damping. The two regions of low ΔV_{xs} are typical, have been found over wide ranges of problem definition and guidance-logic optimization, and are due to the tradeoff between rapid correction at longer range with low

damping and reduced overcorrection with high damping.

The smaller of the two minimum values of ΔV_{xs} depends on problem definition; thus, with with larger measurement or initial perigee errors, the more heavily damped system is favored with k_{DM} about 1.35. For smaller errors or to cause the system to be less sensitive to ΔV execution and measurement errors, the damping coefficient of about 0.25 to 0.5 is preferred.

The effect of k_{DM} on the maximum number of corrective maneuvers is shown in figure 13(h). The minimum requirement, 6 corrections, occurs at a damping coefficient of 0.5, influencing a slight compromise in ΔV_{xs} in selecting the reference value. The region of low ΔV_{xs} at $k_{DM}=1.35$ is associated with $N_{max}=8$, and it is not generally possible to reduce N_{max} by reoptimization of other logic while using high damping.

It is concluded that the optimization of guidance logic permits selection of good performance over a wide range of optimization criteria, with a significant choice of parameters available to allow near-optimum performance for those criteria not specifically desired. Thus, when particular system requirements and tradeoff costs are available, the logic (including herein the sampling-rate schedule k_R and ΔR_{max}, and the dead bands and damping k_m, k_{DB}, and k_{DM}) can be optimized to yield the desired combination of ΔV_{xs}, N_{max}, sensitivity to errors, computing problems, and target accuracy.

REQUIREMENTS ON SYSTEM COMPONENTS

As an indication of the interaction between component systems of the guidance scheme and as an evaluation of requirements on component system performance, the sensitivity of guidance-system performance to the capabilities of associated components is analyzed parametrically. Of particular interest are the sizing of propulsion devices, accuracy requirements for corrective maneuvers, and the factors associated with data-reduction speed.

Sizing of propulsion devices.—Relations for corrective maneuvers (appendix B) were derived assuming that trajectory modification results from essentially impulsive velocity increments followed by periods of coasting flight to account for the time of firing finite-thrust engines. The effects of changing vehicle acceleration capability A_v, or engine size, are thus interpreted from the effects of changing the duration of coasting after an impulsive correction. The excess velocity increment ΔV_{xs} is shown as a function of A_v in figure 14(a). Decreasing A_v from the reference value of 0.1 (6.4 ft/sec^2) causes only slight increases in ΔV_{xs}. Because of the cutoff criteria, the range of the final readings must be increased until, with A_v about 0.01 (0.6 ft/sec^2), the accuracy of guidance is reduced. The variation of N_{max} as A_v is decreased (fig. 14(b)) is also insignificant except for the mismatched point at 0.03.

Some caution should be exercised in interpreting the limiting value of 0.01 (0.6 ft/sec^2), or a thrust-weight ratio of 0.02, because of the optimistic

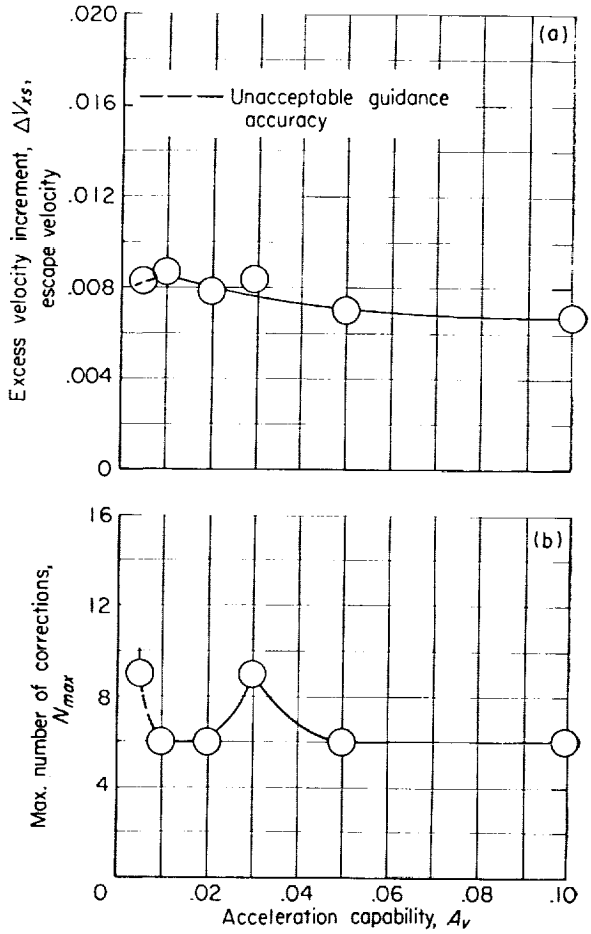

(a) Effect of acceleration capability on velocity-increment requirements.

(b) Effect of acceleration capability on number of corrective maneuvers.

FIGURE 14.—Evaluation of control engine requirements. Assumed values from table II.

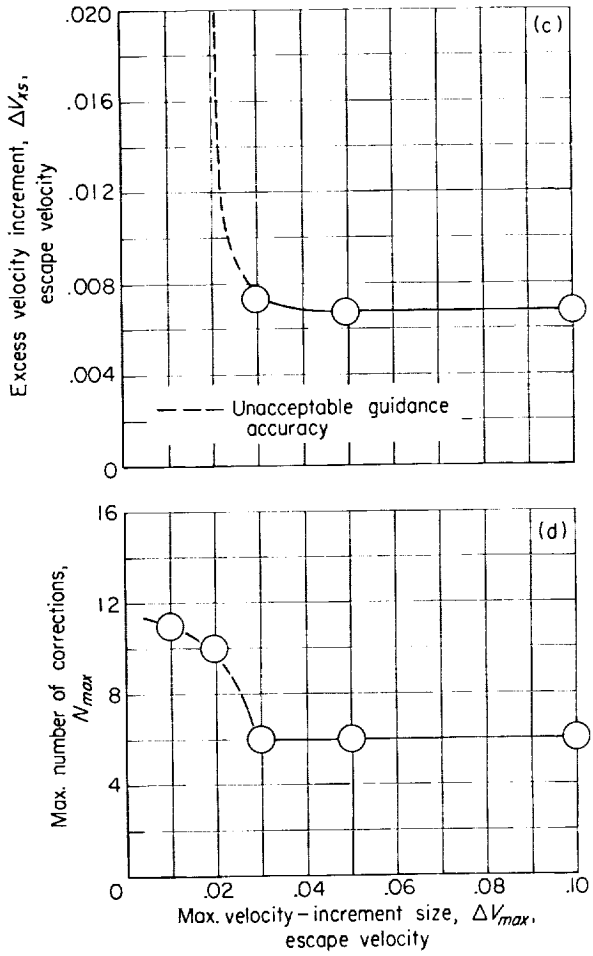

(c) Effect of limiting maximum individual ΔV on velocity-increment requirements.

(d) Effect of limiting maximum individual ΔV on number of corrective maneuvers.

FIGURE 14.—Continued. Evaluation of control engine requirements. Assumed values from table II.

nature of the assumptions. On the other hand, there is no limit on the maximum acceleration capability; but problems of accuracy in measuring ΔV and attitude control make the use of large control engines impractical.

Limits on the maximum velocity increment for any single correction ΔV_{max} are considered primarily to determine the problems associated with the use of uncooled propulsion devices. For fixed acceleration capability, ΔV_{max} becomes a limit of firing time. The ΔV_{max} assumed for the reference case, 0.1 escape velocity (3670 ft/sec), is not a limit, since the maximum demand is 0.04 escape velocity. The effect of reduced ΔV_{max} on ΔV_{xs} is shown in figure 14(c); and, as anticipated, no effect is indicated for ΔV_{max} of 0.05 escape velocity (1835 ft/sec), since the limit is still larger than the demand. With ΔV_{max} of 0.03 escape velocity, there is some delay in making initial corrections, and ΔV_{xs} increases slightly; but for smaller ΔV_{max} the delays in executing corrective maneuvers become important and ΔV_{xs} more than triples; in addition, the target of ± 0.0025 radii (± 10 miles) is missed. The effect on N_{max} (fig. 14(d)) is similar, in that for ΔV_{max} greater than 0.03 escape velocity there is no effect. For ΔV_{max} less than 0.03 escape velocity, the large initial ΔV are replaced by several smaller corrections, and N_{max} increases.

It is concluded that propulsion devices must be capable of velocity increments for a single correction of about 0.03 escape velocity (1100 ft/sec) or about three-fourths of the maximum ideal velocity-increment requirement of the reference case. The assumptions concerning impulsive trajectory modification with finite coasting periods do not materially influence this result, since the effects are noted at long range where time increments along the trajectory are relatively long. The data-sampling rate in guidance logic (ΔR_{max} and k_R) and the assumed initial trajectory and errors, however, do influence ΔV_{max} limitations significantly. Thus, the guidance system will be more sensitive to limitation of individual corrections if fewer correction points are available (i.e. larger ΔR_{max} and k_R). As the $\Delta V_{id,max}$ is varied with the assumptions of initial trajectory and errors, such as E and σ_P, it is anticipated that the limit ΔV_{max} will remain of the order $(\frac{3}{4})\Delta V_{id,max}$.

Limitation of the minimum allowable velocity increment for a single corrective maneuver ΔV_{min} may be desirable to reduce the startup and shutdown losses for the majority of corrections. The limit does not apply to the final ΔV prior to cutoff (fig. 11), since guidance accuracy would be considerably reduced if the final trimming correction were omitted. In addition, ΔV_{min} has been indicated previously to be useful in reducing the number of corrections used during the approach. The effect of varying ΔV_{min} from the reference value of 0.001 escape velocity is shown in figures 14(e) and (f). Reducing ΔV_{min} to 0.0005 or 0.0002 escape velocity causes N_{max} to increase to 11 or 14 of a possible 15 or 16 corrections. Since ΔV_{min} acts essentially as a dead band in guidance

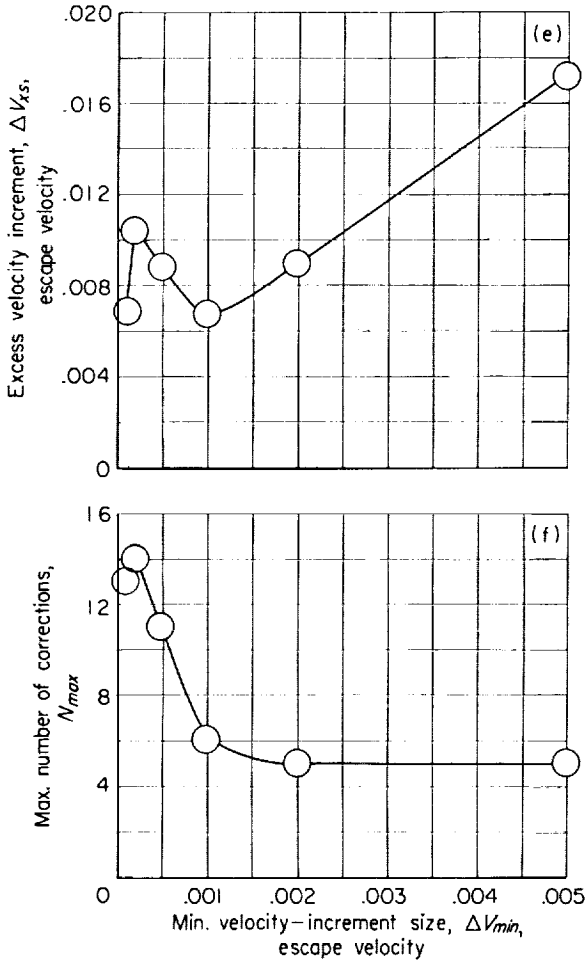

(e) Effect of limiting minimum individual ΔV on velocity-increment requirements.

(f) Effect of limiting minimum individual ΔV on number of corrective maneuvers.

FIGURE 14.—Concluded. Evaluation of control engine requirements. Assumed values from table II.

logic, ΔV_{xs} increases as ΔV_{min} decreases, but decreases again at 0.0001 escape velocity as a good combination of logic is established, much in the manner of figure 13(g). Reoptimization of logic may permit ΔV_{xs} of about the reference value for ΔV_{min} between 0.0001 and 0.001 escape velocity, but the attempts at reoptimization indicate that N_{max} cannot be effectively reduced using dead bands and damping alone.

Increasing the minimum allowable velocity increment above 0.001 escape velocity reduces the number of corrective maneuvers from 6 to 5 but results in an essentially overrestrained system requiring larger ΔV_{xs}, which increases to 0.017 escape velocity (625 ft/sec) for ΔV_{min} of 0.005 escape velocity as shown, then leads to complete failure in guidance accuracy for ΔV_{min} between 0.005 and 0.01 escape velocity (not shown).

Accuracy requirements for corrective maneuvers.—The purpose of distinguishing errors in the control of ΔV from errors in the knowledge of the resultant increment after execution is discussed in deriving the relations used in the analysis (appendix B). Briefly, again, it is desired to separate the requirements for dynamic control from the accuracy requirement of ΔV measurement.

The performance of the guidance system is expected to be insensitive to errors in controlling the

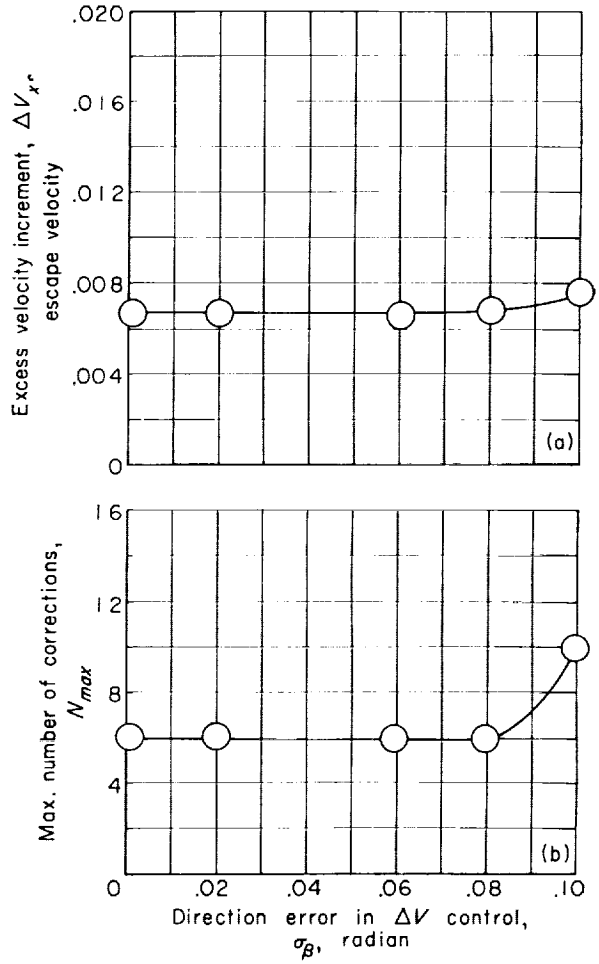

(a) Effect of errors in direction of ΔV control on velocity-increment requirements.

(b) Effect of errors in direction of ΔV control on number of corrective maneuvers.

FIGURE 15.—Accuracy requirements for trajectory modification. Assumed values from table II.

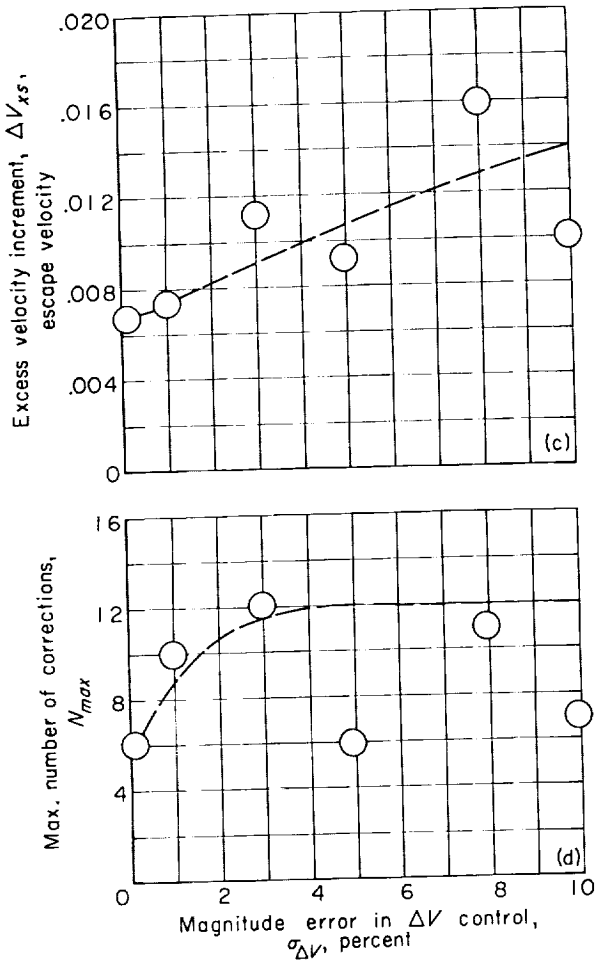

(c) Effect of errors in magnitude of ΔV control on velocity-increment requirements.

(d) Effect of errors in magnitude of ΔV control on number of corrective maneuvers.

FIGURE 15.—Continued. Accuracy requirements for trajectory modification. Assumed values from table II.

relatively small corrective maneuvers during the approach, simply because control errors in one ΔV are corrected in a later ΔV. As the cutoff range is approached and accuracy becomes critical, the error coefficients decrease and ΔV is generally small.

The effect of errors in controlling the direction of ΔV on ΔV_{xs} and N_{max} is shown in figures 15(a) and (b), where the standard deviation of β_{meas} is varied from 0.0004 radian (80-sec arc) to 0.1 radian (6°). There is no effect on the velocity-increment requirement or the maximum number of corrective maneuvers for errors as large as 0.08 radian rms (4.5°). For larger σ_β, N_{max} increases to 10, but ΔV_{xs} increases only slightly.

The effects of magnitude errors $\sigma_{\Delta V}$ are shown in figures 15(c) and (d) for $\sigma_{\Delta V}$ larger than the reference value of 0.1 percent rms. Primarily because of the low probabilities of several successive large control errors, the maximum values are not well defined, and a clear trend of ΔV_{xs} and N_{max} variation with $\sigma_{\Delta V}$ is obscure. The important result, however, is that the guidance system will perform at all with errors as large as 10 percent rms.

The effect on ΔV_{xs} and N_{max} of errors in measuring the direction β_{meas}, $\sigma_{\delta\beta}$, simultaneously with

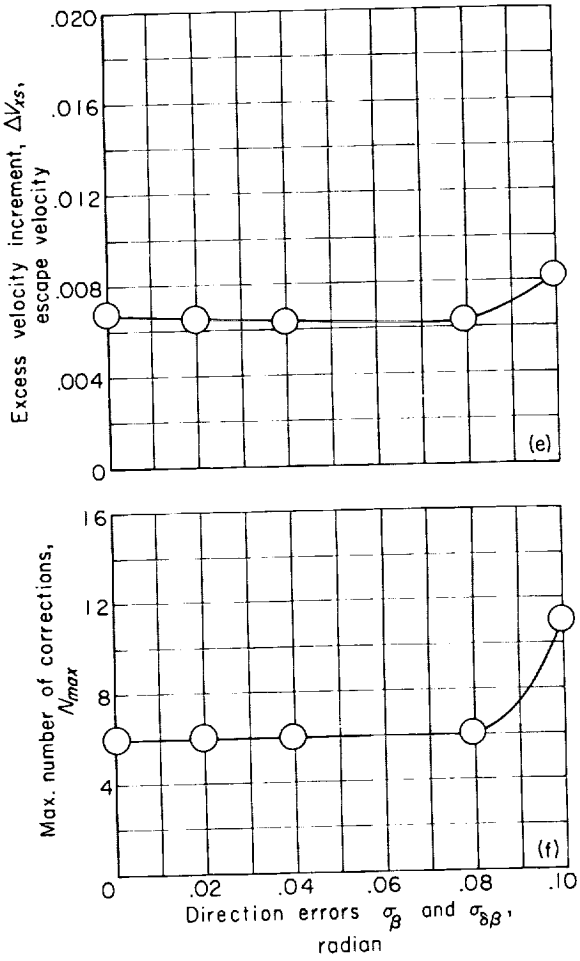

(e) Effect of errors in controlling and measuring direction of ΔV on velocity-increment requirements.

(f) Effect of errors in controlling and measuring direction of ΔV on number of corrective maneuvers.

FIGURE 15.—Continued. Accuracy requirements for trajectory modification. Assumed values from table II.

errors in controlling the direction σ_β is shown in figures 15(e) and (f). The trend is approximately that of figures 15(a) and (b) for control errors alone, indicating that the loss of trajectory knowledge due to $\sigma_{\delta\beta}$ is negligible in effect on guidance-system performance.

The magnitude errors, $\sigma_{\Delta V}$ and $\sigma_{\delta\Delta V}$, however, have more effect on ΔV_{xs} and N_{max}, as shown in figures 15(g) and (h). Again, the details of the trends are obscure, but guidance to the ± 0.0025-radius (± 10-mile) corridor is possible with independent errors $\sigma_{\Delta V}$ and $\sigma_{\delta\Delta V}$ both as large as 10 percent rms, but at a cost in ΔV_{xs} of double to triple the cost with 0.1-percent errors.

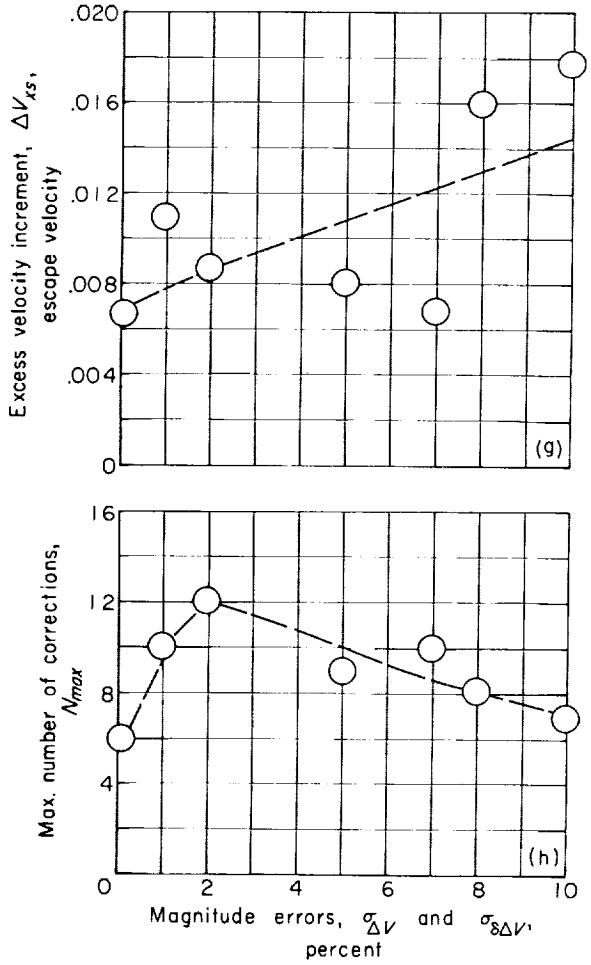

(g) Effect of errors in controlling and measuring magnitude of ΔV on velocity-increment requirements.

(h) Effect of errors in controlling and measuring magnitude of ΔV on number of corrective maneuvers.

FIGURE 15.—Concluded. Accuracy requirements for trajectory modification. Assumed values from table II.

Limiting values of the four errors associated with corrective maneuvers, namely σ_β and $\sigma_{\Delta V}$ in execution, and $\sigma_{\delta\beta}$ and $\sigma_{\delta\Delta V}$ in measurement, have not been evaluated, since accuracy of the order 10 percent in magnitude and 6° in direction should be easily obtained by present standards (ref. 8 or 17). The large tolerance of the system could then be applied to other problem areas.

It cannot be overemphasized that these large tolerances to errors in corrective maneuvers are due, for the most part, to the use of multiple-correction guidance. If a fixed number of corrections (say, 3) were used, the accuracy requirements would be much more exacting.

Computation-speed requirements.—Time increments along the trajectory, such as the minimum reading increment $\Delta\tau_{min}$, and the time increment for data reduction, orienting the vehicle to execute a correction, and reorienting the vehicle to commence data acquisition, are of interest, since component system requirements can be estimated from the sensitivity of the guidance system to these delays.

The minimum reading increment size $\Delta\tau_{min}$ has two functions in guidance logic: (1) to establish the time, or range, of the initiation of cutoff logic, and (2) to prevent very small reading increments where accuracy could be unsatisfactory. Increasing $\Delta\tau_{min}$ from the reference value of 0.5 (about 5 min for Earth, Mars, or Venus) causes a small increase in ΔV_{xs}, since the second-last ΔV is made at longer range where σ_P is larger. Therefore, the last correction requires larger ΔP and thus larger ΔV, since the cost increases as range decreases.

The times required to reduce data, reorient the vehicle, and so forth, associated with the use of corrective maneuvers and lumped into one term called "reorientation time" $\Delta\tau_{stop}$, affect directly the range and thus the accuracy of the last reading increment. Thus, accuracy is reduced as $\Delta\tau_{stop}$ increases, but ΔV_{xs} is also reduced. For $\Delta\tau_{stop}$ of the order 1.5 (15 min) the second-last readings are also affected significantly and ΔV_{xs} then increases. For the reference case $\Delta\tau_{stop}$ is assumed as 0.5 (5 min) as a compromise between low ΔV_{xs} and a reasonable accuracy margin at the ± 0.0025-radius corridor.

The limitations on data-reduction time can be inferred by assuming the attitude-control-system response fast relative to minutes and varying

$\Delta\tau_{min}$ and $\Delta\tau_{stop}$ together. Since data must be reduced before a correction is determined whether it is executed or not, $\Delta\tau_{min}$ and $\Delta\tau_{stop}$ both must be at least the time required by the computation. Effects on ΔV_{xs} and N_{max} are shown in figure 16, where the number of corrections and the velocity increments increase with data-reduction time, and with times of the order 2.5 (25 min) resulting in acceptable guidance accuracy. As $\Delta\tau_{min}$ and $\Delta\tau_{stop}$ are increased to 3.0 (½ hr), target accuracy is not attained, however.

The data-reduction time limitation of about 25 minutes for either vehicle-contained or ground-based computers for approaches to entry at Earth does not present a difficult problem. (The simulated computation, though simplified, requires about ¼ sec.) The use of Earth-based computers for approaches to entry at Mars or Venus may be difficult because of relatively long transport times (from 6 to 30 min for two-way communication) and the high power requirements for rapid transmission of data (ref. 8).

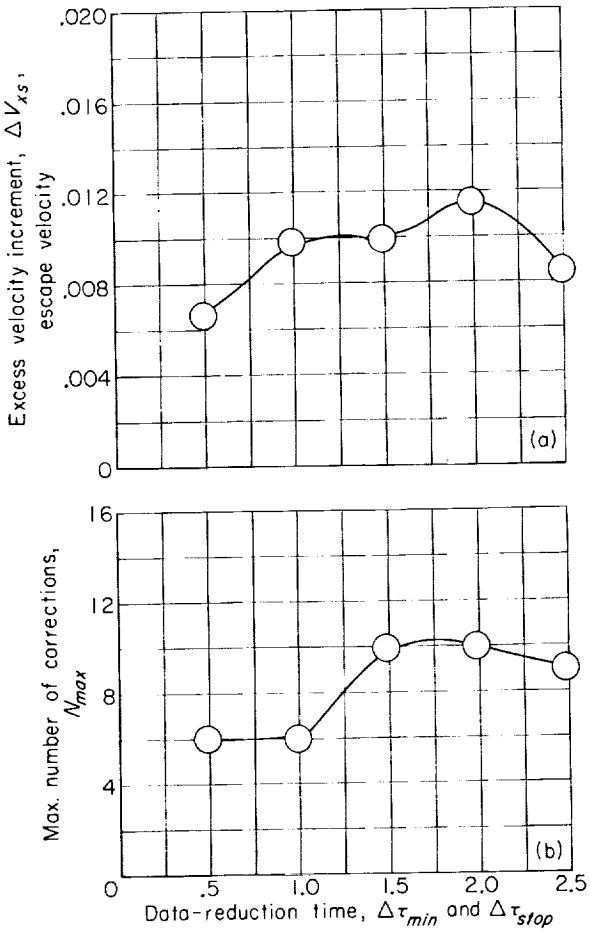

(a) Effect of data-reduction time on velocity-increment requirements.

(b) Effect of data-reduction time on number of corrective maneuvers.

FIGURE 16.—Computation-speed requirements. Assumed values from table II.

Great caution should be exercised in interpreting this limitation, since the sensitivity of the guidance system varies considerably with problem definition.

It should be noted first that $\Delta\tau_{min}$ and $\Delta\tau_{stop}$, or A_v, have significant effects only at short range near entry and therefore are not influenced by problems of assuming initial errors in trajectory. The data-reduction time ($\Delta\tau_{min}$ and $\Delta\tau_{stop}$) and the engine size are competing for the same time and thus influence each other.

Mission energy, entry-corridor size, planet surface uncertainties, and basic measurement accuracy all have a major influence, however. Therefore, from the specified corridor size, the range at which sufficient accuracy can be attained is determined from the instrument errors and the surface uncertainty. From the energy, then, the time to entry can be determined and is the time available to reduce data as well as to execute the correction. For example, allowable data-reduction time varies roughly as the inverse of entry velocity. For an entry at 60,000 feet per second, the allowable time is reduced from 25 to 16 minutes.

EFFECTS OF ERROR, TARGET, AND TRAJECTORY ASSUMPTIONS

The discussion of guidance logic and requirements for system components has centered on the assumed measurement errors, trajectory errors, and problem definition of the reference case as summarized in table II. The effects of these assumptions on the guidance system are considered in the following sections.

Results are presented in parametric form to illustrate the effects of individual assumptions; in general, trends are presented without reoptimization of guidance logic. Though reoptimization has been performed in many cases, and because improvement in performance over that of the reference logic is relatively small, the results will illustrate the logic of the reference case where possible. However, since the maximum number of corrective maneuvers during the approach to

entry is sensitive to the guidance logic, results without reoptimization are of little interest and will not be illustrated. As shown in the discussion of guidance logic, the number of corrections can be minimized at small cost in total velocity-increment requirements.

Because the assumption of initial errors in trajectory, namely perigee errors, causes the greatest uncertainty in ΔV costs of approach guidance, it is considered first. It is not the purpose here to predict the performance of midcourse guidance systems; on the contrary, it is desired to illustrate the costs in approach guidance resulting from residual errors in midcourse guidance. Thus, the costs of inaccuracies in approach guidance systems can be assessed, and some tradeoff considerations reflecting requirements for midcourse systems can be implied.

Second, the effects of entry-corridor limitations on the cost of guidance are presented to show some tradeoff considerations with the entry vehicle requirements. In this section a choice of "representative" corridor-size specification is described for use in the final section, where the effects of mission energy and basic measurement accuracy are illustrated.

Effects of initial errors in trajectory.—The initial data acquisition of the approach guidance system is assumed to occur at a range R along a trajectory given by energy E and perigee P. Errors are assumed in the initial values of the three parameters.

The initial range is assumed to be 100 radii (400,000 miles, 350,000 Int. naut. miles) with a standard deviation of 10 radii (40,000 miles, 35,000 Int. naut. miles). Since it is desired to avoid specifications that by implication require the vehicle to monitor range, large errors are anticipated. The specific value of 10 radii, however, is used to avoid unique sampling-rate schedules and causes the maximum ideal ΔV requirements to increase about 15 percent because of the reduced range of the first correction. With a single measurement of 0.0002 radian rms (40-sec arc), the initial range error would be about 1 radius rms if monitoring were assumed.

The assumed initial error in energy σ_E is 0.01 (units of escape velocity squared) and has little effect on results.

Details of the generation of initial perigee errors are shown in appendix D. Results are presented as a function of the standard deviation of the linear components used to generate the bivariate distribution. The ΔV costs of correcting given errors in perigee are shown in appendix B, and the maximum ΔV is indicated to occur when the direction of rotation around the target planet must be changed. The cumulative frequency distribution for errors assumed in the reference case is shown in figure 12(c).

The ΔV costs of guidance presented herein are interpreted from the worst probable cases; thus, only the combinations of initial errors in perigee, energy, and range that cause the maximum ΔV for correction reflect in system requirements. It would be feasible to define the maximum errors in initial conditions rather than the distributions if errors from which maximum ΔV costs would result could be determined. Knowledge of distributions, however, is needed to define the frequency of occurrence of "worst" probable cases. In addition, other causes of mission failure such as too many corrections, breakdown in computation methods, or missing the entry corridor are not correlated with maximum ΔV requirements; and distributed errors are necessary in system evaluation.

The ideal velocity-increment requirements resulting from 10,000 samples and the assumptions of the reference case are shown in figure 17 as a function of σ_P. The curves are the maximum, tenth, and hundredth ranked ΔV and should be exceeded 0.01, 0.1, and 1 percent of the time in one additional trial, respectively. The probability of not exceeding the curves is then 99.99, 99.9, and 99 percent, respectively. The rapid increase in ΔV_{id} with σ_P in the range of σ_P from 0.3 to 0.7 radius is again due to the nonlinearities of the parameter P and the specification of a given direction of rotation. The ΔV_{id} varies from 0.001 to 0.15 escape velocity (37 to 5500 ft/sec) for the range from 0.1 to 10 radii (400 to 40,000 miles, 350 to 35,000 Int. naut. miles) in the standard deviation of the linear distribution used to generate the bivariate distribution of perigee errors.

The ΔV_{id} required during the approach phase because of residual errors in midcourse guidance can be evaluated easily for any given maximum ΔP or, with a little more effort, from any given distribution of trajectory errors, the results shown in figure 17 being just one example.

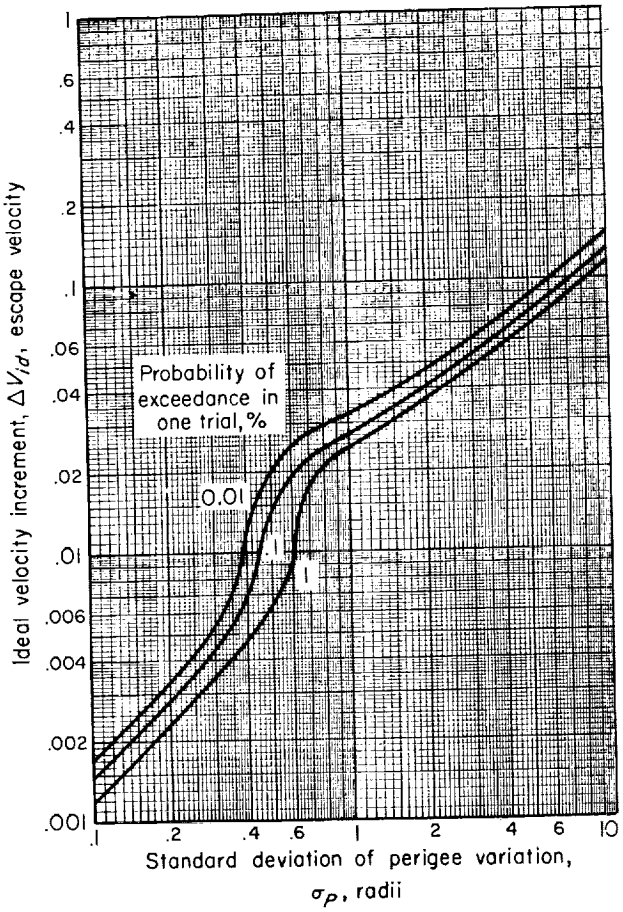

FIGURE 17.—Ideal velocity-increment requirements. Assumed values from table II.

The additional ΔV required to execute the corrections due to errors in the approach guidance system is shown in figure 18, again as a logarithmic function of σ_P. The excess velocity increment ΔV_{xs} varies from 0.005 to 0.0115 escape velocity (185 to 420 ft/sec) as σ_P varies from 0.1 to 5 radii. For the same range of σ_P, ΔV_{id} varied from 0.001 to 0.08, or 80:1 relative to about 2:1 change in ΔV_{xs}. Roughly, then, the ΔV cost due to the approach guidance system remains almost constant as σ_P is varied, with the result that the total velocity-increment cost of approach guidance can be predicted readily for given ideal ΔV requirements.

In greater detail, ΔV_{xs} in figure 18 increases with σ_P for σ_P greater than 1 because of the greater errors in perigee determination for large P (fig. 7). For σ_P less than 1, ΔV_{id} is smaller; therefore, ΔV_{xs} is roughly the maximum of the entire family,

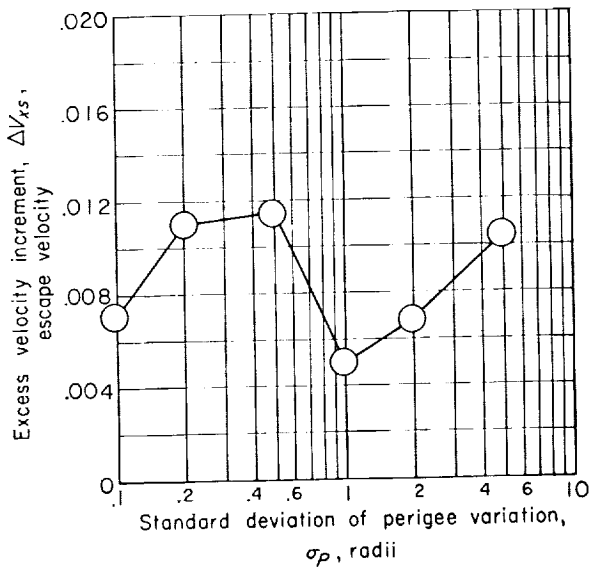

FIGURE 18.—Effects of initial trajectory errors on excess velocity-increment requirements. Assumed values from table II.

not the maximum associated with large ΔV_{id} as for larger σ_P where optimization was performed.

Effects of entry-corridor size.—The target of guidance of the reference case and the previous discussion is assumed to be an entry corridor around the nominal target perigee P_{tar}=1 radius of $\pm$0.0025 radius ($\pm$10 miles approaching Earth). The effect of varying the target miss distance allowable ΔP_{limit} is shown in figure 19. Reducing

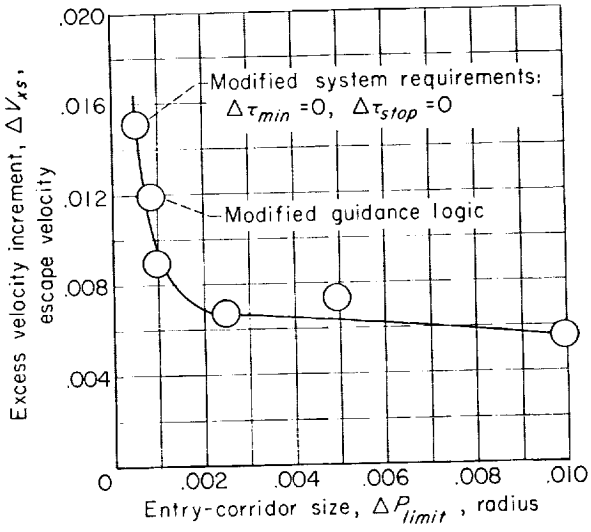

FIGURE 19.—Effect of entry-corridor size. Assumed values from table II.

ΔP_{limit} from the reference value of 0.0025 to 0.001 radius results in an increase in ΔV_{xs} of about 0.002 escape velocity (75 ft/sec). (In computation, this result is obtained by specifying $\Delta P_{limit}=0$ and using the maximum miss distance as the minimum corridor obtainable.) A minimum miss distance of 0.001 radius (4 miles, 3.5 Int. naut. miles) is possible with the guidance logic of the reference case; but, by modifying the logic ($k_{DB}=1.0$, $k_{DM}=1.0$), a corridor of 0.00086 radius is attained at an increase in ΔV_{xs} of about 0.003 escape velocity (110 ft/sec). Even smaller target corridors can be used if the requirements on the performance of the data-reduction computation system are increased; thus, by assuming an essentially zero data-reduction time, a corridor of 0.00055 radius (±2.2 miles, 1.9 Int. naut. miles) is obtained using ΔV_{xs} of 0.015 escape velocity, more than twice the reference value. Smaller targets are not anticipated with the assumed planet uncertainty of 0.0002 radius.

The excess velocity increment ΔV_{xs} decreases only slightly as corridor size increases above 0.0025 radius, since the system can be optimized with little regard for accuracy at the reference value. The ideal velocity-increment requirement also will change only slightly, since ΔP_{limit} is insignificant with respect to initial errors in trajectory.

The minimum corridor attainable with guidance logic optimized to reduce ΔV_{xs} is considered a representative compromise in accuracy and ΔV cost. The value of $\Delta V_{xs}=0.0088$ escape velocity with ΔP_{limit} of 0.001 radius is used in the next section, where the effects of energy level and instrument accuracy are estimated.

Effects of energy and instrument accuracy.—The effects of mission energy level, or hyperbolic velocity, and basic instrument accuracy on the capabilities of the guidance system are illustrated in figure 20, where the total velocity-increment requirements are shown as a function of the minimum efficient corridor size, as described in the previous section (fig. 19). Lines of constant energy are shown at 0.2, 1, and 2 (hyperbolic velocity of 16,400, 36,700, and 52,000 ft/sec or entry velocity of 40,400, 52,000, and 63,500 ft/sec, respectively). Dashed lines of constant instrument accuracy are shown for σ_{meas} of 0.0001 to 0.0006 radian (20-sec arc to 2-min arc, rms), and control of the direction (and measurement of the direction)

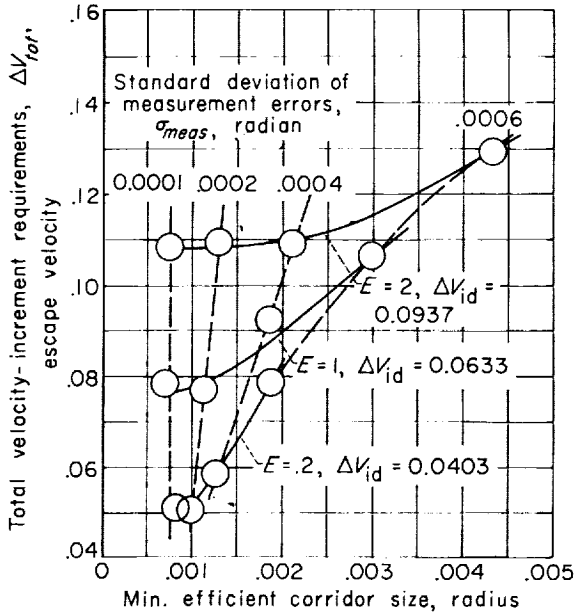

FIGURE 20.—Effects of energy and measurement accuracy on total velocity-increment requirements and target accuracy. (σ_β and $\sigma_{\delta\beta}$ equal twice σ_{meas}; $\Delta R_{max}=15$ radii for $\sigma_{meas}=0.0004$ and 0.0006; ΔV_{last} varied as necessary; other assumed values from table II.)

of ΔV is twice the basic measurement error, but timing errors are fixed at the reference value of 0.01 percent.

It is necessary to increase the estimated size of the last correction ΔV_{last} to prevent attempted firing of control devices in the atmosphere in some cases. Also, the initial reading increment size ΔR_{max} is increased from 10 to 15 radii for the larger measurement errors to reduce the number of special calculations. In other respects, the logic is that of the reference case with ΔP_{limit} set to zero. Data have been adjusted using the 99.9-percent curve of figure 17; therefore, the probability of exceeding the ΔV_{tot} shown is about 1 percent.

The corridor attainable with guidance logic optimized to minimize ΔV_{tot} increases more with energy than anticipated from the standard deviation of trajectory determination (fig. 8), since the times along the trajectory are reduced while the times required for data reduction and the execution of corrective maneuvers remain fixed or increase. Accuracy is still determined almost entirely in the last increment; and R_{cut} is increased, since larger ΔV must be obtained with a fixed acceleration capability A_s in addition to the increases due to data-reduction time.

The ΔV_{xs} increases with energy level (not shown) from roughly 0.009 to 0.014 or 0.025 escape velocity for E_i increases from 0.2 to 1 or 2, in addition to the increases in ΔV_{id} from 0.040 to 0.063 or 0.094 escape velocity. For measurement errors less than 0.0002 radian rms (40-sec arc), then, the ΔV_{tot} increases from about 0.05 (E=0.2) to 0.08 (E=1) or 0.11 (E=2) escape velocity.

As instrument accuracy is increased from the reference value (40-sec arc), the entry corridor is reduced. The effect of uncertainties in planet terrain prevents further reduction, however; and, furthermore, larger $\sigma_{R,o}$ than assumed herein would increase the target obtainable regardless of the instrument accuracy. As instrument errors are increased, the corridor size increases, particularly at high energy where times along the trajectory are reduced. Thus, the ΔV of the last correction increases to about 0.02 escape velocity (730 ft/sec). The ΔV_{tot} also increases, but it should be noted that instruments with an accuracy requirement of 2-minute-arc standard deviation are less precise than current expectations.

Figure 20 is interpreted as a rough demonstration of the ability of the guidance system to control vehicles to entry corridors of the order ± 0.0035 radius (± 14 miles, 12 Int. naut. miles) from approach velocities up to 63,500 feet per second in spite of instrument capabilities of the order 0.0006 radian (2-min arc) rms. The total ΔV requirements increase, naturally, for larger measurement errors and higher velocities, but the total cost is still uncertain because of the residual errors in midcourse guidance. The ΔV chargeable to approach guidance is of the order 0.04 escape velocity (1470 ft/sec) for the worst case shown, where the total requirement is 0.13 escape velocity (4770 ft/sec).

These ΔV requirements may be compared with the retrothrust for decelerating the vehicle without atmospheric braking, about 30,000 feet per second to cause an elliptical orbit and more than 60,000 feet per second for a low-velocity landing or entry.

CONCLUDING REMARKS

The optical guidance system is considered capable of controlling vehicles to entry corridors of the order ± 5 miles (10 miles high) if instruments accurate to about 40-second-arc rms are used, or to about ± 15 miles using 2-minute-arc instruments. Improved instrumentation will not result in smaller entry corridors than about the maximum uncertainty in planet terrain, assumed to be 0.8 mile rms for evaluation purposes and preventing high success probabilities for corridors less than ± 2 to 2.5 miles. Increased mission energy, or velocity, tends to increase the minimum corridor; for example, increasing the hyperbolic velocity from 16,000 to 50,000 feet per second roughly doubles the size of the smallest corridor that can be attained efficiently. The corridor sizes are generally well within the aerodynamic capability of lifting entry vehicles (refs. 1 and 18 to 21).

Relaxation of entry-corridor-size specifications above the values indicated has only minor effects on the total velocity-increment requirements. Some reduction in system component requirements can be obtained, however.

Velocity-increment requirements due to inaccuracies in the approach guidance system vary from about 200 to 1500 feet per second over the entry-velocity range from 40,000 to 63,500 feet per second and instrument accuracy range from 40-second- to 2-minute-arc rms. To this velocity-increment requirement must be added the cost of correcting residual errors in midcourse guidance, assumed herein, but contributing velocity increments as high as 5000 feet per second or possibly more, if midcourse guidance is not used (ref. 22). Unpublished analyses of midcourse guidance systems with component accuracies comparable with those herein have been made by the authors. Results indicate that an ideal velocity increment of 150 to 500 feet per second may be required to correct residual errors from such a midcourse system. Even smaller requirements may result if a system such as that described in reference 8 is considered.

For the purpose of rough estimation, total velocity-increment requirements, with systems of accuracy level 40-second-arc rms, can be considered of the order 1 percent of the entry velocity.

The ability of the system to guide efficiently using instrumentation of modest capability is principally the result of allowing multiple corrections to reduce trajectory errors at long range where velocity-increment costs are lower. The maximum number of corrections required can be reduced to, say, 6 through the optimization of guidance logic with little additional cost in total velocity-increment requirements. *The develop-*

ment of propulsion devices capable of multiple firing with high reliability is considered necessary.

Engines may be as small as needed to accelerate the vehicle at a rate of $\frac{2}{3}$ foot per second squared, though larger acceleration capability results in increased tolerance to other system component errors. Minimum engine size increases with instrument errors, mission velocity, and data-reduction time requirements. Corrective maneuvers are executed perpendicular to the direction to the planet and so will vary in direction with respect to vehicle velocity.

The individual velocity increment, which varies up to the maximum requirement for correcting assumed initial errors in trajectory, is interpreted herein as the change in firing time for fixed acceleration-rate devices. Attempts to reduce the maximum individual velocity increment result in increased total velocity-increment requirements. The individual corrections just prior to entry must be variable from zero to about 700 feet per second in extreme cases or to 150 feet per second with lower mission velocity or smaller instrument errors. Except for the final trimming correction, very small velocity increments are omitted to reduce the maximum number of corrections at no cost in total velocity increment or guidance accuracy.

Tolerance of the system to errors in controlling and measuring the direction and magnitude of corrective maneuvers can be large (of the order 0.1 radian and 10 percent rms) and so should cause no new measurement or attitude control problems. In addition, attitude control or position monitoring between the 15 to 20 readings is not required, but an attitude knowledge may be desirable to avoid search modes before reading and to make oblateness corrections in data reduction.

The time available for data reduction may be as high as 20 or 25 minutes using 40-second-arc instruments for an entry velocity of 1.1 escape velocities at Earth, Venus, or Mars. The time available decreases with increased mission velocity or measurement errors and with decreased engine size or entry-corridor size. Twenty minutes may be insufficient for Earth-based computation when approaching Mars or Venus but is more than sufficient for vehicle-contained computers.

Guidance logic, including the rate of data sampling and the use of dead band and damping, can be used to reduce the total velocity increment, the number of corrections, and the number of data reductions, or to increase the target accuracy and the tolerance to errors in system components, but not necessarily simultaneously. For the subject feasibility study, a reasonable compromise is used; but, for a specific system, the guidance logic would be optimized to the criteria of interest or to eliminate problem areas.

LEWIS RESEARCH CENTER
NATIONAL AERONAUTICS AND SPACE ADMINISTRATION
CLEVELAND, OHIO, *December 19, 1960*

APPENDIX A

SYMBOLS

Underscored symbols are used to symbolize matrix notation. Matrix terms are not summarized here, however, but are developed in appendix E.

A,B,C	angles in triangulation of basic data (appendix C)
A_v	nondimensional acceleration capability of vehicle control propulsion engines
a,b,c	sides of triangle opposite angles A,B,C in reduction of basic data (appendix C)
E	nondimensional total energy per unit mass (eq. (5))
$\mathscr{E}$	total energy per unit mass; discrepancy in appendixes D and E
F	function
G	universal gravitational constant
H	nondimensional angular momentum per unit mass (eq. (6))
h	angular momentum per unit mass
k_{DB}	dead-band coefficient in guidance logic (eq. (19) or (20))
k_{DM}	damping coefficient in guidance logic (eq. (22a))
k_m	target-miss confidence coefficient in guidance logic (eqs. (21) and (22b))
k_R	step-size coefficient in guidance logic (eq. (18))
M	mass of target body
m	rank from maximum value (eq. (23))
N	number of corrections during approach or number of additional vehicles to be considered (eq. (23))
n	number of vehicles in sample from which prediction is made (eq. (23))
P or R_p	nondimensional perigee range, r_p/r_o
R	nondimensional range, r/r_o
r	range, miles
t	time, sec
V	nondimensional velocity, v/v_e
v	velocity, miles/sec or ft/sec
x,y	coordinates
$\bar{x}_m$	mean number of exceedances over rank m (eq. (23))
z	substituted quantity (eq. (D4))
β	angle from normal to R to ΔV (fig. 23), radians
γ	angle from normal to R to V (fig. 1), radians
Δ	finite difference; increment
δ	finite difference due to errors
ϵ	eccentricity
θ	angle from perigee to range (fig. 1), radians
μ	angle from vehicle x-axis to line between two stars (appendix C), radians
σ	standard deviation
τ	nondimensional time, tv_e/r_o
τ_{go}	nondimensional time to perigee passage
$\Delta\tau_{stop}$	reorientation time
φ	angle from inertial reference direction to range (fig. 1), radians
ω	angle subtended by apparent disk of planet (fig. 3), radians

Subscripts:

Capital letters used as subscripts refer to the notation of the primary symbol.

a	actual
atm	sensible atmosphere
cut	last data point (eq. (17))
des	desired
e	escape
end	first point in final reading pair
ex	expected from calibration data
h	hyperbolic
i	initial
id	ideal
last	last point
limit	entry-corridor half size
max	maximum
meas	measured, measurement
min	minimum
nom	nominal
o	at planet surface
p	perigee
r	in radial direction

s	variable normally positive but used with sign to indicate direction of rotation (appendix D)	θ	in circumferential direction
		$\Delta\tau$	time increment
		$\Delta\varphi$	angular displacement
tar	target	0	at planet center; zero
tot	total	1	before thrust; first data point of reading pair
v	vehicle		
x,y	in x or y direction	2	after thrust; second data point of reading pair
xs	excess (eq. (25))		

APPENDIX B

ANALYSIS OF TRAJECTORY MODIFICATION

Discussion of corrective maneuvers is treated in three parts. First, the methods by which the desired ΔV is obtained and the basic cost of idealized maneuvers are illustrated. Second, the effects of inexact control of the desired velocity increment on the trajectory after correction and the basic sensitivity to control errors are briefly considered. Finally, the significance of errors in measuring the resultant ΔV after execution and the effect of these measurement errors on knowledge of orbital elements are studied.

DESIRED VELOCITY INCREMENTS

The velocity increment is assumed impulsive in effect; that is, ΔV is applied for relatively short periods of time compared with trajectory times. In order to maintain a first-order functional approximation of the time required to correct the trajectory with finite propulsion devices, however, the execution time $\Delta\tau$ is considered. Assuming a constant acceleration capability A_v, the execution time is

$$\Delta\tau=\frac{\Delta V}{A_v} \tag{B1}$$

These assumptions permit closed-form calculation during corrective maneuvers rather than stepwise integration along the trajectory. Where ΔV is small and A_v relatively large (so that $\Delta\tau$ is short), the errors introduced should be negligible. If, though, significant errors occur, the computed results will be in error in a direction tending to underestimate system requirements.

It is of major importance in guidance to minimize total ΔV requirements for the approach phase of a mission. It is logical, then, to minimize ΔV for individual corrections. The iterative solution for optimum perigee modification is discussed and evaluated in reference 23, where it is also shown that the optimum correction is accurately approximated by applying ΔV normal to range, or in a circumferential direction. The tedious, iterative, optimum solution is then replaced by a direct calculation. The circumferential ΔV is sufficiently close to the optimum that no further justification for its use is necessary. But, aside from the obvious simplification in analysis herein, the simplification in computing and control aboard a vehicle makes the use of circumferential corrections desirable.

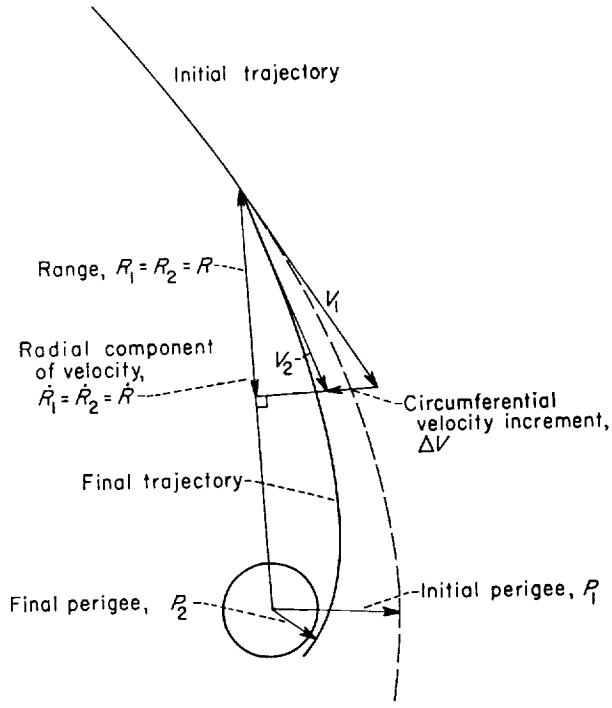

FIGURE 21.—Circumferential corrective maneuver.

Using the notation of figure 21, the components of velocity are

$$\left.\begin{aligned} V_\theta&=\frac{H}{R} \quad \text{(from eq. (6))}\\ V_r&=\dot{R}=V\sin\gamma \end{aligned}\right\} \tag{B2}$$

so that, for circumferential trajectory modification where V_r is constant and $R_1=R_2=R$,

$$\Delta V=V_{\theta,2}-V_{\theta,1}=\frac{H_2-H_1}{R} \tag{B3}$$

Solving equations (5a), (6a), and (7) for angular momentum,

$$H=\pm\sqrt{P^2E+P} \tag{B4}$$

where the sign is determined from the direction of rotation of the vehicle around the planet. Using the components of velocity in the energy equation (5) for any point on the trajectory,

$$\dot{R}^2=E+\frac{1}{R}-V_\theta^2=E+\frac{1}{R}-\frac{H^2}{R^2}=E+\frac{1}{R}-\frac{P^2E+P}{R^2} \tag{B5}$$

Equating $\dot{R}_1^2=\dot{R}_2^2$ and solving for E_2,

$$E_2=\frac{E_1(R^2-P_1^2)+P_2-P_1}{R^2-P_2^2} \tag{B6}$$

which is used in equation (B4) to find H_2, and ΔV can be obtained by equation (B3). Thus, the velocity increment is directly computed knowing the initial trajectory elements P_1 and E_1, the desired perigee P_2, and the range of the impulsive correction. (Where $R\gg P$ the change in trajectory energy is small relative to the change in perigee, P_2-P_1, and ΔV is readily estimated using equations (B3) and (B4) with energy constant.)

An example of the ΔV cost of perigee modification is shown in figure 22(a) on logarithmic scales as a function of range. As indicated by the dashed curve, the ΔV is approximately inversely proportional to range except close to the perigee of the initial trajectory, in this case 2 radii. The initial energy is 0.2, representing a hyperbolic velocity of 0.45 escape velocity. The cost of correcting the assumed error of 1 radius (4000 miles) varies from 0.006 (220 ft/sec) at 100 radii (400,000 miles) to 0.4 (14,680 ft/sec) at 2 radii, the perigee of the initial trajectory.

It is apparent from figure 22(a) that corrective maneuvers should be executed at as long range as is feasible, and that the ΔV costs of delaying action become substantial, even prohibitive, as range decreases.

The variation of ΔV with the error in trajectory is shown in figure 22(b), where the error ΔP varies from large positive values, 8 radii (32,000 miles, 28,000 Int. naut. miles), to large negative values, which represent the opposite direction of rotation. Results illustrate ΔV for correction at 100 radii (400,000 miles). The increased slope near ΔP of -1 reflects the nonlinearity in the parameter P as it approaches zero. The dashed curve shows the

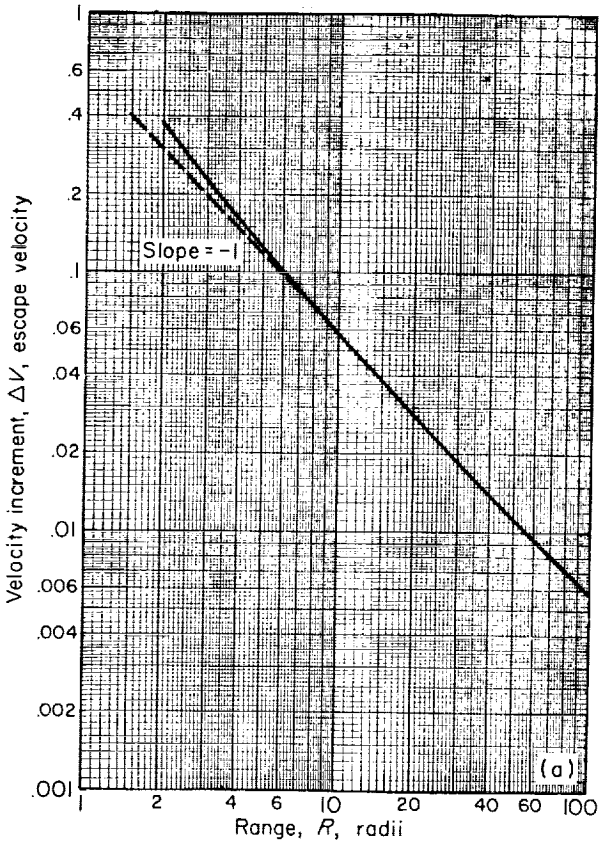

(a) Variation with range; $P_1=2$ radii.

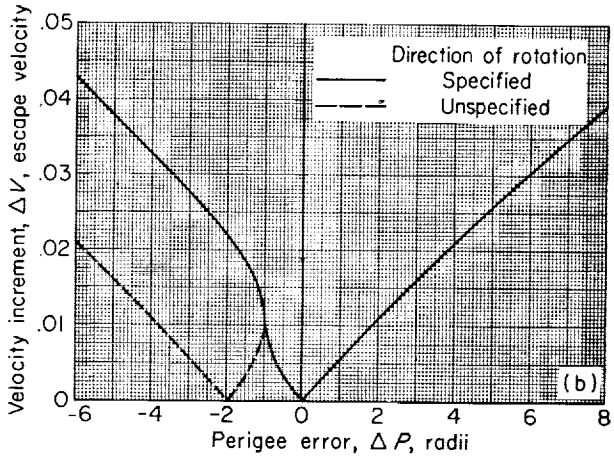

(b) Variation with initial error; $R=100$ radii.

FIGURE 22.—Velocity-increment cost of corrective maneuvers. Initial energy, 0.2; $P_2=P_{tar}=1$ radius.

ΔV required to correct to a perigee of 1 regardless of the direction of rotation, and reflects the increased cost incurred by specifying the direction of rotation in the target of guidance. The difference, for perigee errors greater than -2 radii, is about 0.022 escape velocity (800 ft/sec) in figure 22(b).

The ΔV illustrated can be considered the ideal ΔV required to correct the trajectory. The same method is used by the vehicle computer to compute desired corrective action. As will be considered shortly, the knowledge of range and orbital elements P and E available to the vehicle results from measurements including errors. As a result, the final trajectory is expected to differ from the desired trajectory.

EFFECT OF ERRORS IN MEASURING VELOCITY INCREMENT

Variations in the direction β_{meas} of the resultant ΔV_{meas} from the desired circumferential correction ΔV_{des} ($\beta_{des}=0$) are shown in figure 23(a). Assuming small directional errors, the components of velocity after correction are

$$\left.\begin{aligned} V_{r,2}&=\dot{R}_2=\dot{R}_1+\Delta V_{meas}\sin\beta_{meas}\\ V_{\theta,2}&=R\dot{\theta}_2=R\dot{\theta}_1+\Delta V_{meas}\cos\beta_{meas}\end{aligned}\right\} \quad \text{(B7)}$$

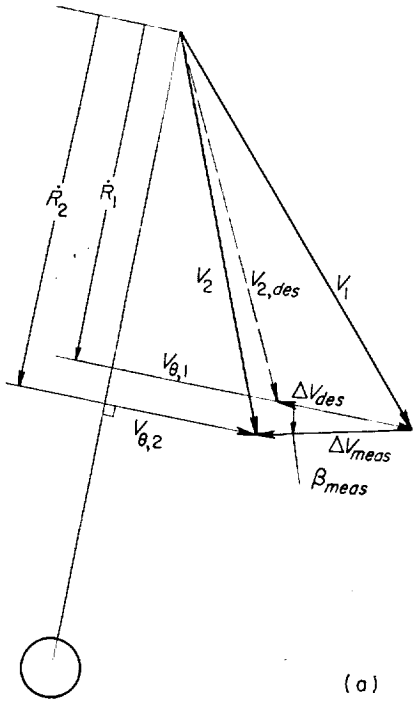

(a) Notation.

FIGURE 23.—Effect of errors in corrective maneuvers.

Substituting into equations (5) and (6), the orbital elements after corrections are

$$\left.\begin{aligned} E_2&=(\dot{R}_1+\Delta V_{meas}\sin\beta_{meas})^2\\ &\quad+(R\dot{\theta}_1+\Delta V_{meas}\cos\beta_{meas})^2-\frac{1}{R}\\ H_2&=R(R\dot{\theta}_1+\Delta V_{meas}\cos\beta_{meas})\end{aligned}\right\} \quad \text{(B8)}$$

from which the perigee P_2 can be found with the use of equations (5a), (6a), and (7).

Knowledge of the resultant velocity increment is hypothesized to result from an inertial measurement scheme using accelerometers and gyroscopes. The control scheme hypothesized is shown functionally in figure 23(b). The desired corrective maneuver ($\Delta V_{des},\beta_{des}$) results in some actual correction ($\Delta V_a,\beta_a$), which is indicated as the measured correction ($\Delta V_{meas},\beta_{meas}$) due to measurement errors $\delta\Delta V$ and $\delta\beta$. The modified trajectory is computed using equations (B8), ΔV_{meas}, and β_{meas}.

The effect of measurement errors on the modified trajectory can be estimated as follows. Linearizing equations (B8) and writing in terms of small finite errors give

$$\left.\begin{aligned} \delta E_2&=2\left(\dot{R}_2\Delta V_{meas}\cos\beta_{meas}\right.\\ &\quad\left.-\frac{H_2}{R}\Delta V_{meas}\sin\beta_{meas}\right)\delta\beta\\ &\quad+2\left(\dot{R}_2\sin\beta_{meas}+\frac{H_2}{R}\cos\beta_{meas}\right)\delta\Delta V\\ \delta H_2&=(R\cos\beta_{meas})\delta\Delta V\\ &\quad-(R\Delta V_{meas}\sin\beta_{meas})\delta\beta\end{aligned}\right\} \quad \text{(B9)}$$

For small errors, assume

$$\sin\beta_{meas}\approx\beta_{meas},\qquad \cos\beta_{meas}\approx 1$$

Then, simplifying and dropping second-order terms,

$$\left.\begin{aligned} \delta E_2&=2(R\dot{\theta}_2\delta\Delta V+\dot{R}_2\Delta V_{meas}\delta\beta)\\ \delta H_2&=R\delta\Delta V\end{aligned}\right\} \quad \text{(B10)}$$

Finally, since the perigee is significant to the guidance problem, the angular momentum is elimi-

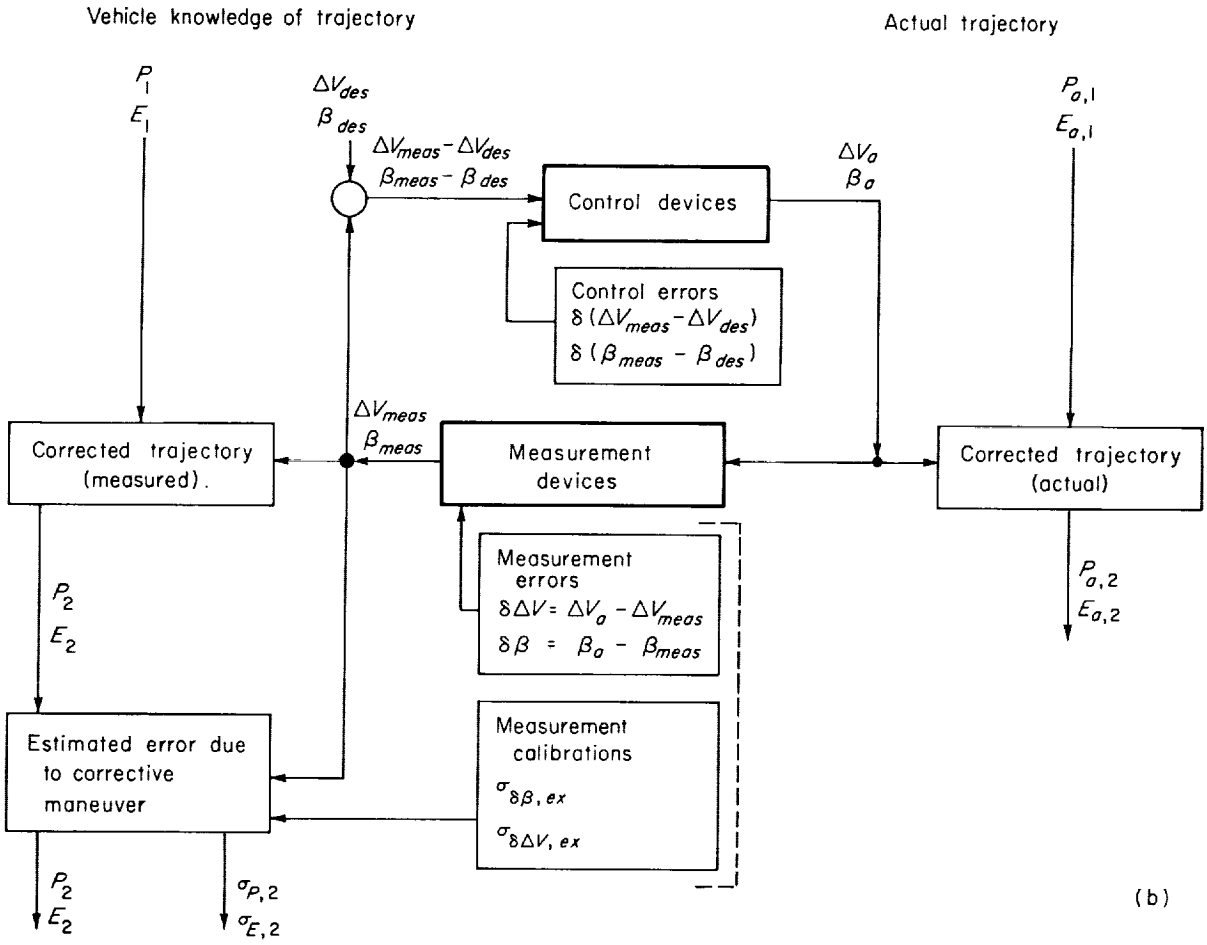

(b) Schematic of control scheme.

FIGURE 23.—Concluded. Effect of errors in corrective maneuvers.

nated using equations (5a), (6a), and (7) as

$$\delta P_2 = \frac{1}{\epsilon_2}\left(2H_2\delta H_2 - P_2^2\delta E_2\right) \tag{B11}$$

where ϵ is the eccentricity. Simplifying, and noting that $\dot{R} = \pm\sqrt{\dot{R}^2}$ is always positive for the inbound vehicle,

$$\left.\begin{aligned}\delta P_2 &= \frac{2}{\epsilon_2}\left[\left(1-\frac{P_2^2}{R^2}\right)H_2 R\,\delta\Delta V - P_2^2\dot{R}_2\Delta V_{meas}\delta\beta\right]\\ \delta E_2 &= 2\left(\frac{H_2}{R}\,\delta\Delta V + \dot{R}_2\Delta V_{meas}\delta\beta\right)\end{aligned}\right\} \tag{B12}$$

The significance of ΔV measurement errors is considered in detail in reference 23. The major effects can be determined here by inspection of equations (B12). The directional error $\delta\beta$ is dominated by the coefficient ΔV_{meas} in both equations, so that for small corrections the effect is small. In addition, the radial velocity $\dot{R}$ is small at long range where large corrections may be used. The error in measuring the magnitude $\delta\Delta V$ may contribute significant uncertainty in energy at short range, but less as range increases in the denominator.

The most important effect is that of $\delta\Delta V$ on the perigee at long range where correction to the desired trajectory is advantageous with respect to ΔV expenditure (fig. 22). This is not surprising, however, since ΔV is applied in a direction chosen to permit perigee modification with minimum ΔV expenditure (i.e., a direction in which the perigee is sensitive to ΔV).

Uncertainties in the knowledge of the orbital elements available to the vehicle can be ex-

pressed as variances σ_P^2 and σ_E^2, as considered in the ANALYSIS section. Assuming that the magnitude and direction errors are uncorrelated, and that the standard deviations $\sigma_{\delta\Delta V,ex}$ and $\sigma_{\delta\beta,ex}$ of the measurement instruments are available from calibrations, the uncertainty due to measurement errors in corrective maneuvers is, from equation (B12),

$$\left.\begin{aligned}\sigma_P^2&=\left[\frac{2}{\epsilon_2}\left(1-\frac{P_2^2}{R^2}\right)H_2R\right]^2\sigma_{\delta\Delta V,ex}^2\\&\quad+\left[\frac{2}{\epsilon_2}P_2^2\dot{R}_2\Delta V_{meas}\right]^2\sigma_{\delta\beta,ex}^2\\\sigma_E^2&=\left[\frac{2H_2}{R}\right]^2\sigma_{\delta\Delta V,ex}^2+[\dot{R}_2\Delta V_{meas}]^2\sigma_{\delta\beta,ex}^2\end{aligned}\right\}\quad\text{(B13)}$$

The increase in uncertainties in trajectory knowledge, expressed as σ_P^2 and σ_E^2, is dependent on the errors in the measurement instruments $\sigma_{\delta\Delta V,ex}$ and $\sigma_{\delta\beta,ex}$, the size of the measured velocity increment ΔV_{meas}, the trajectory after correction, and the range. The control errors influence the variances only indirectly.

EFFECT OF CONTROL ERRORS

In most closed-loop control systems, a strong control feedback is used to cause the measured output to agree with the desired value. It is desired in most systems, moreover, to obtain perfect correlation of $\Delta V_{meas},\beta_{meas}$ with $\Delta V_{des},\beta_{des}$; and any differences result from small errors in calibration of cutoff decay curves or dynamic response limitations in the control system. In current practice, however, this precise control is often attained using systems requiring substantial power supplies and violent cutoff techniques. It is of interest here to investigate relaxation of these requirements. To do so, differences in the measured correction $\Delta V_{meas},\beta_{meas}$ and the desired correction $\Delta V_{des},\beta_{des}$ are assumed uncorrelated with measurement errors. In other words, errors in controlling the ΔV are considered independent of errors in measuring the resultant correction.

The effects of errors in control action, σ_β and $\sigma_{\Delta V}$, have been shown with numerical results in figure 14.

APPENDIX C

COMPUTATION OF RANGE AND ANGULAR ROTATION FROM BASIC MEASUREMENTS

The following discussion of range determination using the apparent size of the planet assumes visibility of the entire disk, inferring that some wavelength is used that permits definition of both light and dark sides of the planet. The more complex methods required when only a crescent is visible are presented in reference 8. It is also inferred that sharp definition of planet boundaries is possible, which may require quantitative calibration of fringe effects.

The measurements picked from the hypothetical image were indicated to include the maximum and minimum intercepts of the planet along some vehicle reference axes, say x_v and y_v. The two values of apparent size of the planet are

$$\left.\begin{aligned}\omega_x &= x_{max} - x_{min} \\ \omega_y &= y_{max} - y_{min}\end{aligned}\right\} \tag{C1}$$

Simply averaging the two values,

$$\omega = \frac{\omega_x + \omega_y}{2} \tag{C2}$$

where the image is considered scaled in radians to avoid writing a scale factor in each equation. The range is

$$R = \frac{R_o}{\sin(\omega/2)} \tag{C3}$$

where the nominal value of R_o is 1 radius. Considering uncertainties in planet size or local terrain as well as in the measurements, the error in range is

$$\begin{aligned} dR &= \frac{\partial R}{\partial \omega} d\omega + \frac{\partial R}{\partial R_o} dR_o \\ &= -\frac{R_o \cos(\omega/2)}{2 \sin^2(\omega/2)} d\omega + \frac{dR_o}{\sin(\omega/2)} \end{aligned} \tag{C4a}$$

which simplifies by virtue of equation (C3) to

$$dR = -\frac{R}{2}\sqrt{R^2-1}\, d\omega + R\, dR_o \tag{C4b}$$

where

$$d\omega = \frac{1}{2}(dx_{max} - dx_{min} + dy_{max} - dy_{min}) \tag{C5}$$

Assuming now that the four basic points have uncorrelated normally distributed errors of equal σ_{meas}, and noting that the sum of normally distributed values is also normally distributed with the standard deviation equal to the square root of the sum of the squares,

$$\sigma_\omega = \frac{1}{2}\sqrt{4}\sigma_{meas} = \sigma_{meas}$$

The uncertainty in range, approximated in terms of finite differences due to errors, is

$$\delta R = R\left(-\frac{\sqrt{R^2-1}}{2}\delta_{meas} + \delta R_o\right) \tag{C6a}$$

Then

$$\delta_{meas} = \sigma_{meas}[\delta] \tag{C7}$$

where $[\delta]$ is a normally distributed random error, and each $[\delta]$ is different,

$$\delta R = -\frac{R}{2}\sqrt{R^2-1}\sigma_{meas}[\delta] + R\sigma_{R,o}[\delta] \tag{C6b}$$

and the variance in range determination is

$$\sigma_R^2 = \frac{R^2(R^2-1)}{4}\sigma_{meas}^2 + R^2\sigma_{R,o}^2 \tag{C8}$$

The determination of $\Delta\varphi$ from two successive readings requires the use of a matching pair of stars, say 1 and 2, as well as the two sets of planet data (sketches (a) and (b)). The center of the planet (x_0, y_0) is

$$\left.\begin{aligned} x_0 &= \frac{x_{max} + x_{min}}{2} \\ y_0 &= \frac{y_{max} + y_{min}}{2} \end{aligned}\right\} \tag{C9}$$

and the sides of the triangle are, for example,

$$b = \sqrt{(x_C - x_0)^2 + (y_C - y_0)^2} \tag{C10}$$

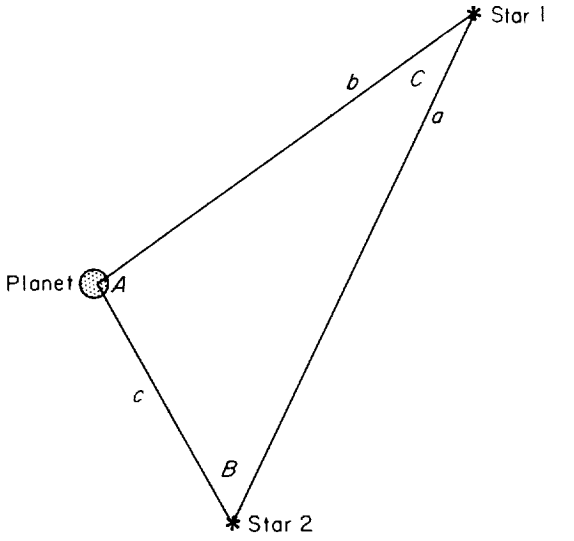

(a)

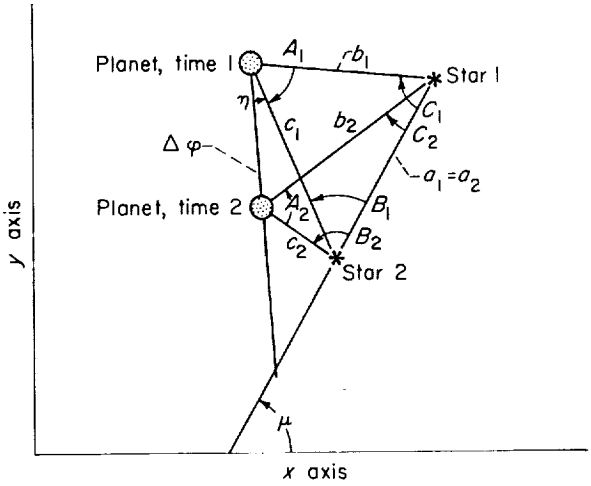

(b)

The angles of the triangle can be found using the law of cosines. For example,

$$B=\cos^{-1}\left(\frac{c^2+a^2-b^2}{2ca}\right) \tag{C11}$$

From two such readings the angular displacement in the plane of motion $\Delta\varphi$ is

$$\Delta\varphi=\pm\left(c_1^2+c_2^2-2c_1c_2\cos|B_1-B_2|\right)^{1/2} \tag{C12}$$

The plane of motion relative to the line between stars a is

$$\eta=\left|\cos^{-1}\left(\frac{\Delta\varphi^2+c_1^2-c_2^2}{2c_1\Delta\varphi}\right)\right|+|B_1|\pi \tag{C13}$$

which can be related to the vehicle axis at time 2 for the purpose of orienting relative to an inertial system for use in corrective maneuvers by

$$\mu=\tan^{-1}\left(\frac{y_b-y_c}{x_b-x_c}\right) \tag{C14}$$

A suitable sign convention is required to establish the directions of $\Delta\varphi$ and η, but problems would not be anticipated.

Errors associated with the determination of $\Delta\varphi$ and η are difficult to assess because of the dependence on the particular positions of stars used. It is readily shown, however, that, if the stars are in the plane of motion, the maximum accuracy with a given measurement error is obtained.

Assume, then, that the vehicle has the ability to pick stars near the plane of motion. As an alternative, consider the recording of many stars, with the final calculation using those found in the plane on previous check calculations.

The calculation of $\Delta\varphi$ then becomes, still considering the image scaled in radians,

$$\begin{aligned}\Delta\varphi=\frac{1}{2}\Bigg[&\left(\frac{x_{max}+x_{min}}{2}-x_c\right)_1-\left(\frac{x_{max}+x_{min}}{2}-x_c\right)_2\\&+\left(\frac{x_{max}+x_{min}}{2}-x_b\right)_1-\left(\frac{x_{max}+x_{min}}{2}-x_b\right)_2\Bigg]\\=\frac{1}{2}\{&[x_{max}+x_{min}-(x_c+x_b)]_1-[x_{max}+x_{min}\\&-(x_c+x_b)]_2\}\end{aligned} \tag{C15}$$

Therefore,

$$\begin{aligned}\delta\Delta\varphi=\frac{1}{2}\{&[\delta x_{max}+\delta x_{min}-(\delta x_c+\delta x_b)]_1\\&-[\delta x_{max}+\delta x_{min}-(\delta x_c+\delta x_b)]_2\}\end{aligned} \tag{C16}$$

$$\begin{aligned}\sigma^2_{\Delta\varphi}&=\frac{1}{4}\left(4\sigma^2_{\text{planet}}+4\sigma^2_{\text{star}}\right)\\&=\sigma^2_{\text{planet}}+\sigma^2_{\text{star}}\end{aligned} \tag{C17}$$

$$\sigma_{\Delta\varphi}=\sqrt{\sigma^2_{\text{planet}}+\sigma^2_{\text{star}}} \tag{C18}$$

Therefore, the error in $\Delta\varphi$ is equally due to errors in observing the planet and observing the stars. For the hypothesized measurement scheme, the accuracy in reading data is equal; thus,

$$\sigma_{\Delta\varphi}=\sqrt{2}\sigma_{meas}$$

APPENDIX D

DETAILS OF COMPUTATION METHOD

Time and time increments along the trajectory are required repeatedly in calculation. The integration of conic equations is indicated here so that duplicate presentation can be avoided elsewhere. In general, however, the methods of computation are presented approximately in the order used in calculation. From angular momentum and the polar equation for a conic section, in nondimensional form,

$$\left.\begin{aligned} H &= R^2\dot{\theta} = R^2\frac{\mathrm{d}\varphi}{\mathrm{d}\tau} \\ R &= \frac{2H^2}{1+\epsilon\cos\varphi} \end{aligned}\right\} \tag{D1}$$

Proceeding parallel to methods of references 5 and 6,

$$\int_0^{\tau_{go}} \mathrm{d}\tau = \frac{1}{H}\int_0^{\varphi} R^2\mathrm{d}\varphi \tag{D2}$$

where limits of integration are chosen to yield the time from any point given by R (or θ) to the time of perigee passage. Results of integration in terms of the variables used herein for elliptic, parabolic, or hyperbolic trajectories are shown in reference 2. Restricting this analysis to the hyperbolic approach, the result of integration, after simplification, is

$$\tau_{go} = \frac{1}{E^{3/2}}\left[z - \frac{1}{2}\ln\frac{(1/2)+ER+z}{\epsilon/2}\right] \qquad E>0 \tag{D3}$$

where

$$z = [E^2(R^2-P^2)+E(R-P)]^{1/2} \tag{D4}$$

and z is strictly a dummy variable to indicate substitution. This solution can be represented in functional notation by

$$\tau_{go} = \tau_{go}(P,E,R) \tag{D5}$$

From knowledge of orbital elements P and E, the time from range R to perigee passage is computed in closed form. Closed-form solution is not available, however, to compute range knowing P, E, and τ_{go}; therefore, an iterative solution is used. Since trial values R_1 and τ_{go} are available herein from previous computation, the first approximation is made (using an arbitrary convergence equation in lieu of $\partial R/\partial\tau$) as follows:

$$R = P+(R_1-P)\left(\frac{\tau_{go,des}}{\tau_{go,1}}\right) \tag{D6}$$

where $\tau_{go,des}$ is the time for which range is desired. The iterative loop is then

$$\left.\begin{aligned} \tau_{go} &= \tau_{go}(P,E,R) \\ R &= P+(R-P)\left(\frac{\tau_{go}}{\tau_{go,des}}\right) \\ \tau_{go} &\overset{?}{=} \tau_{go,des} \end{aligned}\right\} \tag{D7}$$

until the desired accuracy is obtained. The iteration is rapidly convergent if the starting conditions are acceptable; namely, $E>0$, $\tau_{go}>0$, and $R>P\geq 0$. Digital rounding prevents accuracy greater than 5 of 8 figures unless additional care is used. Solution for range knowing time and orbital elements is functionally noted as

$$R = R(P,E,\tau_{go}) \tag{D8}$$

and refers to the iterative solution.

CUTOFF CRITERIA

Since active guidance is cut off only when no further corrective maneuvers can be accomplished before entry into the sensible atmosphere, cutoff criteria simply limit the time (or range) of the last data-acquisition points. By assuming vehicles close to the target trajectory, it is possible to precompute the time of cutoff rather than to include computation in the logic of each sample vehicle. The assumption should be valid, since guidance that uses sufficient ΔV to modify the energy or that does not have vehicles near the target at cutoff will be unacceptable regardless of cutoff approximations.

Noting first that all corrective action must be completed before entry into the sensible atmosphere, and assuming $R_{atm}=R_o+0.02$ (80 miles), then

$$\tau_{go,atm}=\tau_{go,atm}(P_{tar},E,R_{atm}) \tag{D5a}$$

Sufficient time for data reduction, orientation of the vehicle to execute a correction, execution, and reorientation to entry attitude must be provided. The time of the second point of the last pair is then

$$\tau_{go,cut}=\tau_{go,atm}+\Delta\tau_{stop}+\frac{\Delta V_{last}}{A_v} \tag{D9}$$

and

$$R_{cut}=R_{cut}(P_{tar},E,\tau_{go,cut}) \tag{D8a}$$

The first point of the last pair should precede the second by the specified minimum increment of time $\Delta\tau_{go,min}$. Thus, no reading increment should be initiated after

$$\tau_{go,end}=\tau_{go,cut}+\Delta\tau_{go,min} \tag{D10}$$

which is used in guidance logic by specifying the range of last initiation as

$$R_{end}=R_{end}(P_{tar},E,\tau_{go,end}) \tag{D8b}$$

INITIALIZATION OF VEHICLE RUNS

The nominal values and standard deviations for residual errors resulting from previous guidance are assumed. Denoting normally distributed random numbers by $[\delta]$, where each $[\delta]$ is different, the actual or true trajectory is generated as

$$\left.\begin{aligned} R_a&=R_{nom}+\sigma_{R,nom}[\delta]\\ E_a&=E_{nom}+\sigma_{E,nom}[\delta]\\ P_{a,x}&=P_{nom}+\sigma_{P,nom}[\delta]\\ P_{a,y}&=\sigma_{P,nom}[\delta]\\ P_a&=\sqrt{P_{a,x}^2+P_{a,y}^2}\\ H_a&=\frac{P_{a,x}}{|P_{a,x}|}\sqrt{P_a^2E_a+P_a} \end{aligned}\right\} \tag{D11}$$

where the actual perigee P_a is generated as a normal bivariate distribution around the nominal point $(P_{nom},0)$. The sign of angular momentum H_a determines direction of rotation around the planet, where the target trajectory is considered to have positive rotation.

Some additional properties of the actual trajectory are computed as

$$\left.\begin{aligned} \epsilon_a&=1+2P_aE_a\\ \tau_{go,a}&=\tau_{go,a}(P_a,E_a,R_a) \end{aligned}\right\} \tag{D11a}$$

and, from the polar equation for a conic trajectory (eq. (D1)), the angular displacement from the perigee, the true anomaly, is

$$\theta_a=\cos^{-1}\frac{1}{\epsilon_a}\left(\frac{2H_a^2}{R_a}-1\right) \tag{D12a}$$

where θ_a is in the first two quadrants when H_a is positive, but

$$\theta_a=2\pi-\theta_a \tag{D12b}$$

when $H_a<0$.

IDEAL VELOCITY-INCREMENT CALCULATION

The ideal velocity increment ΔV_{id} is herein defined as the minimum ΔV required to correct the initial trajectory, at the initiation of guidance, to within the entry corridor. The initial error in perigee is

$$\Delta P=\frac{H_a}{|H_a|}P_a-P_{tar} \tag{D13}$$

When $\Delta P\leq\Delta P_{limit}$, no ΔV is required. In general,

$$P_{2,id}=P_{tar}+\frac{\Delta P}{|\Delta P|}\Delta P_{limit} \tag{D14}$$

So the ideal correction is to the near boundary of the entry corridor. Then,

$$E_{2,id}=\frac{R_a^2E_a-H_a^2+P_{2,id}}{R_a^2-P_{2,id}^2} \tag{D15}$$

$$H_{2,id}=+\sqrt{P_{2,id}^2E_{2,id}+P_{2,id}} \tag{D16}$$

$$\Delta V_{id}=\frac{H_{2,id}-H_a}{R_a} \tag{D17}$$

The ΔV_{id} represents the minimum requirements of ΔV to correct the assumed error in perigee at the assumed initial point R_a and with the assumed energy E_a; ΔV_{id} can be considered the cost of residual errors in midcourse guidance not chargeable to the approach guidance system.

STEP-SIZE LOGIC

Henceforth, discussion will consider the n^{th} increment of computation and guidance logic.

Initially, the first step or reading increment is based on assumed trajectory elements. The effect of other assumptions on the step size is not considered herein, and P_{ex} and E_{ex} are assumed equal to P_{tar} and E_{nom}. When knowledge is available to the vehicle, the step size is based on its current best estimate of trajectory elements. In any case, the range of the first point of the reading pair is measured. The measurement is simulated in computation using the true range R_a and the assumed measurement errors. From equation (C6b),

$$R_1=R_{a,1}\left(1-\frac{\sqrt{R_{a,1}^2-1}}{2}\,\sigma_{meas}[\delta]+\sigma_{R,o}[\delta]\right) \quad \text{(D18)}$$

If $R_1<R_{end}$, however, sufficient time to complete two reading increments and corrections is not available, as discussed in the previous section "Cutoff Criteria." Logic is then modified for the final increment, following which the approach is thus terminated, and the results of the guidance problem are tabulated statistically. When $R_1\geq R_{end}$, time remains and computation continues, using only knowledge available to the vehicle:

$$\left.\begin{aligned}\epsilon&=1+2PE\\ H^2&=P^2E+P\\ \tau_1&=\tau_1(P,E,R)\end{aligned}\right\} \quad \text{(D19)}$$

The desired range of the next reading R_2 is tentatively computed as shown in figure 10:

$$R_2=\text{the larger of}\begin{cases}R_1(1-k_R)\\ R_1-\Delta R_{max}\end{cases} \quad \text{(D20)}$$

so that either the proportional increment or the maximum allowable increment ΔR_{max} is used, whichever leads to the smaller increment. The time at R_2 is then

$$\tau_2=\tau_2(P,E,R) \quad \text{(D19a)}$$

and the increment of coasting flight is then

$$\Delta\tau=\text{the larger of}\begin{cases}\tau_1-\tau_2\\ \Delta\tau_{min}\end{cases} \quad \text{(D21)}$$

so that the minimum step size, in terms of time, is used to prevent bad readings or undesired short increments. Since the proportional step sizes are usually larger than $\Delta\tau_{min}$ steps, this logic is seldom used.

The vehicle is considered to coast for the period $\Delta\tau$ as indicated by its clock. The actual coasting period is

$$\Delta\tau_{go}=\Delta\tau(1+\sigma_{\Delta\tau}[\delta]) \quad \text{(D21a)}$$

where the error is considered proportional to the time increment and $[\delta]$ is again a normally distributed random number. The true time of the second reading is found as

$$\tau_{go,2}=\tau_{go,1}-\Delta\tau_{go} \quad \text{(D21b)}$$

and the range $R_{a,2}$ is obtained from the iterative solution of the time equations

$$R_{a,2}=R_{a,2}(P_a,E_a,\tau_{go,a,2}) \quad \text{(D8c)}$$

The measured range R_2 and the angular displacement from the perigee $\theta_{a,2}$ are obtained as previously (eqs. (C6b) and (D1)). The measured angular increment is generated as (from eq. (C18))

$$\Delta\varphi=\theta_{a,1}-\theta_{a,2}+\sigma_{meas,1}[\delta]+\sigma_{meas,2}[\delta] \quad \text{(D22)}$$

where the errors due to planet and star sightings are considered independently.

The expected errors in measured values are obtained using the standard deviations from calibration data,

$$\left.\begin{aligned}\sigma_{R,1}^2&=R_1^2\left[(R_1^2-1)\,\frac{\sigma_{meas,1,ex}^2}{4}+\sigma_{R,o,ex}^2\right]\\ \sigma_{R,2}^2&=R_2^2\left[(R_2^2-1)\,\frac{\sigma_{meas,1,ex}^2}{4}+\sigma_{R,o,ex}^2\right]\\ \sigma_{\Delta\tau}^2&=\Delta\tau^2\sigma_{\Delta\tau,ex}^2\\ \sigma_{\Delta\varphi}^2&=\sigma_{meas,1,ex}^2+\sigma_{meas,2,ex}^2\end{aligned}\right\} \quad \text{(D23)}$$

and the terms required for data reduction are complete.

DATA REDUCTION

The condition equations for this study are

$$\left.\begin{aligned}\Delta\tau+\tau_{go,2}-\tau_{go,1}&=\mathscr{E}_1\\ |\Delta\varphi|+\theta_2-\theta_1&=\mathscr{E}_2\end{aligned}\right\} \quad \text{(D24)}$$

where $\mathscr{E}$ is the discrepancy as defined in appendix E.

Written in terms of the variables of interest and considering for the moment that the orbital elements will be either parameters ($\gamma°$) or observations ($x°$), equation (D24) is

$$\left.\begin{aligned} F_1(R_1,R_2,\Delta\tau,0,P_s,E)&=\mathscr{E}_1\\ F_2(R_1,R_2,0,\Delta\varphi,P_s,E)&=\mathscr{E}_2\end{aligned}\right\} \tag{D25}$$

where the perigee range P_s is used as a signed variable to indicate the direction of rotation around the planet. The use of the perigee in guidance logic forces eventual computation of this element, so that the use of a more convenient term in this stage of data reduction only delays the problem.

The specific working functions used in the condition equations are shown parametrically, where in concept they should be considered as fully substituted for the variables in the preceding functional notation. From equations (D1), (D3), and (D4),

$$\left\{\begin{aligned} &\Delta\tau+\frac{1}{E^{3/2}}\left(z_2-z_1-\frac{1}{2}\ln\frac{2z_2+2R_2E+1}{2z_1+2R_1E+1}\right)=\mathscr{E}_1\\ &z_i=[E^2(R_i^2-P^2)+E(R_i-P)]^{1/2}\qquad i=1,2\end{aligned}\right\}$$

$$\left\{\begin{aligned} &\Delta\varphi+\cos^{-1}\frac{1}{\epsilon}\left(\frac{2H^2}{R_2}-1\right)-\cos^{-1}\frac{1}{\epsilon}\left(\frac{2H^2}{R_1}-1\right)=\mathscr{E}_2\\ &H^2=P^2E+P,\qquad \epsilon=1+2PE\end{aligned}\right\} \tag{D26}$$

Differentiation to obtain the coefficient matrices of the observations and/or the unknown parameters, after simplification, yields the following:

$$\frac{\partial\mathscr{E}_1}{\partial R_1}=-\frac{1}{\sqrt{E}}\left(\frac{1-\dfrac{1}{1+2ER_1+2z_1}}{z_1}\,\frac{2ER_1+1}{2}-\frac{1}{1+2ER_1+2z_1}\right) \tag{D27a}$$

$$\frac{\partial\mathscr{E}_1}{\partial R_2}=\frac{1}{\sqrt{E}}\left(\frac{1-\dfrac{1}{1+2ER_2+2z_2}}{z_2}\,\frac{2ER_2+1}{2}-\frac{1}{1+2ER_2+2z_2}\right) \tag{D27b}$$

$$\frac{\partial\mathscr{E}_1}{\partial\Delta\tau}=1 \tag{D27c}$$

$$\frac{\partial\mathscr{E}_1}{\partial\Delta\varphi}=0 \tag{D27d}$$

$$\frac{\partial\mathscr{E}_1}{\partial P_s}=\frac{\epsilon}{2}\left(\frac{P_s}{P}\right)\frac{1}{\sqrt{E}}\left(\frac{1-\dfrac{1}{1+2ER_1+2z_1}}{z_1}-\frac{1-\dfrac{1}{1+2ER_2+2z_2}}{z_2}\right) \tag{D27e}$$

$$\frac{\partial\mathscr{E}_1}{\partial E}=\frac{1}{E^{3/2}}\left[\frac{1-\dfrac{1}{1+2ER_2+2z_2}}{z_2}(R_2-P)\left(ER_2+\frac{\epsilon}{2}\right)-\frac{R_2}{1+2ER_2+2z_2}-\frac{1-\dfrac{1}{1+2ER_1+2z_1}}{z_1}(R_1-P)\times\left(ER_1+\frac{\epsilon}{2}\right)+\frac{R_1}{1+2ER_1+2z_1}\right]-\frac{3}{2}\frac{\Delta\tau}{E} \tag{D27f}$$

$$\frac{\partial\mathscr{E}_2}{\partial R_1}=\frac{-|H|}{R_1^2\sqrt{E+\dfrac{1}{R_1}-\dfrac{H^2}{R_1^2}}} \tag{D27g}$$

$$\frac{\partial\mathscr{E}_2}{\partial R_2}=\frac{|H|}{R_2^2\sqrt{E+\dfrac{1}{R_2}-\dfrac{H^2}{R_2^2}}} \tag{D27h}$$

$$\frac{\partial\mathscr{E}_2}{\partial\Delta\tau}=0 \tag{D27i}$$

$$\frac{\partial\mathscr{E}_2}{\partial\Delta\varphi}=\frac{P_s}{P} \tag{D27j}$$

$$\frac{\partial\mathscr{E}_2}{\partial E}=\frac{P}{\epsilon|H|}\left(\frac{\dfrac{P}{R_2}-1}{\sqrt{E+\dfrac{1}{R_2}-\dfrac{H^2}{R_2^2}}}-\frac{\dfrac{P}{R_1}-1}{\sqrt{E+\dfrac{1}{R_1}-\dfrac{H^2}{R_1^2}}}\right) \tag{D27k}$$

$$\frac{\partial \mathscr{E}_2}{\partial P_s}=\frac{\frac{P}{P_s}}{\epsilon|H|}\left[\frac{E\left(\frac{2H^2}{R_2}-1\right)-\frac{\epsilon^2}{R_2}}{\sqrt{E+\frac{1}{R_2}-\frac{H^2}{R_2^2}}}-\frac{E\left(\frac{2H^2}{R_1}-1\right)-\frac{\epsilon^2}{R_1}}{\sqrt{E+\frac{1}{R_1}-\frac{H^2}{R_1^2}}}\right] \quad H\neq 0 \quad \text{(D27l)}$$

where $H=\sqrt{P^2E+P}\to 0$ as the vehicle falls directly toward the center of the planet. The angular increment and discrepancy become independent of R_1, R_2, and E, and the respective coefficients vanish; $\partial\mathscr{E}_2/\partial P_s$ approaches infinity, however, since small changes in perigee result in undefined or large changes in θ and thus $\mathscr{E}_2$. In other words, for $P\to 0$, infinitesimal changes in $\Delta\varphi$ have no effect on P. In the condition equations this discontinuity occurs as a result of the cosine function, but in the physical problem it is a direct result of the fact that a trajectory toward $P=0$ must be modified by a finite increment before θ differs from 180°.

For the data reduction considered herein, the occurrence of a mathematical zero perigee range does not constitute a significant value, since data considered are valid only to 10^{-6} at best, but most often 10^{-4}, where problems may be encountered. It is realistic, therefore, to consider

$$|H|=|H|+\delta H \qquad \text{as} \qquad H\to 0$$

so that the unbounded slope is avoided. The discontinuity around $P\approx 0$ cannot be avoided, however, and linearization is expected to be poor in this region.

When past history is used, these coefficients are then used with equations (E9) and (E8) in solution for residuals. In direct solution using the least-squares technique to obtain parameter adjustments, equations (E6) and (E7) are used. In either case, the results include P, σ_P^2, E, and σ_E^2; R_2 and $\sigma_{R,2}^2$ are available either as indicated or as adjusted when past history is used.

CORRECTIVE MANEUVERS

Only the knowledge available to the vehicle is used in determining and executing corrective maneuvers. Thus, the guidance logic is based strictly on the results of data reduction (not on the actual trajectory, which is unknown to the vehicle).

The indicated value and expected standard deviation of perigee error are

$$\left.\begin{aligned}\Delta P&=P_s-P_{tar}\\ \sigma_P&=\sqrt{\sigma_P^2}\end{aligned}\right\} \qquad \text{(D28)}$$

Corrective action is omitted unless both of the following conditions are met, as shown in figure 11:

$$|\Delta P|>k_{DB}\sigma_P \qquad \text{(19a)}$$

$$|\Delta P|+k_{DB}\sigma_P>\Delta P_{limit} \qquad \text{(20a)}$$

so that the tentative use of thrust is considered only if the indicated perigee error ΔP is larger than the significance placed in the data as reflected by k_{DB}, and the error plus the significance $\sigma_P k_{DB}$ is greater than the entry corridor ΔP_{limit}.

Using now the subscripts 1 for before and 2 for after the ΔV, the error in perigee after the correction is the larger of

$$\left.\begin{aligned}&\Delta P_{limit}-k_m\sigma_P\\ &k_{DM}\sigma_P\end{aligned}\right\}=\Delta P_2 \qquad \text{(22)}$$

or

so that the vehicle is corrected to "k_m sigmas" within the corridor or to "k_{DM} sigmas" from the target, whichever is larger. The perigee after ΔV is then

$$P_{s,2}=P_{tar}+\frac{\Delta P}{|\Delta P|}\Delta P_2 \qquad \text{(D29)}$$

so that the vehicle is corrected toward, but never intentionally beyond, the target. The corrective velocity increment is computed as indicated in equations (B2) and (B3), where $R_1=R_2=R$. Again,

$$E_2=\frac{E_1(R^2-P_1^2)+P_2-P_1}{R^2-P_2^2} \qquad \text{(B6)}$$

$$H_2=\frac{P_{s,2}}{|P_{s,2}|}\sqrt{P_2^2E_2+P_2} \qquad \text{(D16a)}$$

$$\Delta V=\frac{H_2-H_1}{R} \qquad \text{(B3)}$$

The ΔV must be within the limits imposed (arbitrarily herein) by the propulsion devices. If the ΔV is smaller than ΔV_{min}, thrust is omitted;

therefore, for thrust to be used, the condition required is $\Delta V \geq \Delta V_{min}$. If, however, $\Delta V > \Delta V_{max}$, too large an increment is demanded, and ΔV is set to $\Delta V = \Delta V_{max}$. In either case the execution of the correction is made. The resulting ΔV measured by the vehicle is generated using random numbers,

$$\left.\begin{aligned} \Delta V_{meas} &= \Delta V(1+\sigma_{\Delta V}[\delta]) \\ \beta_{meas} &= \sigma_{\beta}[\delta] \end{aligned}\right\} \tag{D30}$$

and the trajectory as known to the vehicle is computed as

$$\left.\begin{aligned} \dot{R}_2 &= \dot{R}_1 + \Delta V_{meas} \sin \beta_{meas} \\ R\dot{\theta}_2 &= R\dot{\theta}_1 + \Delta V_{meas} \cos \beta_{meas} \end{aligned}\right\} \tag{B7}$$

$$\left.\begin{aligned} H_2 &= R(R\dot{\theta}_2) \\ E_2 &= \dot{R}_2^2 + (R\dot{\theta}_2)^2 - \frac{1}{R} \\ \epsilon_2^2 &= 1 + 4E_2H_2^2 \\ P_2 &= \frac{1}{2E_2}\sqrt{\epsilon_2^2 - 1} \\ P_{s,2} &= \frac{H_2}{|H_2|} P_2 \end{aligned}\right\} \tag{D31}$$

where $P_{s,2}$ is the argument of the perigee with the sign of the direction of rotation.

The variance of the corrected trajectory is (from eqs. (B13) and (15))

$$\left.\begin{aligned} \sigma_P^2 &= \sigma_P^2 + \frac{4\Delta V_{meas}^2}{\epsilon_2^2}\left[\frac{H_2^2}{R^2}(R^2 - P_2^2)^2\sigma_{\Delta V,ex}^2 + P_2^4 R_2^2 \sigma_{\beta,ex}^2\right] \\ \sigma_E^2 &= \sigma_E^2 + 4\Delta V_{meas}^2\left(\dot{R}_2^2\sigma_{\beta,ex}^2 + \frac{H_2^2}{R^2}\sigma_{\Delta V,ex}^2\right) \end{aligned}\right\} \tag{D32}$$

where the error $\sigma_{\Delta V}$ and the expected error $\sigma_{\Delta V,ex}$ are considered percentage errors rather than fixed ΔV errors.

CORRECTION OF ACTUAL TRAJECTORY

The actual (or true) corrective action is determined from the measured $(\Delta V, \beta)$ correction using random measurement errors,

$$\left.\begin{aligned} \Delta V_a &= \Delta V_{meas}(1+\sigma_{\Delta V,a}[\delta]) \\ \beta_a &= \sigma_{\beta,a}[\delta] \end{aligned}\right\} \tag{D30a}$$

and the actual trajectory after correction is computed using equations (B2) to (B4) but with true values, P_a, E_a, and so forth. The position on the trajectory is computed assuming the coasting period as representative of the first-order approximations to the effects of finite engines, and so forth:

$$\left.\begin{aligned} \Delta\tau &= \Delta\tau_{stop} + \frac{|\Delta V_a|}{A_p} \\ \Delta\tau_a &= \Delta\tau(1+\sigma_{\Delta\tau}[\delta]) \\ \tau_{go,a,2} &= \tau_{go,a,1} - \Delta\tau_a \\ R_a &= R_a(P_a, E_a, \tau_{go,a,2}) \end{aligned}\right\} \tag{D33}$$

The step-size logic is then repeated, and the sequence of data acquisition, data reduction, and corrective action is continued until cutoff logic interrupts and signifies the final correction before entry. The modified guidance logic is then substituted as described in discussion of figure 11.

APPENDIX E

LEAST-SQUARES DATA REDUCTION

The general problem of least squares and error propagation is treated in the literature (e.g., refs. 9 and 16). A brief discussion is presented here only to develop the nomenclature used in analysis. The method and symbolism are directly shortened from those of Brown (ref. 11) and others.

Introduce first the elements $x_1^\circ, x_2^\circ, \ldots x_n^\circ$ of a set of observations, and a set of unknown parameters $\gamma_1, \gamma_2, \ldots \gamma_p$. The number of independent condition equations, m, is $m=n-n_0+p$, where n_0 is the minimum number to determine the set of observations.

The condition equations are

$$\left.\begin{aligned} &f_1(x_1, x_2, \ldots x_n, \gamma_1, \gamma_2, \ldots \gamma_p)=0 \\ &f_2(x_1, x_2, \ldots x_n, \gamma_1, \gamma_2, \ldots \gamma_p)=0 \\ &\cdot \\ &\cdot \\ &\cdot \\ &f_m(x_1, x_2, \ldots x_n, \gamma_1, \gamma_2, \ldots \gamma_p)=0 \end{aligned}\right\} \qquad \text{(E1)}$$

The adjusted observation will be

$$x_i=x_i^\circ+v_i \qquad i=1, 2, \ldots n \qquad \text{(E2)}$$

where the residuals v are presently unknown, and the adjusted parameters are

$$\gamma_j=\gamma_j^\circ+\delta\gamma_j \qquad j=1, 2, \ldots p \qquad \text{(E3)}$$

where the γ_j° are initial estimates and the $\delta\gamma_j$ are presently unknown corrections.

If equations (E2) and (E3) are substituted into (E1) and the residuals and parameter corrections are small, the resulting equations can be approximated by the zero- and first-order terms of Taylor expansions. The discrepancy $\mathscr{E}$ is then

$$\mathscr{E}_i=f_i(x_1^\circ, x_2^\circ, \ldots x_n^\circ, \gamma_1^\circ, \gamma_2^\circ, \ldots \gamma_p^\circ) \qquad i=1, 2, \ldots m$$

$$a_{ij}=\frac{\partial \mathscr{E}_i}{\partial x_j^\circ}, \qquad j=1, 2, \ldots n$$

$$b_{ik}=\frac{\partial \mathscr{E}_i}{\partial \gamma_k^\circ}, \qquad k=1, 2, \ldots p$$

and

$$\left.\begin{aligned} &a_{11}v_1+a_{12}v_2+\ldots+a_{1n}v_n+b_{11}\delta\gamma_1+b_{12}\delta\gamma_2+\ldots+b_{1p}\delta\gamma_p+\mathscr{E}_1=0 \\ &a_{21}v_1+a_{22}v_2+\ldots+a_{2n}v_n+b_{21}\delta\gamma_2+b_{22}\delta\gamma_2+\ldots+b_{2p}\delta\gamma_p+\mathscr{E}_2=0 \\ &\cdot \\ &\cdot \\ &\cdot \\ &a_{m1}v_1+a_{m2}v_2+\ldots+a_{mn}v_n+b_{m1}\delta\gamma_1+b_{m2}\delta\gamma_2+\ldots+b_{mp}\delta\gamma_p+\mathscr{E}_m=0 \end{aligned}\right\} \qquad \text{(E4)}$$

There are n unknown residuals and p unknown parameter corrections in m equations, and the set is overdetermined when $m<n+p$.

The result desired is that which minimizes the weighted sum of the squares of the residuals. Assuming that the observations are uncorrelated,

$$S=\frac{v_1^2}{\sigma_1^2}+\frac{v_2^2}{\sigma_2^2}+\ldots\frac{v_n^2}{\sigma_n^2} \qquad \text{(E5)}$$

where the unit variance of reference 11 is multiplied out for this development, and the weight of an observation is inversely proportional to its variance σ^2.

The diagonal matrix of the variances of the observations is denoted as

$$\underline{\sigma}=\begin{bmatrix}\sigma_1^2 & 0 & \cdots & 0\\ 0 & \sigma_2^2 & \cdots & 0\\ \cdot & \cdot & & \cdot\\ \cdot & \cdot & & \cdot\\ \cdot & \cdot & & \cdot\\ 0 & 0 & \cdots & \sigma_n^2\end{bmatrix}$$

and

$$\underline{A}=\begin{bmatrix}a_{11} & a_{12} & \cdots & a_{1n}\\ a_{21} & a_{22} & \cdots & a_{2n}\\ \cdot & \cdot & & \cdot\\ \cdot & \cdot & & \cdot\\ \cdot & \cdot & & \cdot\\ a_{m1} & a_{m2} & \cdots & a_{mn}\end{bmatrix},\quad \underline{v}=\begin{bmatrix}v_1\\ v_2\\ \cdot\\ \cdot\\ \cdot\\ v_n\end{bmatrix},\quad \underline{\mathscr{E}}=\begin{bmatrix}\epsilon_1\\ \epsilon_2\\ \cdot\\ \cdot\\ \cdot\\ \epsilon_m\end{bmatrix}$$

are, respectively, the coefficient of the observations matrix $\underline{A}$, the residual vector $\underline{v}$, and the discrepancy vector $\underline{\mathscr{E}}$. The coefficient matrix of the parameters $\underline{B}$ and the vector of parameter adjustments $\underline{\delta}$ are

$$\underline{B}=\begin{bmatrix}b_{11} & b_{12} & \cdots & b_{1P}\\ b_{21} & b_{22} & \cdots & b_{2P}\\ \cdot & \cdot & & \cdot\\ \cdot & \cdot & & \cdot\\ \cdot & \cdot & & \cdot\\ b_{m1} & b_{m2} & \cdots & b_{mP}\end{bmatrix},\quad \underline{\delta}=\begin{bmatrix}\delta\gamma_1\\ \delta\gamma_2\\ \cdot\\ \cdot\\ \cdot\\ \delta\gamma_P\end{bmatrix}$$

In matrix notation equation (E4) becomes

$$\underline{A}\underline{v}+\underline{B}\underline{\delta}+\underline{\mathscr{E}}=0$$

and equation (E5) for the weighted sum of squares of the residuals is

$$S=\underline{v}^T(\underline{\sigma})^{-1}\underline{v}$$

The derivation of reference 11 will not be repeated herein. The reduced normal equations that result are

$$[\underline{B}^T(\underline{A\sigma A}^T)^{-1}\underline{B}]\underline{\delta}+\underline{B}^T(\underline{A\sigma A}^T)^{-1}\underline{\mathscr{E}}=0 \qquad \text{(E6)}$$

which can usually be solved for the parameter corrections δ, which can then be used in

$$\underline{v}=-\underline{\sigma A}^T[(\underline{A\sigma A}^T)^{-1}(\underline{B\delta}+\underline{\mathscr{E}})]$$

to determine the residuals. The covariance matrix of the adjusted parameters is

$$\sigma_{\delta\delta^T}=[\underline{B}^T(\underline{A\sigma A}^T)^{-1}\underline{B}]^{-1} \qquad \text{(E7)}$$

The covariance matrix of the adjusted observations is obtained by subtracting the covariance matrix of the residuals σ_{vv^T} from that of the original observations $\underline{\sigma}$ (or $\sigma_{zz^T}=\underline{\sigma}-\sigma_{vv^T}$):

$$\sigma_{vv^T}=(\underline{A\sigma})^T\{(\underline{A\sigma A}^T)^{-1}-[\underline{B}^T(\underline{A\sigma A}^T)^{-1}]^T [\underline{B}^T(\underline{A\sigma A}^T)^{-1}\underline{B}]^{-1}\underline{B}^T(\underline{A\sigma A}^T)^{-1}\}\underline{A\sigma}$$

For the data reduction of this analysis, however, only special cases of these results are required to solve for the residuals and the covariance matrix of the adjusted observations. When no parameters are used,

$$\underline{v}=-\underline{\sigma A}^T(\underline{A\sigma A}^T)^{-1}\underline{\mathscr{E}} \qquad \text{(E8)}$$

$$\sigma_{vv^T}=(\underline{A\sigma})^T(\underline{A\sigma A}^T)^{-1}\underline{A\sigma} \qquad \text{(E9)}$$

When the orbital elements of this study are used as parameters, such as is done to use the least-squares method in direct calculation, the equations are not overdetermined, and $\underline{v}$ and σ_{vv^T} are not required. In that case only $\underline{\delta}$ and $\sigma_{\delta\delta^T}$ are computed, and the equations are iterated until $\underline{\delta}$ becomes negligible.

APPENDIX F

SENSITIVITY OF TRAJECTORY DETERMINATION TO ERRORS IN BASIC MEASUREMENTS

Expected errors in trajectory determination resulting from assumed errors in the measurement system are presented in the ANALYSIS (figs. 6 to 9). The sensitivity to each of the component measurement errors is considered here.

The form of illustration is that of figures 6 and 7, except that error coefficients are shown rather than the expected standard deviation of trajectory elements. Where coefficients are multiplied by probable errors to illustrate the relative sensitivity to various components of the measurement system, the usual limitations of the linearization process should be considered. The results are shown for a trajectory of 0.2 energy (v_h=16,400 ft/sec) and 1 perigee (tangent to the surface) as a function of ΔR for a series of R_2. The region (R_2,ΔR) of interest to multiple-correction guidance is not noted, but is shown in figures 6, 7, or 10.

The error coefficient in perigee determination due solely to the measurement of range and the direction of range is shown in figure 24(a). Since the direction of range enters into the computation of $\Delta\varphi$, $\Delta\varphi$ is not considered errorless even though errors in determination of star positions are not considered. This interpretation results from the use of the range-measuring instruments to determine the direction $\hat{R}$ and is not a result of the use of occultation. Range is computed from apparent planet size (eq. (C3)), and it has been indicated that errors increase rapidly with range. This is reflected in the error coefficient for perigee determination. In the region of interest to multiple-correction guidance schemes, the error coefficient varies from about 1.25 with ΔR=1 radius and R_2=1.2 radii to about 800 with ΔR=10 and R_2=100 radii. The variation with range is about 640:1. Minimum error coefficient, or maximum accuracy, occurs with ΔR of the same order as R_2; in other words, $R_2 \simeq R_1/2$. Accuracy decreases with larger ΔR because of increasing R_1 terms; while, for ΔR smaller than those of maximum accuracy, large difference terms cause accuracy to decrease, and for $\Delta R \ll R_2$ the error coefficient is inversely proportional to ΔR.

To illustrate the standard deviation in the region of interest, assume a measurement system of 0.0002-radian standard deviation (40-sec arc). The variation with range is then from 0.00025 to 0.16 radius (perigee error of 1 to 640 miles, 0.9 to 555 Int. naut. miles).

The error coefficient in perigee determination due to errors in star-position measurement is shown in figure 24(b). The sensitivity to $\Delta\varphi$ is *not* illustrated, only that portion of $\Delta\varphi$ due to star-position measurement or, in other words, only the portion not contributed by range instrumentation. The rapid increase in error coefficient with range is again noted in figure 24(b). Maximum accuracy occurs with very large step sizes, and for $\Delta R \ll R_2$ the error coefficient increases approximately as $1/\Delta R$. For R_2=1.2 and ΔR=1 radius, the error coefficient is 1.1 radii per radian, or about 0.00022 radius (0.9 mile, 0.8 Int. naut. mile) assuming errors of 40-second-arc rms. Similarly, for R_2=100 and ΔR=10 radii, the error coefficient is 800 radii per radian, or 0.16 radius (640 miles).

In the range of interest for multiple-correction guidance, the uncertainties in perigee determination due to range sensing instruments and star-position sensing instruments are of equivalent significance, varying less than 1.2:1. The measurement scheme hypothesized in this analysis, however, measures star and planet positions with the same instrumentation. The error coefficients are illustrated separately to permit a brief look at other possibilities, such as the use of an inertial reference direction determined with precision position gyroscopes (refs. 17 and 24). With equivalent sensitivity for errors in the planet observations and errors in inertial reference direction, increased errors in either portion will be reflected in reduced performance of the guidance system. Gains in system performance up to 30

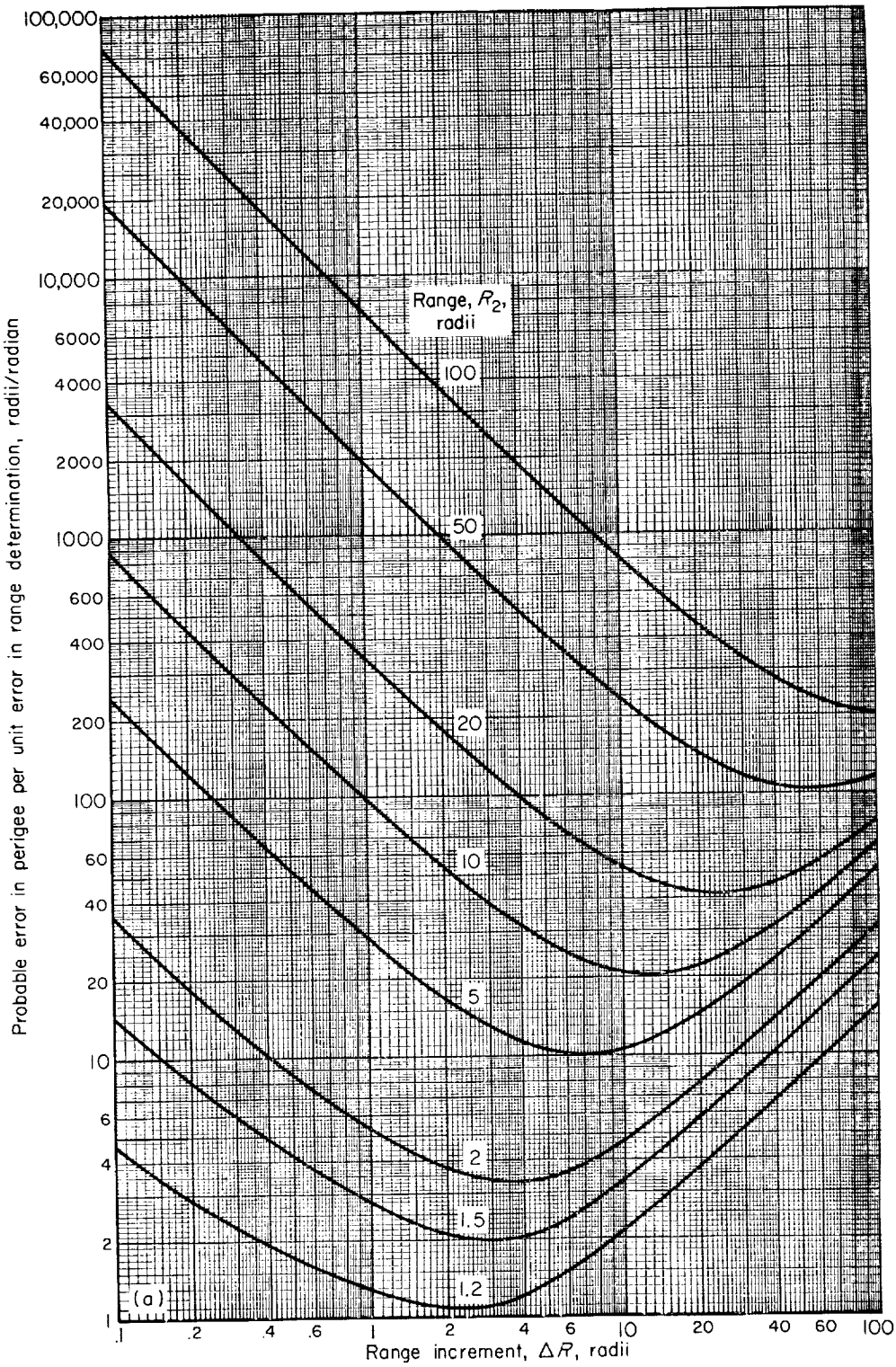

(a) Errors in measuring magnitude and direction of range.

FIGURE 24.—Probable errors in perigee determination. Perigee range, P, 1; energy, 0.2.

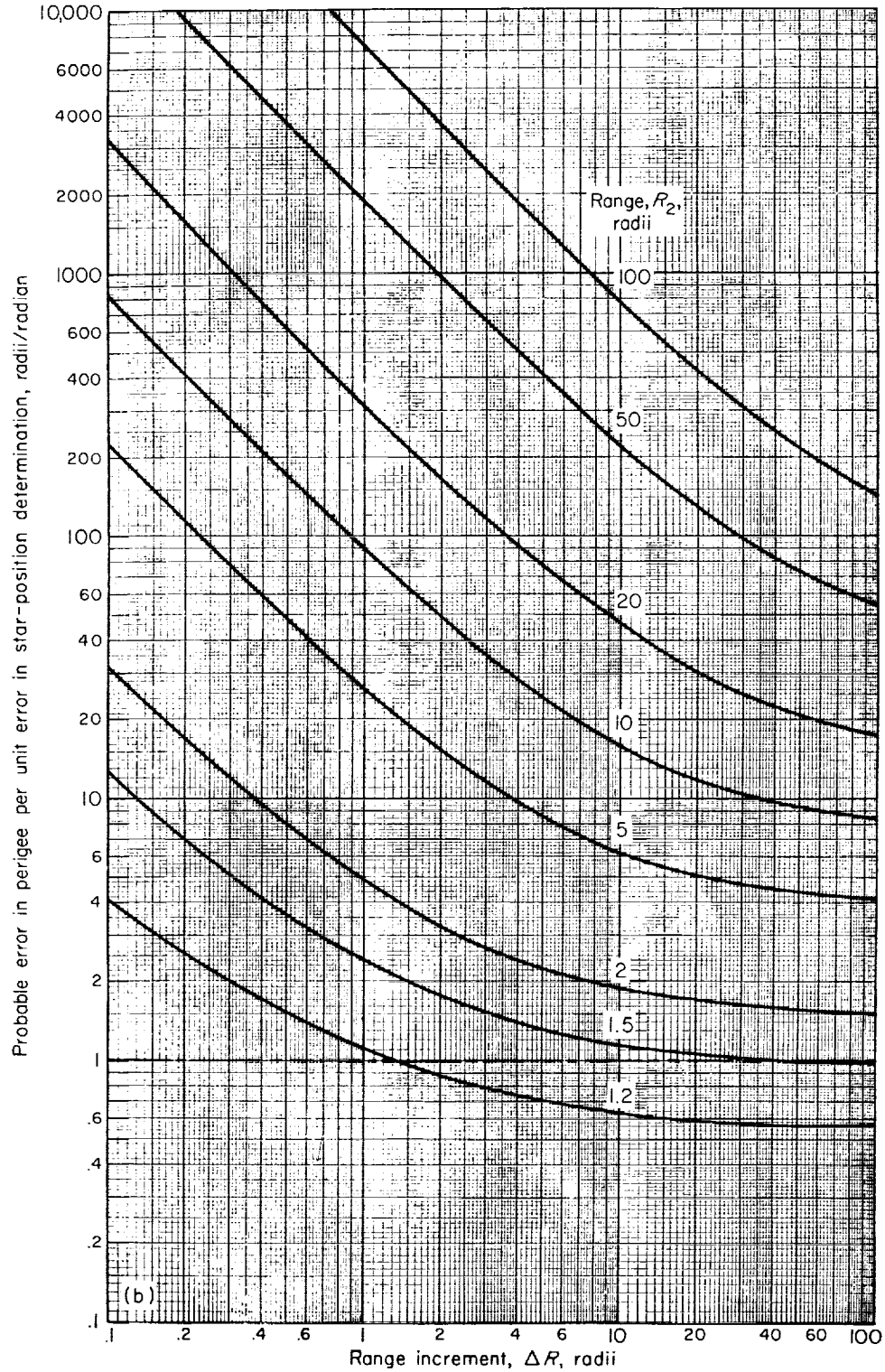

(b) Errors due to star-position determination.

FIGURE 24.—Continued. Probable errors in perigee determination. Perigee range, P, 1; energy, 0.2.

or 40 percent, however, are possible if errors due to the gyroscopic or star-tracking system are significantly less than errors in the range-measuring system.

The error coefficient for perigee determination due to errors in the optical system as hypothesized in this analysis is shown in figure 24(c). At large ΔR the errors due to range measurement are much larger than those due to star-position measurement, and the curves assume approximately the shape of figure 24(a), with broad regions of $\Delta R \approx 2R_2$ yielding near-optimum error coefficients. In the region of interest to the multiple-correction scheme presented herein, the error coefficient is roughly $\sqrt{2}$ larger than for either of the component measurements separately (figs. 24(a) and (b)). Thus, at $R_2=1.2$ radii and $\Delta R=1$ radius, the error coefficient is 1.7 radii per radian; and at $R_2=100$ and $\Delta R=10$ radii, it increases to 1150 radii per radian. With a measurement accuracy of 40-second arc, these become uncertainties of 1.36 to 920 miles rms.

The optical system as hypothesized herein observes the surface of the target planet. The sensitivity of perigee determination to uncertainties in planet size or terrain is shown in figure 24(d). For short range and large ΔR the error in perigee approaches the uncertainty, but for small increments the error coefficient increases inversely with ΔR. With $R_2=1.2$ radii and $\Delta R=1$ radius, the error coefficient is 1.7 radii per radius; and, with $R_2=100$ and $\Delta R=10$ radii, it increases to 5 radii per radius. At long range this error sensitivity is small and usually insignificant with respect to others errors. The assumption of distribution shape and numerical size of planet surface uncertainties is subject to question. In no case, however, can guidance accuracy exceed the knowledge in the observed portion of the target planet. (Herein, the surface is used.) Thus, if the uncertainty is assumed as 0.0002 radius rms, as herein, the error becomes 0.00034 radius or 1.36 miles rms. In other words, by assuming an uncertainty of 0.8 mile rms, the minimum corridor attainable with high success probability is about $\pm 3\sigma \times 0.8$ miles, or roughly a 5-mile altitude, even with otherwise perfect systems.

The value of planet surface errors assumed is intended to represent the uncertainties that might occur approaching Earth where mountains 4 miles high may be observed occasionally and the average terrain may vary from sea level to 1.6 miles or ± 0.8 mile. This error would not be representative of errors due to cloud cover or due to planet oblateness. Judicious choice of optical wavelengths is one possibility of avoiding cloud-cover problems, and oblateness can be considered in data reduction if a rough knowledge of range orientation with respect to the equatorial plane is available.

The final measurements used in perigee determination are time increments. The error coefficients of timing errors are shown in figure 24(e) for errors assumed proportional to the time increment. The sensitivity to errors in timing is of the order of 1 decade less than that of the optical errors. For example, with $R_2=100$ and $\Delta R=10$ radii, the probable error is 1.4 radii; and, for $R_2=1.2$ radii and $\Delta R=1$ radius, it is 0.4 radius. With the assumed error of 0.01 percent (9 sec per day), expected errors are 0.56 and 0.16 mile. As a result, timing errors are negligible in effect on perigee determination.

The combined effects of errors in measurement on the accuracy of trajectory determination are shown in figure 6(a), illustrating the σ_P resulting from the components as just discussed, and figure 6(b), illustrating the σ_E as is considered next.

As the guidance problem is considered herein, the trajectory energy is not controlled during the approach to an entry corridor. The accuracy of energy determination is of interest, however, because E is used in determining corrective maneuvers, maintaining the history of past data reductions, and computing the time increments of the sampling-rate schedule. To simplify the interpretation of sensitivities in the determination of trajectory energy, parenthetical values are expressed as the changes in entry velocity for an approach to Earth. The nominal value is 40,400 feet per second for $E=0.2$.

The error coefficients for energy determination due to errors in range measurement, star-position measurement, and measurement using the optical system as hypothesized herein are shown in figures 25(a), (b), and (c), respectively. The characteristics of the variation with range and range-increment size are similar to those illustrated in figure 24(a) for the sensitivity of perigee determination. The effects of star-position errors (fig. 25(b)) are different from those previously illustrated in that range has very small effects,

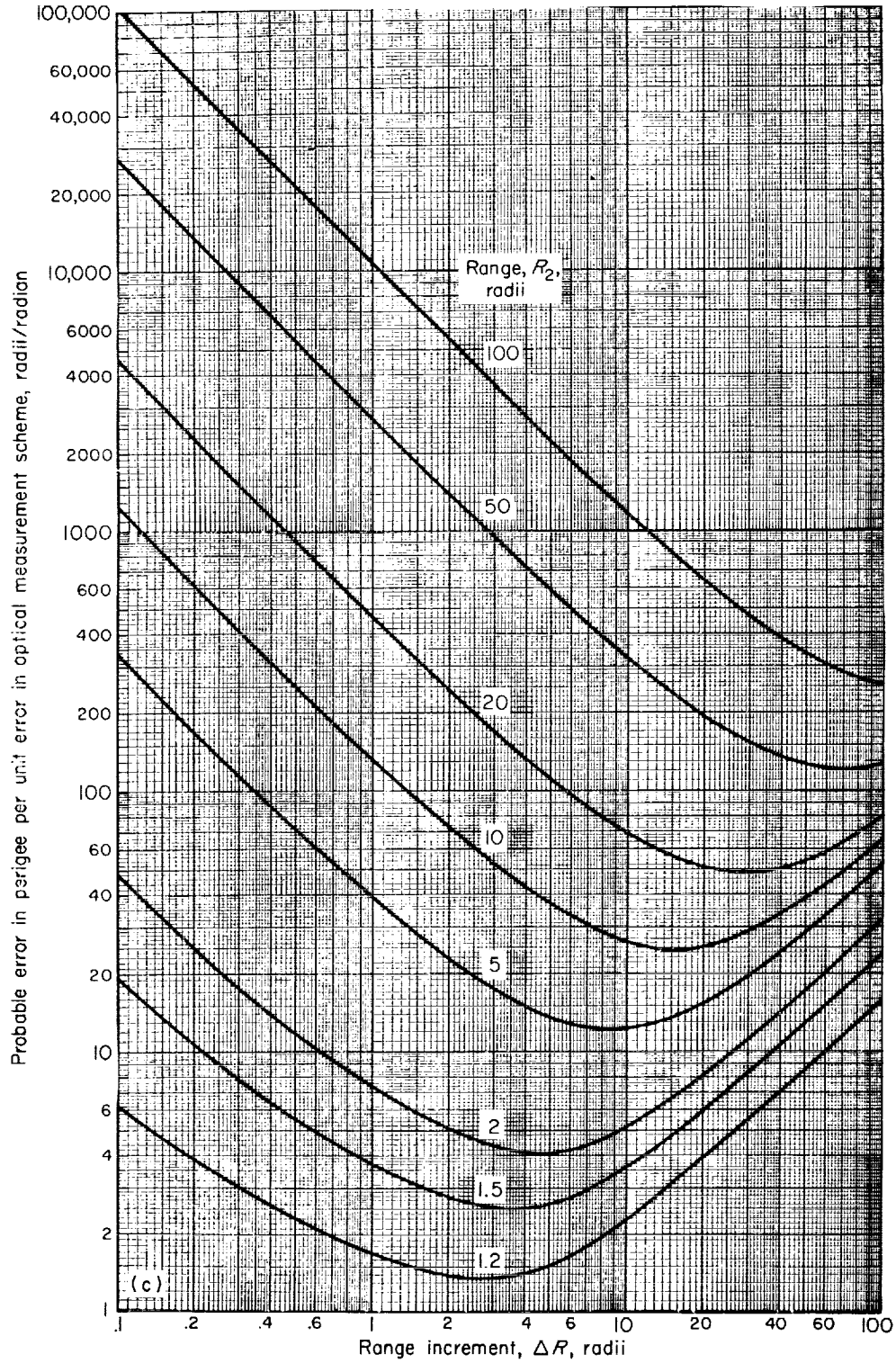

(c) Errors in assumed optical measurement scheme.

FIGURE 21.—Continued. Probable errors in perigee determination. Perigee range, P, 1; energy, 0.2.

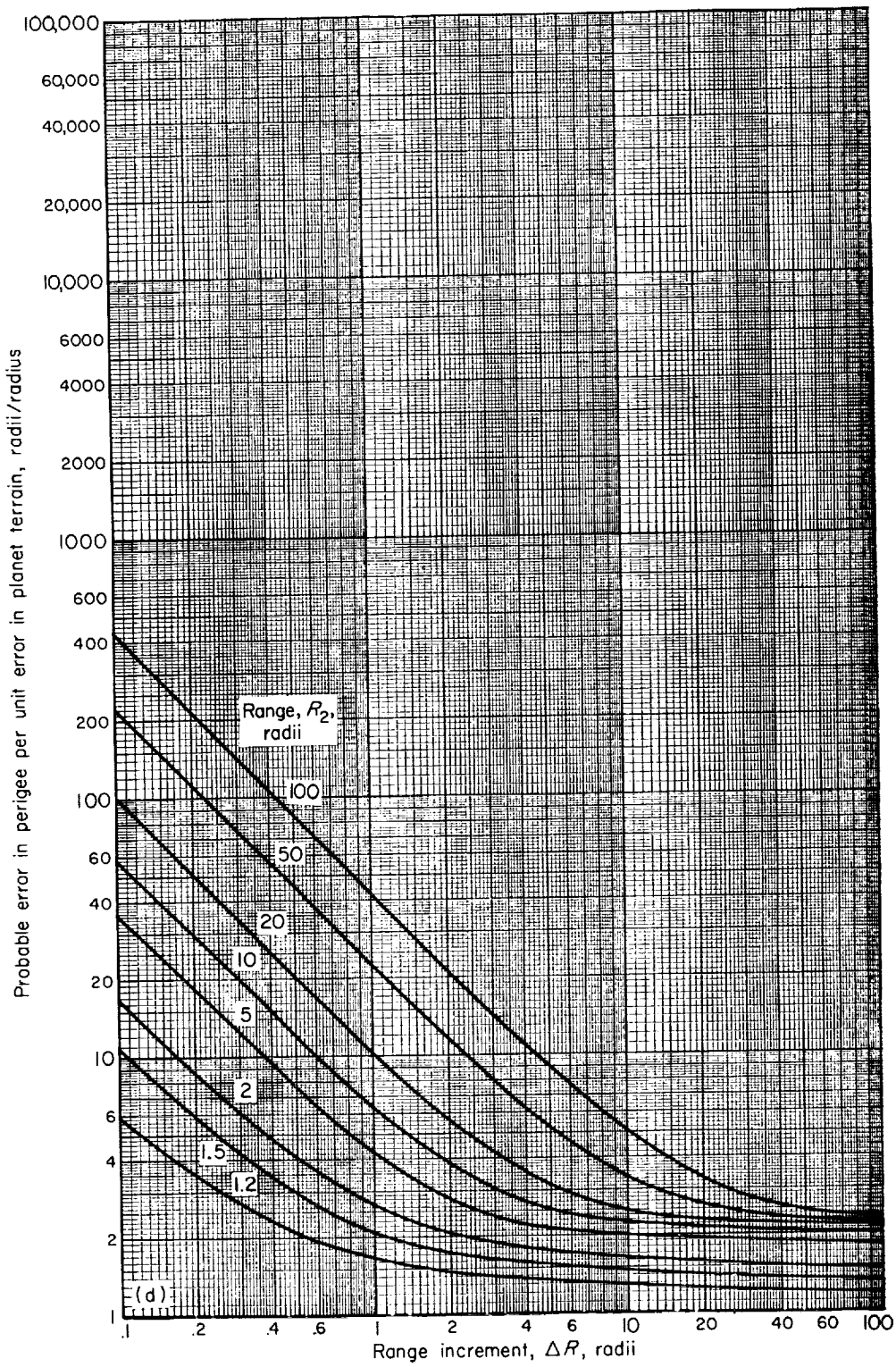

(d) Errors due to uncertainties in planet terrain.

FIGURE 24.—Continued. Probable errors in perigee determination. Perigee range, P, 1; energy, 0.2.

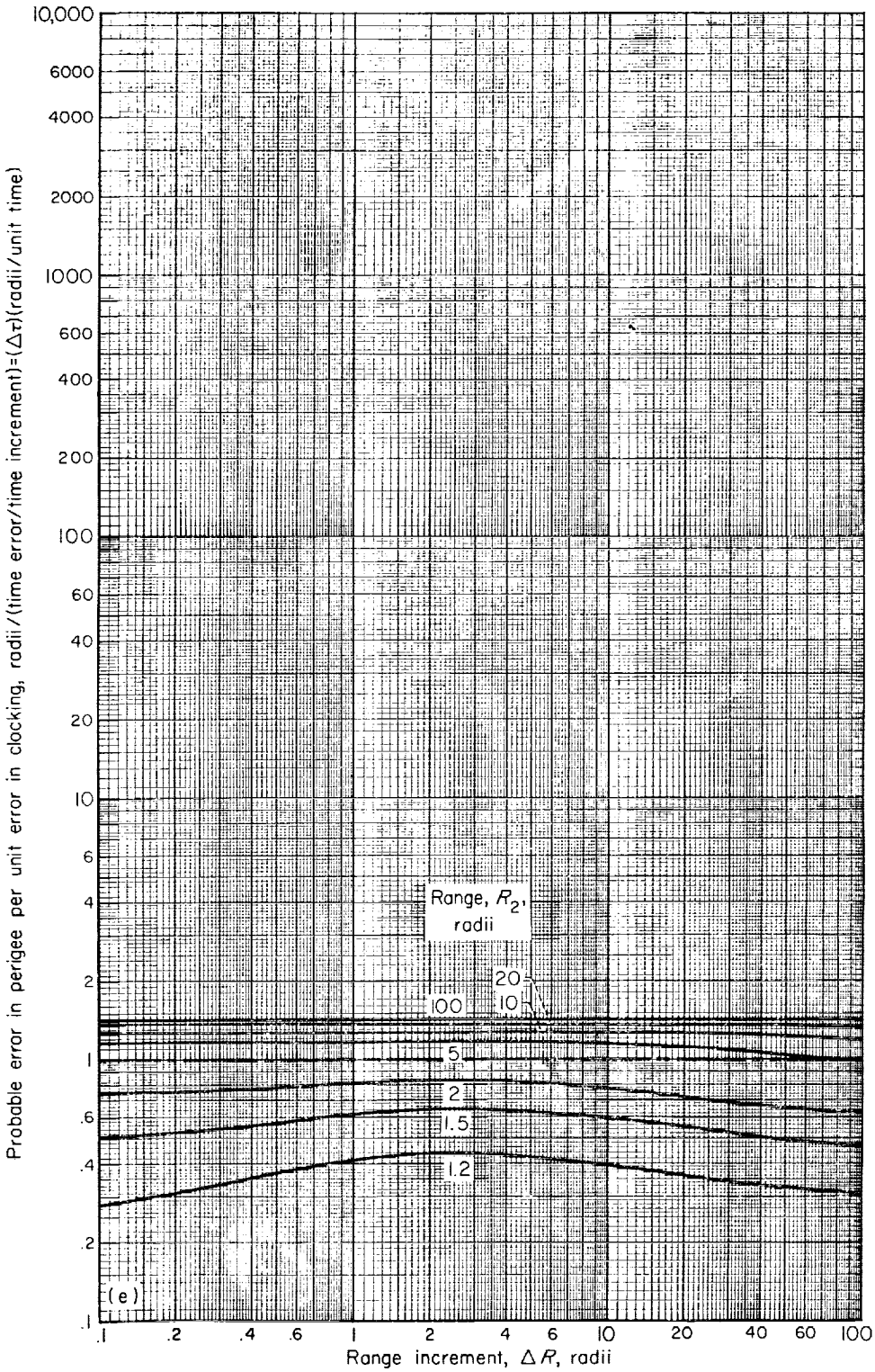

(e) Errors due to clocking errors proportional to time increment.

FIGURE 24.—Concluded. Probable errors in perigee determination. Perigee range, P, 1; energy, 0.2.

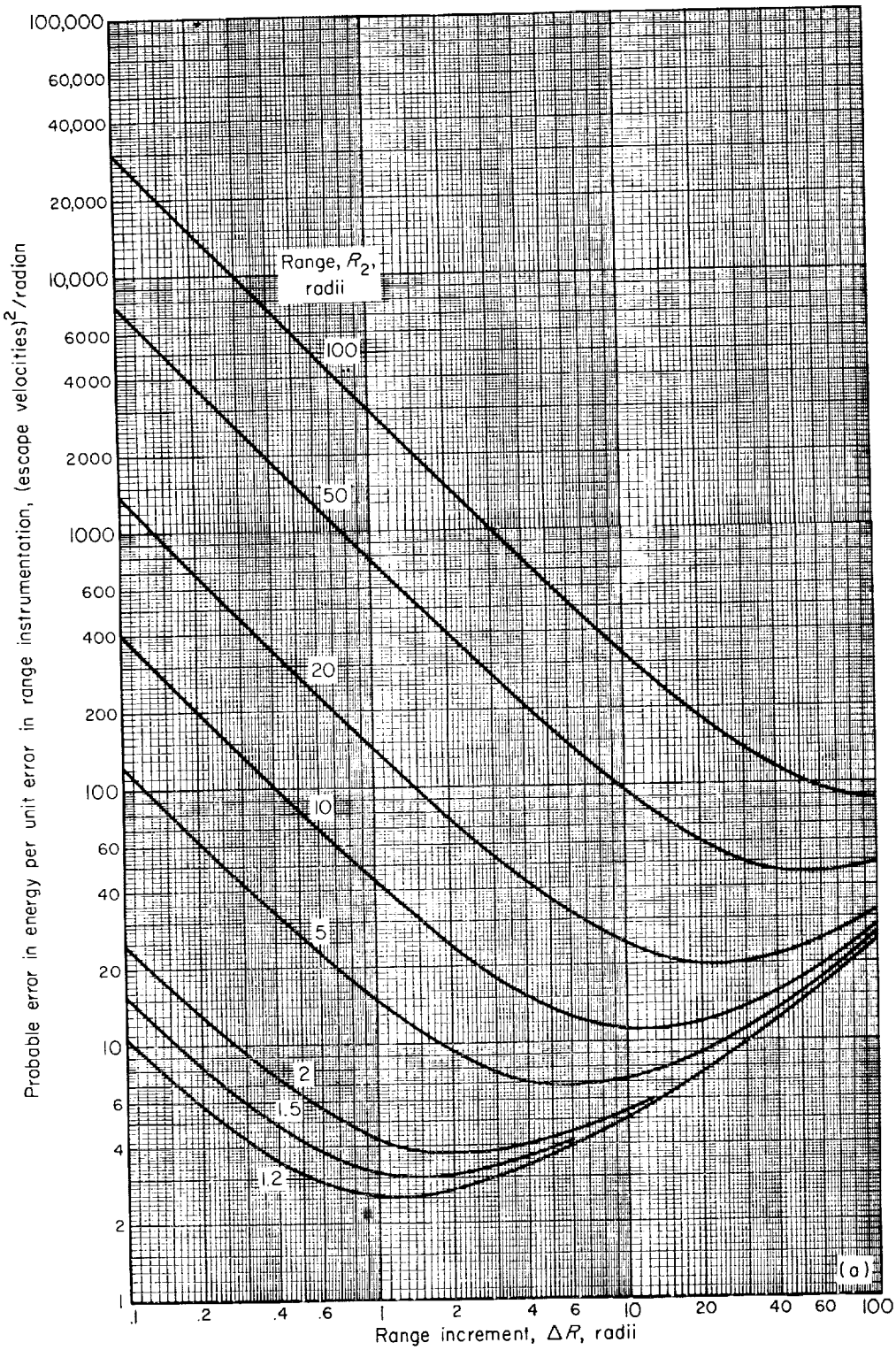

(a) Errors in measuring magnitude and direction of range.

FIGURE 25.—Probable errors in energy determination. Perigee range, P, 1; energy, 0.2.

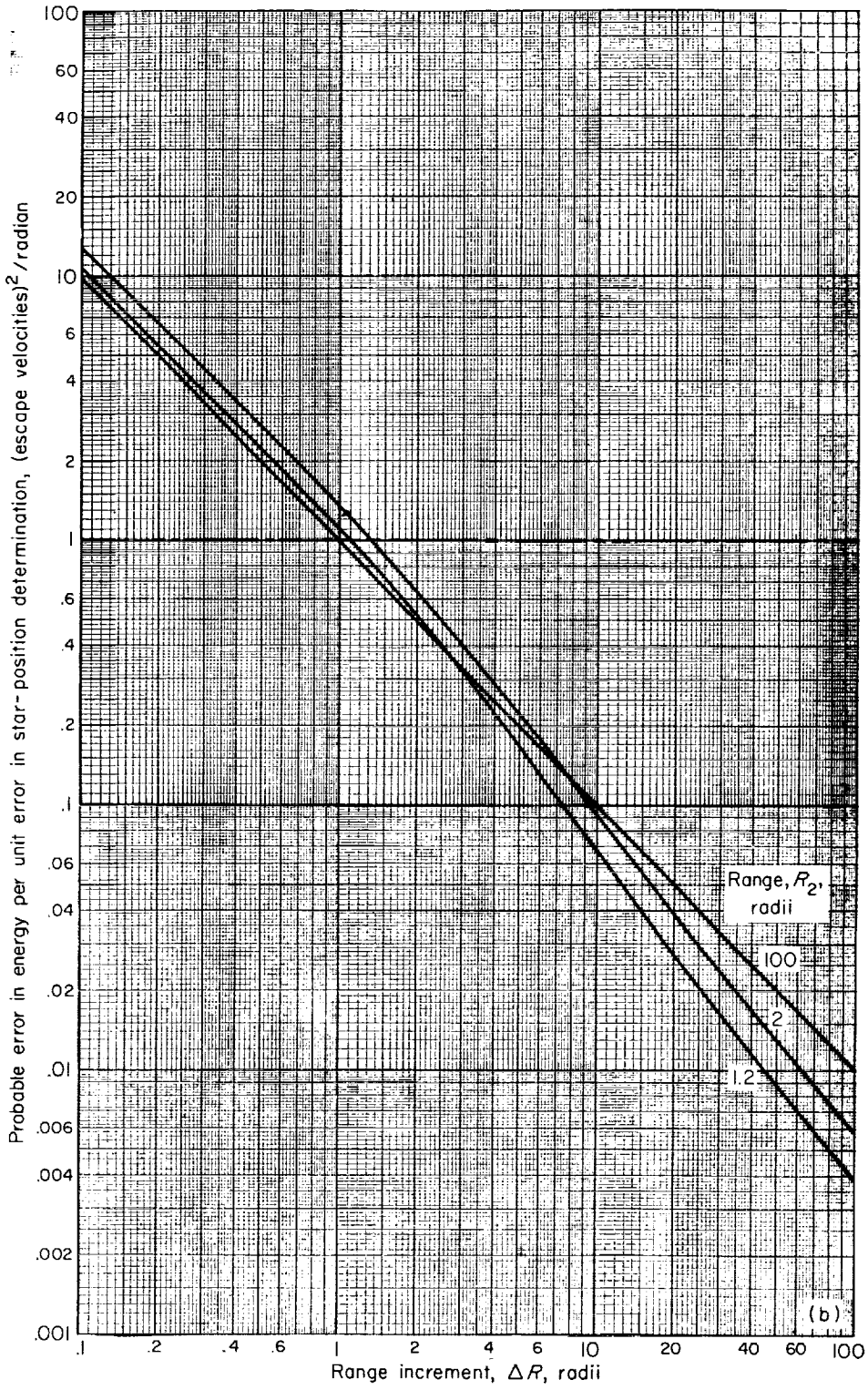

(b) Errors due to star-position determination.

FIGURE 25. Continued. Probable errors in energy determination. Perigee range, P, 1; energy, 0.2.

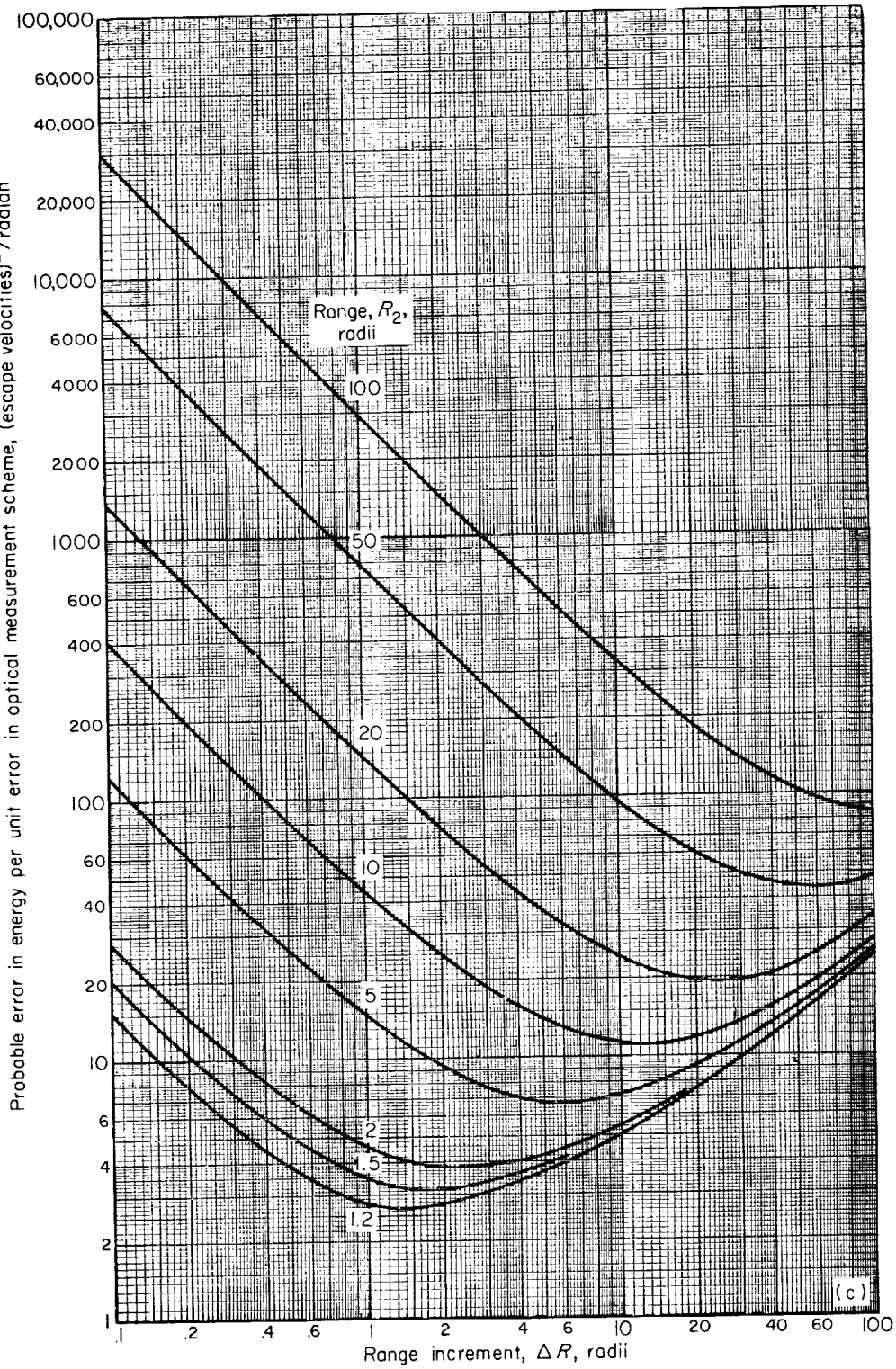

(c) Errors in assumed optical measurement scheme.

FIGURE 25.—Continued. Probable errors in energy determination. Perigee range, P, 1; energy, 0.2.

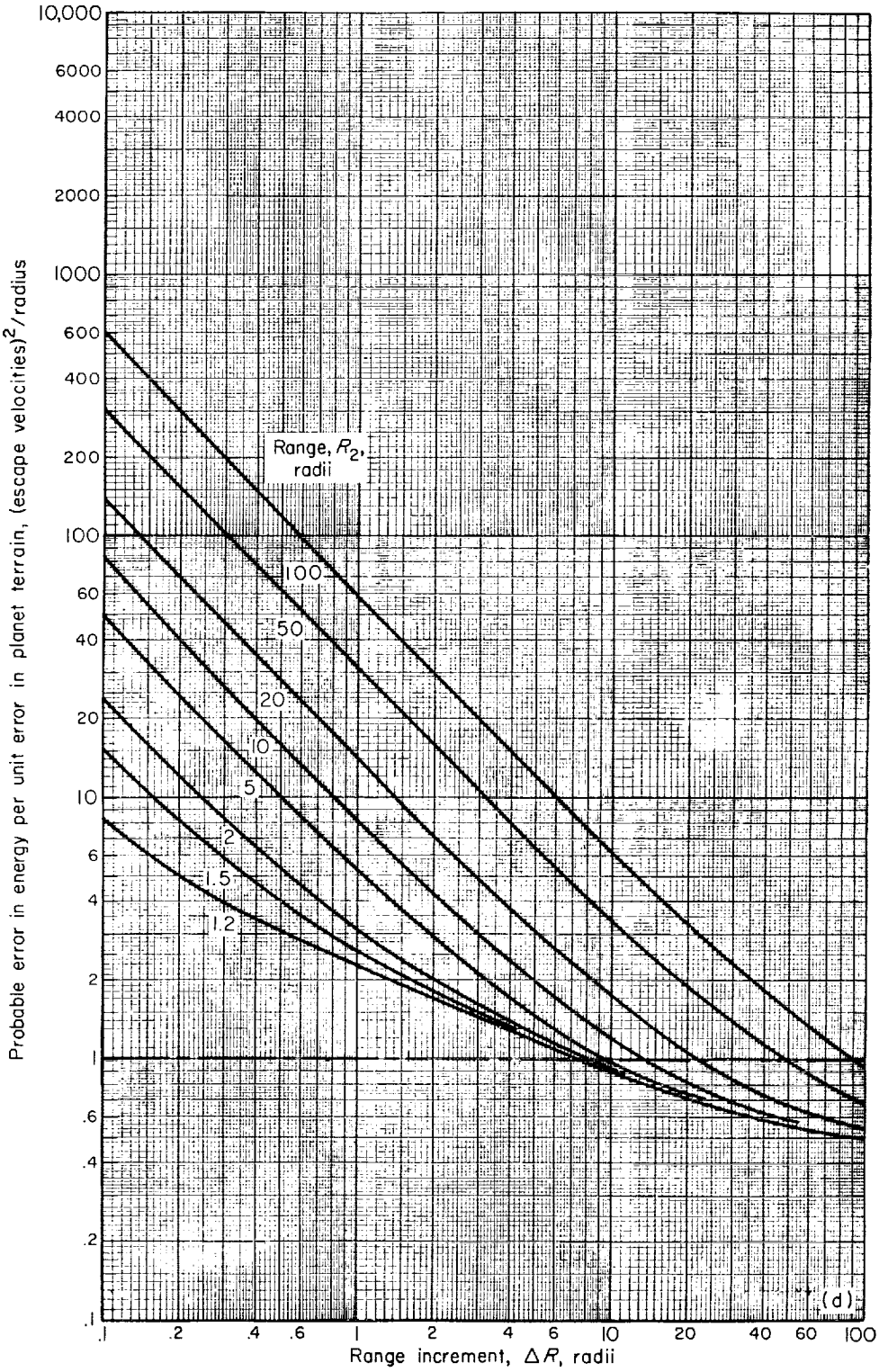

(d) Errors due to uncertainties in planet terrain.

FIGURE 25.—Continued. Probable errors in energy determination. Perigee range, P, 1; energy, 0.2.

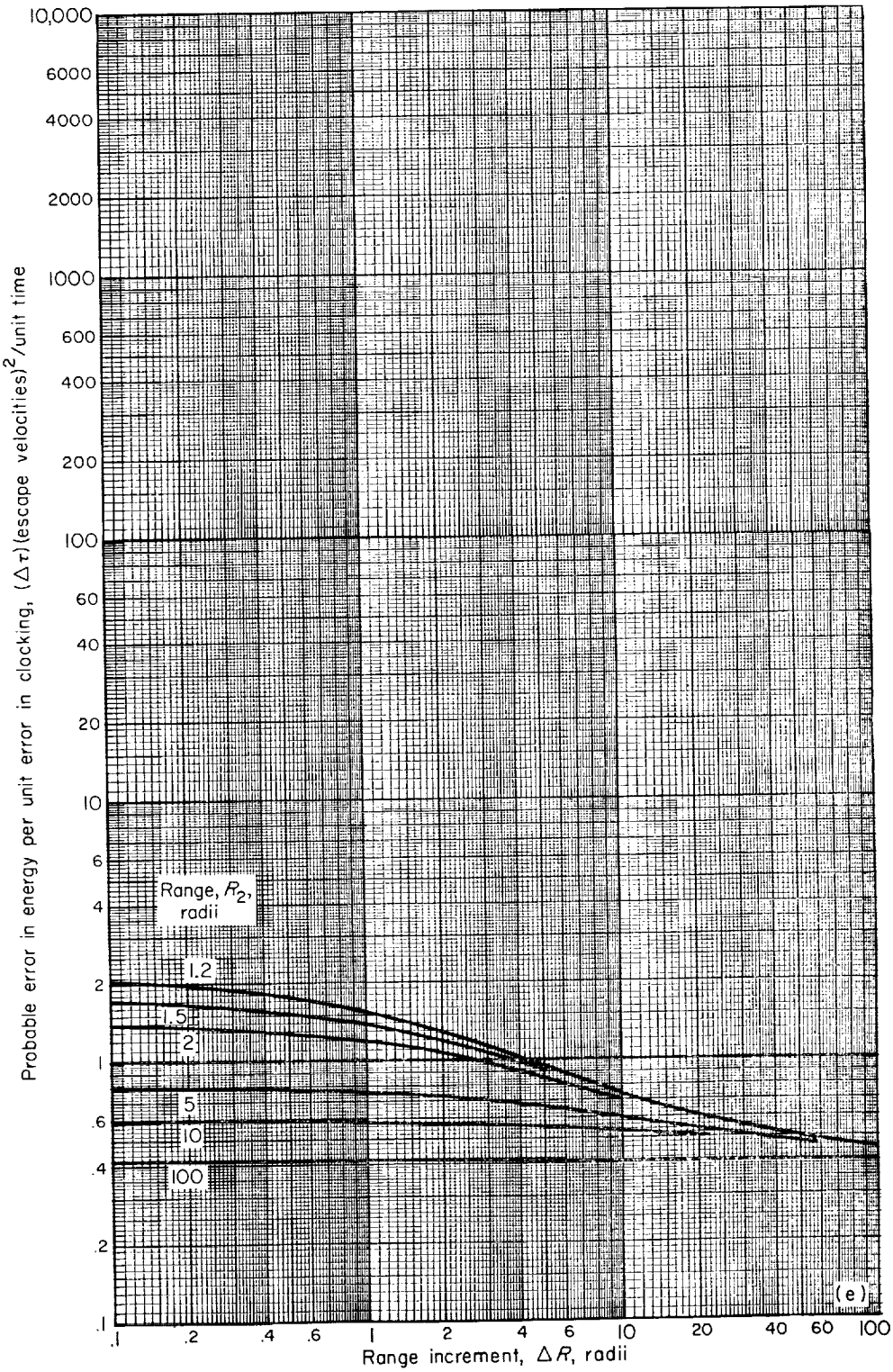

(e) Errors due to clocking errors proportional to time increment.

FIGURE 25.— Concluded. Probable errors in energy determination. Perigee range, P, 1; energy, 0.2.

the sensitivity is small, and the sensitivity varies inversely with the increment size ΔR. The error coefficient for the optical system (fig. 25(c)) varies from 2.7 with $R_2=1.2$ radii and $\Delta R=1$ radius to 325 with $R_2=100$ and $\Delta R=10$ radii, with units 1 per radius-radian or escape velocities squared per radian. With 40-second-arc measurement accuracy, this represents errors of 0.00054 to 0.065 1/radius (or roughly 10 to 1100 ft/sec error in entry velocity). The sensitivity (probable error) in energy is relatively small in comparison with the sensitivity of the perigee in the effects on entry conditions.

The error coefficients for energy determination due to uncertainties in planet terrain are shown in figure 25(d), and the characteristics are similar to those of perigee determination (fig. 24(d)), except that the error coefficients continue to decrease as ΔR increases. The variation with range for the ΔR of interest to the multiple-correction scheme is again about 5 to 2. For the assumed error of 0.0002 radius, the energy is determined to an accuracy of 0.00045 per radius with $R_2=1.2$ radii and $\Delta R=1$ radius (7.5 ft/sec). As indicated previously, this uncertainty is not an instrument inaccuracy, but is a physical limitation due to imperfect knowledge of the planet.

The error coefficients for energy determination due to timing errors (fig. 25(c)) are again considerably smaller than those of the optical measurements, except at short range. The variation with range is inverted, so that larger uncertainties occur at short range, and the variation with ΔR is small at short range and negligible at long range. The significance of errors in timing is slight, as indicated by the maximum error coefficient of 1.5 for the region of increment sizes of interest to multiple-correction guidance. For assumed errors of 0.01 percent, the expected error in energy is then 0.00015 per radius (roughly 2 ft/sec error in entry velocity for an approach to Earth).

REFERENCES

1. Chapman, Dean R.: An Analysis of the Corridor and Guidance Requirements for Supercircular Entry into Planetary Atmosphere. NASA TR R 55, 1960.
2. Harry, David P., III, and Friedlander, Alan L.: Exploratory Statistical Analysis of Planet Approach-Phase Guidance Schemes Using Range, Range-Rate, and Angular-Rate Measurements. NASA TN D 268, 1960.
3. Friedlander, Alan L., and Harry, David P., III.: An Exploratory Statistical Analysis of a Planet Approach-Phase Guidance Scheme Using Angular Measurements with Significant Error. NASA TN D 471, 1960.
4. Harry, David P., III, and Friedlander, Alan L.: Statistical Performance Evaluation of a Self-Contained Optical Guidance System for the Approach of Reentry. Paper Presented at I.A.S. Symposium on Recovery of Space Vehicles, Los Angeles (Calif.), Aug. 31-Sept. 1, 1960.
5. Herget, Paul: The Computation of Orbits. (Available from Paul Herget, Univ. Cincinnati.)
6. Moulton, Forest Ray: An Introduction to Celestial Mechanics. Second rev. ed., The Macmillan Co., 1947.
7. Bock, Charles D., and Mundo, Charles J.: Guidance Techniques for Interplanetary Travel. ARS Jour., vol. 29, no. 12, Dec. 1959, pp. 931-939.
8. Battin, Richard H.: A Recoverable Interplanetary Space Probe. Vol. IV - Appendices. Rep. R-235, Instrumentation Lab., M.I.T., July 1959.
9. Deming, W. Edwards: Statistical Adjustment of Data. John Wiley & Sons, Inc., 1943.
10. Aitken, A. C.: Statistical Mathematics. Seventh ed., Interscience Pub., Inc., 1952.
11. Brown, D. C.: A Treatment of Analytical Photogrammetry with Emphasis on Ballistic Camera Applications. RCA Data Reduction Tech. Rep. 39, AFMTC-TR-57-22, Air Force Missile Test Center, Aug. 20, 1957.
12. Space Guidance and Control Systems Department: Digital Computer Characteristics for Space Applications. Federal Systems Div., Int. Business Machines Corp., June 9, 1959. (Publ. in Electronic Equipment Eng., Oct. 1959.)
13. White, Jack A.: A Study of the Guidance of a Space Vehicle Returning to a Braking Ellipse About the Earth. NASA TN D 191, 1960.
14. Freedman, J., and Meer, F.: RWND2F, Normally Distributed Pseudo-Random Numbers 704 (SAP) and/or 709 (SCAT). Space Tech. Labs., Inc. (Available through Share, IBM.)
15. Gumbel, Emil J.: Statistical Theory of Extreme Values and Some Practical Applications. Appl. Math. Ser. 33, NBS, Feb. 12, 1954.
16. Cramer, Harald: Mathematical Methods of Statistics. Princeton Univ. Press, 1946.
17. Unger, Jurgen H. W.: On the Mid-Course Navigation for Manned Interplanetary Space Flight. DSP-TR-2-58, Army Ballistic Missile Agency, Aug. 28, 1958.

18. Luidens, Roger W.: Approximate Analysis of Atmospheric Entry Corridors and Angles. NASA TN D–590, 1961.
19. Lees, Lester, Hartwig, Frederic W., and Cohen, Clarence B.: The Use of Aerodynamic Lift During Entry into the Earth's Atmosphere. Rep. GM–TR–0165–00519, Space Technology Labs., Inc., Nov. 1958.
20. Wong, Thomas J., and Slye, Robert E.: The Effect of Lift on Entry Corridor Depth and Guidance Requirements for the Return Lunar Flight. NASA TR R–80, 1961.
21. Grant, Frederick C.: Analysis of Low-Acceleration Lifting Entry from Escape Speed. NASA TN D–249, 1960.
22. Spence, William H.: On the Adequacy of ICBM Guidance Capability for a Mars Launch. Preprint 1174–60, ARS, 1960.
23. Friedlander, Alan L., and Harry, David P., III: Requirements of Trajectory Corrective Impulses During the Approach Phase of an Interplanetary Mission. NASA TN D–255, 1960.
24. Ling, Donald P.: Radio-Inertial Guidance. Space Technology, Lecture 12A, Univ. Calif., Apr. 1958.

U.S. GOVERNMENT PRINTING OFFICE, 1961